

令和元年度博士学位論文

Studies on Geranylgeranoic Acid Biosynthesized in Mammals.

D3217003

Yuki Tabata

田端 佑規

2019年12月

長崎県立大学大学院

人間健康科学研究科 栄養科学専攻

専攻分野 細胞生化学

指導教員 四童子 好廣 印

Chapter 1. General Introduction	1
1.1 Isoprenoids.....	2
1.2 Mevalonate pathway biosynthesizes isoprenoids	2
1.3 Acyclic retinoids	8
1.4 Geranylgeranoic acid (GGA)	9
Aims of the study.....	11
Chapter 2. Hepatic monoamine oxidase B is involved in endogenous geranylgeranoic acid synthesis in mammalian cells	12
Abstract.....	13
2-1. Introduction.....	14
2-2. Endogenous GGA in rat tissues	17
2-3. Endogenous 2,3-dihydroGGA in rat tissues.	18
2-4. Inhibition of biosynthesis of cellular GGA by tranlycypromine (TCP).....	24
2-5. Downregulation of cellular GGA by MAOB siRNA.....	26
2-6. Catalytic activity of recombinant human MAOB in oxidation of GGOH to GGal.....	30
2-7. MAOB gene knockout by CRISPR-Cas9/HDR system and the resultant cellular endogenous GGA changes.	33
2-8. Back-transfection of the MAOB gene into MAOB knockout cells restores the MAOB dependence of intracellular GGA.	38

2-9. Discussion	40
Chapter 3. Supplementation with geranylgeranoic acid during mating, pregnancy and lactation improves reproduction index in C3H/HeN mice	45
Abstract.....	46
3-1. Introduction.....	47
3-2. GGA-induced improvement of RI in C3H/HeN mice	49
3-3. Timing effects of GGA supplementation on the RI	54
3-4. Discussion	55
Chapter 4. Unequivocal evidence for endogenous geranylgeranoic acid biosynthesized from mevalonate in mammalian cells	59
Abstract.....	60
4-1. Introduction.....	61
4-2. Changes in endogenous GGA levels when pravastatin and/or ZAA treatment of HuH-7 cells...	62
4-3. ZAA induced upregulation of GGA and cell death in HuH-7 cells	62
4-4. Metabolic labeling of GGA using ¹³ C-MVL in human hepatoma HuH-7 cells	67
4-5. ISA with ¹³ C-MVL in HuH-7 cells	69
4-6. 2,3-DihydroGGA as a metabolite of GGA	73
4-7. Discussion	76
Chapter 5. General Discussion.....	81
Chapter 6. Materials and Methods.....	88

Materials	89
Methods.....	91
7. Acknowledgments.....	105
8. References	106

List of abbreviations

ADH	alcohol dehydrogenase
ARA	arachidonic acid
CRIPR-Cas9	<u>C</u> lustered <u>R</u> egularly <u>I</u> nterspaced <u>S</u> hort <u>P</u> alindromic <u>R</u> epeats <u>C</u> RISPR- <u>A</u> ssociated proteins <u>9</u>
CYP	cytochromes P450
DMAPP	dimethylallyl diphosphate
DMEM	Dulbecco's modified Eagle medium
ESI	electrospray ionization
FAD	flavin adenine dinucleotide
FBS	fetal bovine serum
FOH	farnesol
FPP	farnesyl diphosphate
Fal	farnesal
GGA	geranylgeranoic acid
GGOH	geranylgeraniol
GGPP	geranylgeranyl diphosphate
Gal	geranylgeranial
GGal	geranylgeranial
GOH	geraniol
GPP	geranyl diphosphate
Gal	geranial
HDR	homology directed repair
HMG-CoA	3-hydroxy-3-methylglutaryl-CoA
IPP	isopentenyl diphosphate

ISA	Isotopomer Spectral Analysis
LC/MS(/MS)	liquid chromatography mass spectrometry
MAO	monoamine oxidase
MRM	multiple-reaction-monitoring
MVA	mevalonate
MVL	mevalonolactone
NAD ⁺	nicotinamide adenine dinucleotide
PBS (-)	Dulbecco's Phosphate Buffered Saline, without calcium chloride and magnesium chloride
PCYOX	prenylcysteine oxidase
RAR	retinoic acid receptor
RI	reproduction index
ROR	retinoic acid receptor-related orphan receptors
RXR	retinoid-X-receptor
SAM	senescence-accelerated mouse
TCP	tranylcypramine hydrochloride
WR	weanling rate
ZAA	zaragozic acid A/squalestatin 1
siRNA	small interfering RNA

Chapter 1. General Introduction

1.1 Isoprenoids

Isoprenoids form the most diverse and abundant group of organic compounds in nature (1). They are derived from branched C5 isoprene units. The number of repetitions of this motif, cyclization reactions, rearrangements and oxidation of the carbon skeleton are responsible for the enormous structural diversity. Many types of isoprenoids are essential components of the cellular machinery that are found in all organisms. The isoprenoids participate in a variety of biological processes: 1) as electron carriers, ubiquinone is essentially required for the mitochondrial respiratory chain (2); 2) as components of membranes, hopanoids and steroids are found in eubacteria and eukaryotes, respectively; 3) as a donor for prenylated proteins, farnesyl diphosphate (FPP: C15) and geranylgeranyl diphosphate (GGPP: C20) are involved in isoprenylation of small G-proteins such as Ras and Rho (3); 4) as oligosaccharide carriers, phosphorylated and diphosphorylated dolichols participate in N-linked protein glycosylation (4); 5) as fat-soluble vitamins, many plant-produced isoprenoids are essential nutrients in human diet; and 6) as chemotherapeutic agents, diterpenoid paclitaxel has been widely utilized for therapy of many clinical cancers (5).

1.2 Mevalonate pathway biosynthesizes isoprenoids

Isoprenoids vary greatly in size but are all synthesized ubiquitously among eubacteria, archaeobacteria and eukaryotes through condensations of the five-carbon isopentenyl diphosphate (IPP: C5) and dimethylallyl diphosphate (DMAPP: C5). In mammals, IPP can be synthesized from the mevalonate (MVA) pathway. In 1958, Bloch's group first described the mevalonate pathway in yeasts (6). This pathway starts with a production of acetoacetyl-CoA (C4) from two molecules of acetyl-CoA (C2) in a reaction catalyzed by thiolase. Next, 3-hydroxy-3-methylglutaryl-CoA (HMG-CoA: C6) is synthesized from acetyl-CoA and acetoacetyl-CoA by being condensed by the catalytic reaction of the HMG-CoA synthase. HMG-CoA produces mevalonate (MVA: C6) by HMG-CoA reductase that is a rate-limiting enzyme in this pathway. MVA is sequentially phosphorylated by MVA kinase and MVA-5-phosphate (MVAP: C6) kinase to form MVA-5-diphosphate

(MVAPP: C6). This diphosphate is then decarboxylated by MVAPP decarboxylase to IPP, which is further converted to DMAPP by IPP isomerase. After this isomerization reaction, geranyl diphosphate (GPP: C10) and FPP are sequentially synthesized through a head-to-tail consecutive addition of IPP by FPP synthase (Fig. 1-1).

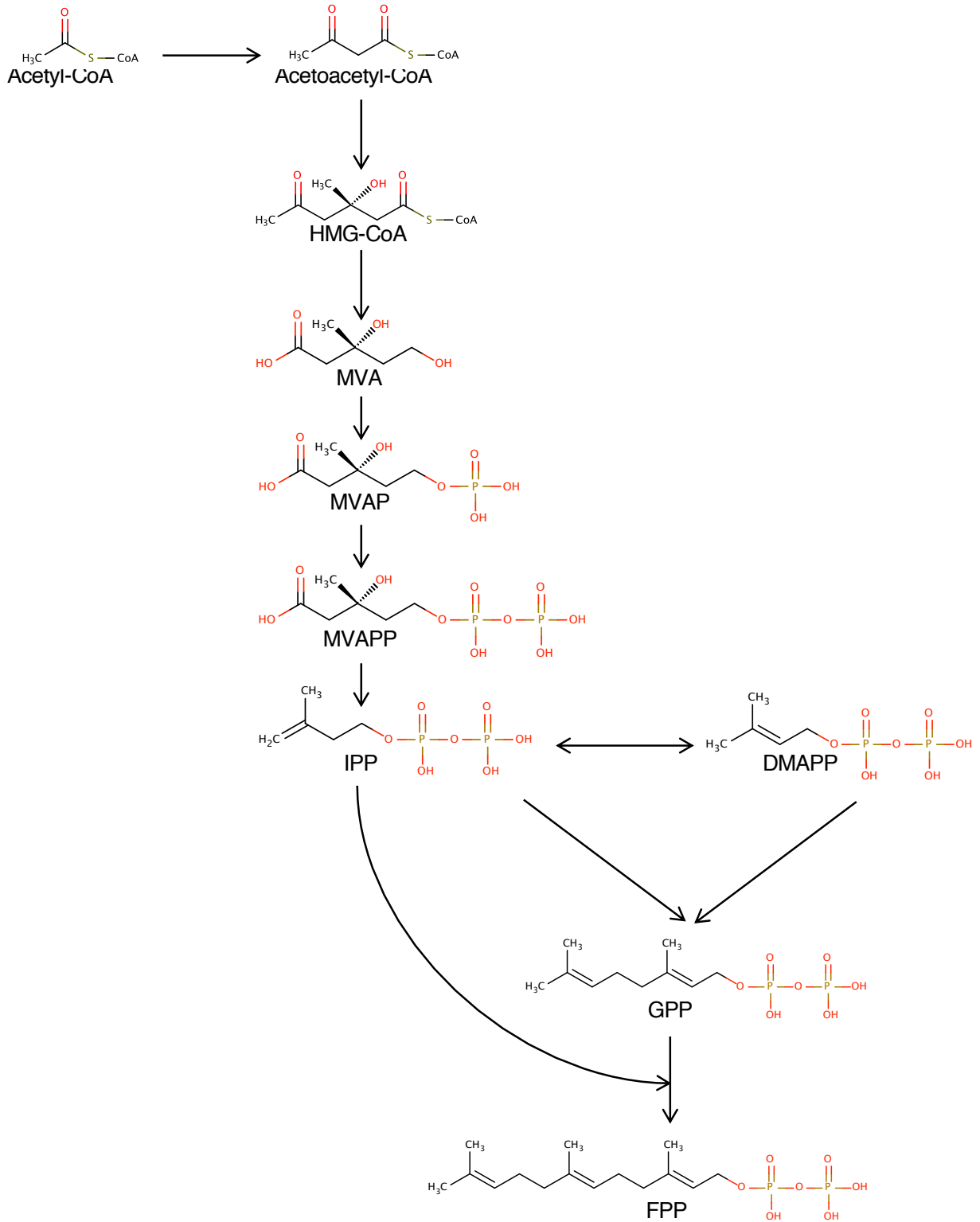


Figure 1-1: Mevalonate pathway: from Acetyl-CoA to FPP.

The details are described in the text.

Metabolic pathway after FPP is divided into two major pathways, steroidogenesis and non-steroidogenesis pathways. The main metabolic pathway from FPP is steroidogenesis. At the first step of steroidogenesis pathway, squalene is synthesized through a tail-to-tail addition of 2 molecules of FPP by squalene synthase as shown below. Squalene is a vital material for the synthesis of cholesterol, steroid hormones, cell membrane maintenance, cell growth, differentiation, and vitamin D in the human body (Fig. 1-2). Another pathway is non-steroidogenesis. In this pathway, GGPP synthase produces GGPP by prenyl transfer reaction from IPP to FPP. From the bottom of Fig. 1-1, a metabolic fate of FPP in non-steroidogenesis is further branched into two major pathways. One is ubiquinone synthesis from all-*trans* GGPP, which is generated from FPP by *trans*-prenyltransferase interacting with FPP synthase (Fig. 1-3). In plants all-*trans* GGPP is a precursor of phytoene (C40), which is a founder of carotenoids (C40) and phytoene is synthesized by condensation of two all-*trans* GGPP molecules in a tail-to-tail manner (7). Another branching pathway is dolichol synthesis from 2-*cis* GGPP, which is generated from FPP by *cis*-prenyltransferase interacting with FPP synthase (Fig. 1-3). All of the above-mentioned metabolites from the MVA pathway are the substrates for biosynthesis of all isoprenoid metabolites including monoterpenes or di-isoprenoids, sesquiterpenes or tri-isoprenoids, diterpenes or tetra-isoprenoids, triterpenes or sterols, ubiquinones, dolichols or polyprenoids, and prenylated proteins. The enzymes of the MVA pathway have been studied from a great number of organisms including humans. It has been well known that inhibition of this pathway is already applied in the treatment of cardiovascular disease, hypercholesterolemia and metabolic bone disease and it could be a possible new therapy in cancer treatment (8–11). For example, HMG-CoA reductase, the best-characterized and rate-limiting enzyme in the pathway, is a target of the statin class of cholesterol-lowering drugs (12), the treatment of cardiovascular disease, and inflammatory processes (13). Several biologically active isoprenoids are found also in insects and plants (14, 15). As mentioned above, many plant-produced isoprenoids such as fat-soluble vitamins (retinoids, vitamin D, tocopherol, and vitamin K) are essential nutrients in human diets.

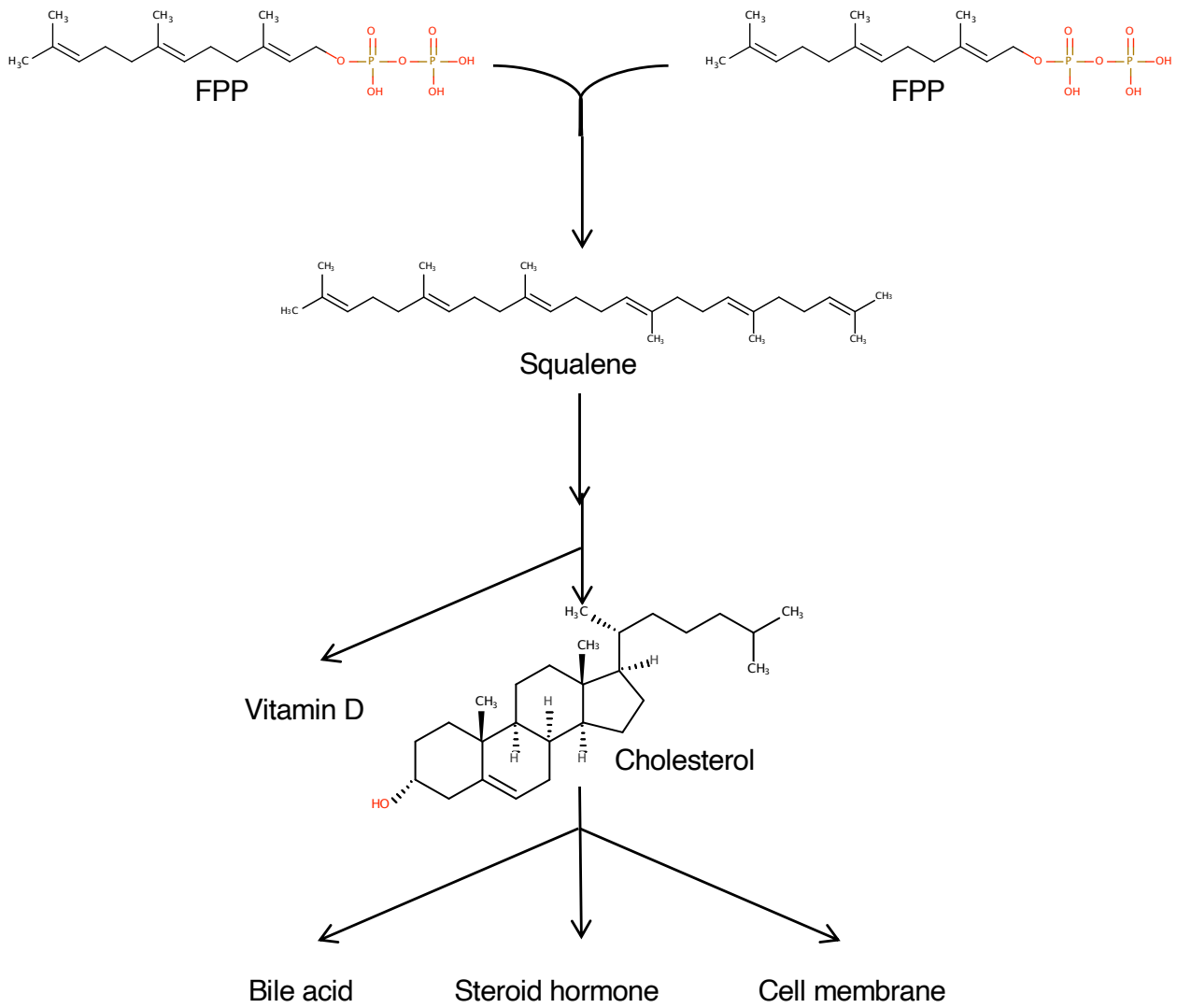


Figure 1-2: Biosynthetic pathway from FPP to Cholesterol.

The details are described in the text.

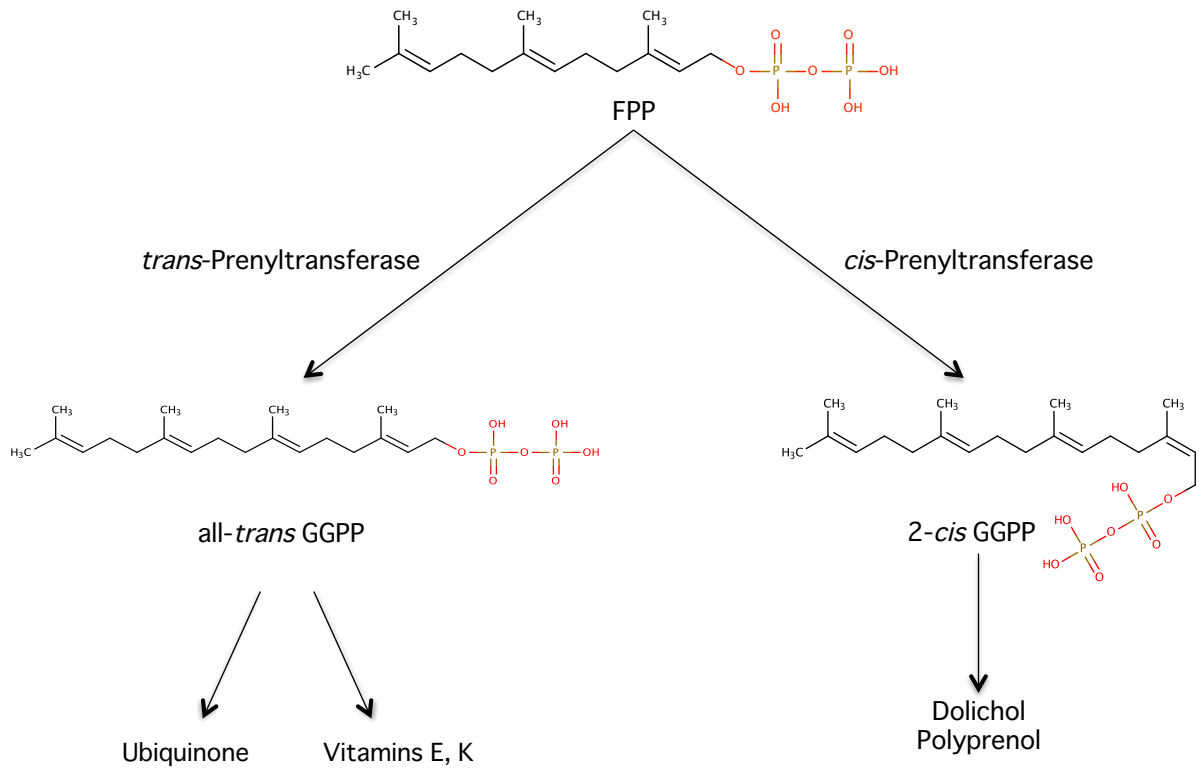


Figure 1-3: From FPP to GGPP and its metabolites.

The details are described in the text.

1.3 Acyclic retinoids

Retinoids including all-*trans* retinoic acid, 9-*cis* retinoic acid and other synthetic retinoic acid derivatives are clinically utilized as chemotherapeutic agents for acute promyelocytic leukemia, but their side effects are sometimes so serious that it becomes difficult to continue administration of the retinoids (16). To solve the problem, acyclic retinoid has been developed as analogues of retinoids in Japan. The clinical efficacy of a chemically synthesized 20-carbon acyclic retinoid (all-*trans* 3,7,11,15-tetramethyl-2,4,6,10,14-hexadecapentanoic acid, 4,5-didehydrogeranylgeranoic acid or a generic name of peretinoin, Fig. 1-4) on prevention of second primary hepatoma has been proven in a placebo-controlled, double-blinded and randomized phase III clinical trial with postoperative hepatoma patients with few side effects (17).

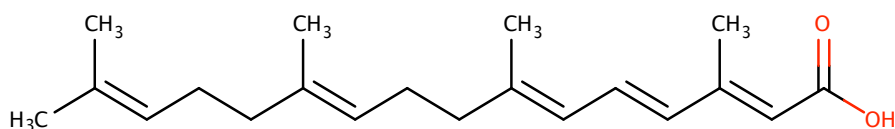


Figure 1-4 Chemical structure of 4,5-didehydrogeranylgeranoic acid

And later it was revealed that peretinoin significantly increased a 5-year survival rate after a radical therapy of primary hepatoma in these patients, in comparison with placebo control (18, 19). It has been also shown that the acyclic retinoid binds to cellular retinoic acid binding protein (CRABP) as well as to nuclear retinoid receptors, exerts transcriptional activation of some hepatocyte-specific genes in hepatoma cells, and has preventive actions in chemical and spontaneous hepato-carcinogenesis (20–23). In this context, this group of compound was named "acyclic retinoid" (19). However, there was a big difference in cell death-inducing activity between acyclic retinoids and natural retinoids such as retinoic acid. In other words, acyclic retinoids efficiently induced cell death in HuH-7 cells, but 5-fold more all-*trans* retinoic acid did not (24). So, "acyclic retinoid" was thought to have non-retinoidal function besides the retinoidal function. Hence, I paid attention to a chemical structure of geranylgeranoic acid (GGA), which is a 4,5-dihydro derivative of peretinoin (Fig. 1-5).

1.4 Geranylgeranoic acid (GGA)

Geranylgeranoic acid (all-*trans* 3,7,11,15-tetramethyl-2,6,10,14-hexadecatetraenoic acid or GGA) is a compound that is chemically categorized as isoprenoids, consisting of 4-isoprene units linked in a tail-to-head manner (Fig. 1-5). GGA has a carboxyl group at its tail terminus and has been developed as one of preventive agents against second primary hepatoma. As for the molecular and cellular mechanisms of GGA-induced cell death, several studies have so far been conducted.

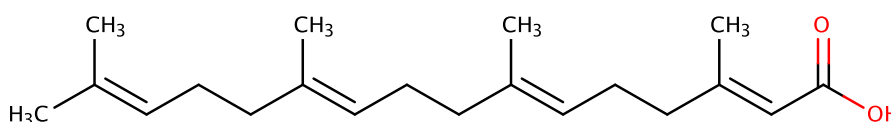


Figure 1-5 Chemical structure of geranylgeranoic acid

The following are descriptions of cellular and molecular events relating to GGA-induced human hepatoma cell death in chronological order. The earliest is cytoplasmic splicing of X-box binding protein 1 (*XBPI*) mRNA, a canonical marker for unfolded protein response (UPR), observed 5 min after adding GGA in culture medium (25), overproduction of superoxide in mitochondria and conversion from LC3-I to LC3-II, a marker for initial autophagic response, can be detected after 15 min (26), and after 30 min, GFP-LC3 granules, a marker for autophagosome, appear (26) and cyclin D1 protein, which is involved in the G1/S checkpoint, disappears (27). Two hours after adding GGA, the *XBPI*s protein is detected in the nucleus (25), the cellular level of phosphorylated p53 at Ser10 is increased (28) and the membrane potential of mitochondria ($\Delta\Psi_m$) is lost (29). Nuclear translocation of the cytoplasmic p53 is induced with a 3-h treatment with GGA (28). The cell death is finally detectable 6–8 h after adding GGA (30). Recently, it has reported that GGA at micromolar concentrations upregulated the cellular protein levels of TP53-induced glycolysis and apoptosis regulator (*TIGAR*) and synthesis of cytochrome c oxidase 2 (*SCO2*) without their transcriptional upregulation and consequently induced a metabolic shift from aerobic glycolysis to mitochondrial respiration, as revealed by metabolomics analysis in 2 h(31). This metabolic shift from glycolysis to aerobic respiration is crucial for

cancer chemoprevention in terms of preventing the Warburg effect, a cancer-specific energy metabolism. In guinea pig fibroblast-derived cell lines, GGA induced a transient increase of mitochondrial superoxide production in 15 min and dissipation of $\Delta\Psi_m$ in 2 h, and cell death became evident in 6 h (32).

GGA has the same physiological activity and characteristics as peretinoin. However, GGA, unlike peretinoin, has been reported to be a natural compound present in some medicinal herbs used in traditional medicine, Kampo and Āyurveda, as well as ordinary herbs (turmeric, basil, rosehip, cinnamon, and so on), indicating that GGA is one of acyclic diterpenoids (33).

Aims of the study

A major aim of my thesis is to unequivocally prove that GGA, a hepatocarcinogenesis inhibitory compound, is biosynthesized in not only plants but also mammalian cells. Therefore, in Chapter 2, I investigated the enzyme involved in the oxidation of GGOH to GGal, the precursor metabolite of GGA, in human hepatoma-derived cells. In chapter 3, I examined biological activities other than the carcinogenesis-preventive effects of GGA, especially the improvement of mouse reproductive function. In chapter 4, I provide unequivocal evidence for endogenous geranylgeranoic acid biosynthesized from mevalonate in mammalian cells.

I sincerely hope that my doctoral dissertation will be the basis for cancer prevention strategies and other bioactivity studies using endogenous bioactive metabolites such as GGA.

Chapter 2. Hepatic monoamine oxidase B is involved in endogenous geranylgeranoic acid synthesis in mammalian cells

Abstract

Geranylgeranoic acid (GGA) has been reported to induce autophagic cell death via upregulation of lipid-induced unfolded protein response in several human hepatoma-derived cell lines, and its 4,5-didehydro derivative has been developed as a preventive agent against second primary hepatoma in clinical trials. Previously, it was reported that GGA is a natural diterpenoid synthesized in several medicinal herbs. On the other hand, it is not clear whether GGA is biosynthesized in mammalian cells. Several cell-free experiments have demonstrated that GGA is synthesized through GGal by oxidation of GGOH with concomitant molecular oxygen consumption. Here, first of all, I show with normal male Wistar rats, the endogenous GGA content in liver were found to be far greater than those in other organs analyzed. Next, in a culture-system of a couple of human hepatoma cell lines, I analyzed possible contribution of monoamine oxidase B (MAOB), which was previously shown to be involved in the oxidation of GGOH by using either HuH-7 cell lysates or recombinant human MAOB. Tranylcypromine, an MAO inhibitor, induced dose-dependent downregulation of endogenous GGA content in HuH-7 cells. Moreover, *MAOB* small interfering RNA (siRNA) treatment reduced the amount of intracellular GGA in HuH-7 and Hep3B cells. In addition, *MAOB*-knockout human hepatoma Hep3B cell (*MAOB*-KO) was established using the Clustered Regularly Interspaced Short Palindromic Repeats CRISPR-Associated proteins 9/homology directed repair (CRISPR-Cas9/HDR) system, but, unexpectedly, I failed to detect any difference in the cellular GGA content between *MAOB*-KO and *MAOB* wild-type cells. However, loss of *MAOB*-siRNA sensitivity of *MAOB*-KO cells was recovered by the transfection of the KO cells with the *MAOB*-expression plasmid, suggesting that some other latent metabolic pathways may be evoked to maintain the cellular endogenous GGA levels in *MAOB*-KO hepatoma cells.

Taken together with the previous findings, the results presented in this chapter strongly suggest that hepatic MAOB is involved in synthesis of endogenous GGA through oxidation of GGOH and I provide new insights into biological role(s) of hepatic MAOB.

2-1. Introduction

Geranylgeranoic acid (all-*trans* 3,7,11,15-tetramethyl-2,6,10,14-hexadecatetraenoic acid or GGA) and its didehydro derivative were demonstrated to be potent ligands for nuclear retinoid receptors (21) so that these isoprenoid compounds have been developed as the preventive agents against second primary hepatoma (17, 18). In the past, it has been reported that GGA is a natural compound present in some medicinal herbs (33).

In mammalian cells, GGA is presumed to be biosynthesized from GGPP, a metabolite derived from the MVA pathway. A previous studies have reported that GGPP is converted to geranylgeraniol (GGOH) by geranylgeranyl pyrophosphatase (GGPPase), the most active at physiologic pH and highly specific for GGPP, in rat liver homogenates (34). GGOH produced by GGPPase had been thought to be oxidized to geranylgeranial (GGal) by cytosolic alcohol dehydrogenase (ADH) in the presence of nicotinamide adenine dinucleotide (NAD^+) (35) and then GGal had been supposed to be further oxidized to GGA by non-specific aldehyde dehydrogenase (35). Indeed, it has confirmed that enzymatic conversion from GGal to GGA is highly dependent on the exogenous NAD^+ in rat liver homogenates (36) and human hepatoma-derived HuH-7 cell lysates (37). However, it found that a putative enzyme in either rat liver or HuH-7 cells involved in the oxidation of GGOH to GGal did not require any exogenous NAD^+ in the cell-free system (36, 37). Taking account that the mitochondrial enzyme was sensitive to tranlycypromine (TCP), an inhibitor against monoamine oxidases (37), I have reasonably speculated that a certain member of monoamine oxidase family might be involved in GGOH oxidation to GGal in the process of GGA biosynthesis (36, 37). There so far have been the following three lines of evidence for monoamine oxidase B (MAOB) as GGOH-oxidizing enzyme; 1) HuH-7 cell lysate or rat liver homogenate enzyme does not require the exogenous NAD^+ to produce GGal, 2) molecular oxygen solubilized in the reaction medium is consumed upon addition of GGOH into HuH-7 cell lysates as enzyme source, and 3) the recombinant human MAOB protein is active to oxidize GGOH to GGal (37).

MAOB, one of the flavin enzymes, located to the outer mitochondrial membrane, generally degrades phenylethylamine and dopamine in the central nervous system (38). When these substrates are oxidized by MAOB, molecular oxygen is consumed and reactive oxygen species such as hydrogen peroxide are generated. Therefore, an increase in the expression level of MAOB in the brain is expected to damage the nervous system due to the reactive oxygen species produced (39). In fact, the expression of MAOB has increased in Alzheimer's disease and Parkinson's disease (40, 41), and MAOB inhibitors have been investigated as treatments for these diseases (42, 43). In contrast to the diverse MAOB studies in the nervous system, the physiological role of MAOB in the liver is hardly clearly defined despite the tissue levels of *MAOB* mRNA expression are not only higher than those in the central nervous system, but also highest among all human organs (44). At present, the liver MAOB enzyme is considered to contribute to the decomposition of xenobiotics, because the liver is one of the major organs that contribute to drug metabolism and MAOB shows relatively broad substrate specificity for aromatic amines (45). In this context, the physiological substrate of liver MAOB has not yet been clearly elucidated. Therefore, if I can show that GGOH is one of the endogenous substrates of hepatic MAOB, as mentioned earlier, I will add a new perspective on the physiological role of hepatic MAOB.

In the first part of this chapter, I demonstrate that endogenous GGA exists in several organs of male rats using liquid chromatography mass spectrometry (LC/MS/MS). The second part of this chapter, by using MAO inhibitors and siRNAs to inhibit and downregulate the cellular MAOB enzyme activity, I demonstrate hepatic MAOB is involved in the maintenance of intracellular GGA content in human hepatoma-derived cells. Then, to ensure that MAOB is involved in GGA biosynthesis more reliably, I performed knockout of the *MAOB* gene using the CRISPR-Cas9 plasmids in human hepatoma cells, but unexpectedly, the intracellular GGA content of *MAOB*-knockout (KO) cells was almost the same as that of wild type cells. However, when the *MAOB*-KO cells were back-transfected with *MAOB* expression plasmid, *MAOB* siRNA-mediated downregulation of endogenous GGA level was recovered. In other words, when MAOB is expressed normally in human

hepatocytes, the intracellular level of GGA is dependent on MAOB activity. The possibility that enzymes other than MAOB in *MAOB*-KO cells are involved in maintaining intracellular GGA content is also described.

2-2. Endogenous GGA in rat tissues

Because it has already reported that endogenous free GGA was identified in the human liver cancer-derived cell line, HuH-7, and blood serum of healthy volunteers using LC/MS, I attempted to detect and quantify endogenous free GGA in each tissue of male Wistar rats. First, I decided to demonstrate endogenous free GGA in livers as compared with free arachidonic acid (ARA), a structural isomer of GGA using LC/MS/MS, which allowed me to separately quantitate GGA and ARA in a single run. As a result, multiple-reaction-monitoring (MRM) tracings of each compound in the liver extract clearly indicated the natural existence of free GGA in the liver, as shown in Fig. 2-1A. Because the standard curves of GGA and ARA were linear ($r^2 = 0.99$ for both), at least in the range shown in supplemental Fig. 2-2, GGA and ARA in each organ of the rat were quantified. Whereas all tissues tested contained endogenous free GGA measured using LC/MS/MS, the hepatic free GGA content was exceptionally high, followed by the reproductive organs, such as prostate and testis, and neuronal tissues of cerebrum and cerebellum (Fig. 2-1B, Table 2-1). Blood serum and epididymal adipose tissue contained only a few free GGA. A tissue distribution of free ARA was in the range of previous reports (46, 47), so the molar ratio of free GGA to free ARA was also highest in the liver (Fig. 2-3A).

Although the epididymis, another reproductive organ, was not listed in supplemental Table 2-1, the tissue concentrations of GGA in each part of the epididymis were calibrated as 28.82 ± 2.13 pmol/g in the caput ($n = 5$), 8.75 ± 3.07 pmol/g in the cauda ($n = 5$), and 5.96 ± 1.13 pmol/g in the corpus ($n = 5$). The epididymal caput was, second to the liver, a tissue with a high GGA concentration.

2-3. Endogenous 2,3-dihydroGGA in rat tissues.

Because Sagami's group (48) reported that rat thymocytes produce 2,3-dihydroGGA from GGal or GGOH through GGA and Dulaney's group (49, 50) found 2,3-dihydroGGA with phytanic acid in the serum and urine of patients with Refsum disease, I also tried to detect and quantify endogenous 2,3-dihydroGGA in male Wistar rat tissues using an MRM mode of LC/MS/MS (Fig. 2-1C, Fig. 2-2). Unlike the tissue distribution of GGA, the 2,3-dihydroGGA content was highest in thymocytes. Furthermore, the hepatic 2,3-dihydroGGA content was the second lowest value after epididymal fat, excluding serum (Fig. 2-1C). When a molar ratio of 2,3-dihydroGGA to GGA in each organ was calculated, it was highest in the thymus (141.2 ± 34.3), second highest in the seminal vesicle (106.0 ± 41.4), and lowest in liver (5.1 ± 1.5); in other organs, it was in the range of 30-75, excluding serum (15.4 ± 1.9), as shown in Fig. 2-1D and Table 2-1.

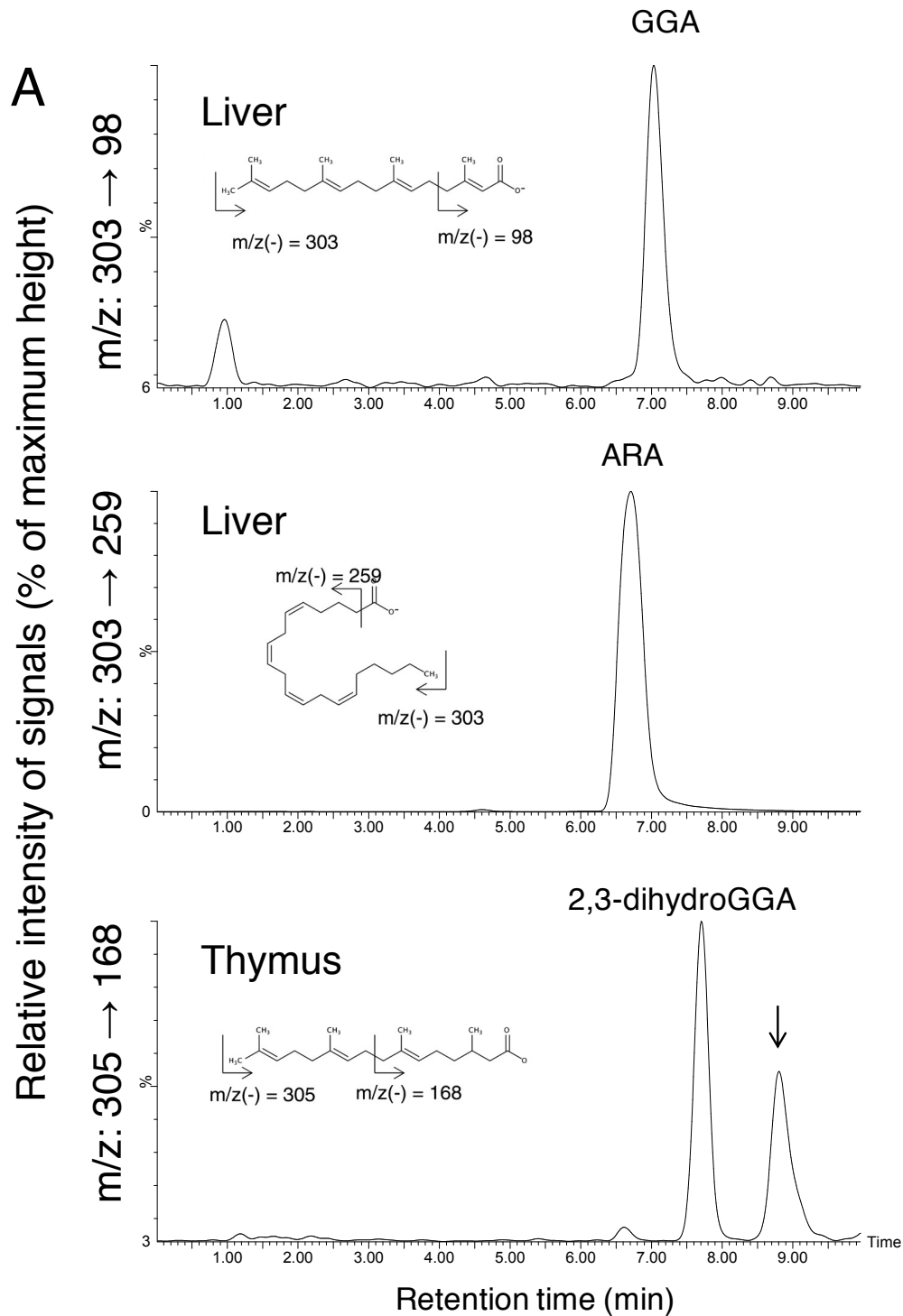


Figure 2-1. Tissue distribution of endogenous free GGA, ARA, and 2,3-dihydroGGA in male Wistar rats measured using reverse phase LC/MS/MS analysis.

(A). Representative chromatograms of the rat hepatic lipid extract tracing GGA ($m/z: 303 \rightarrow 98$) and arachidonic acid ($m/z: 303 \rightarrow 259$), and of the rat thymus lipid extract tracing 2,3-dihydroGGA ($m/z: 305 \rightarrow 168$). Down arrow represents elution times of di-homo- γ -linolenic acid. Tissue distribution of endogenous GGA (B) and 2,3-dihydroGGA (C) in male Wistar rat and a molar ratio of 2,3-dihydroGGA to GGA in each tissue (D) are shown in a bar graph. All bars represent the mean \pm SE ($n = 5$). (B) ***: $p < 0.001$ vs each other organs, (C) ***: $p < 0.001$ vs serum and epididymal fat and, *: $p < 0.05$ vs each organ other than serum and epididymal fat, and (D) *: $p < 0.05$ vs liver (ANOVA with Post HOC Scheffe). GGA, geranylgeranoic acid; ARA, arachidonic acid; LC/MS/MS, liquid chromatography mass spectrometry.

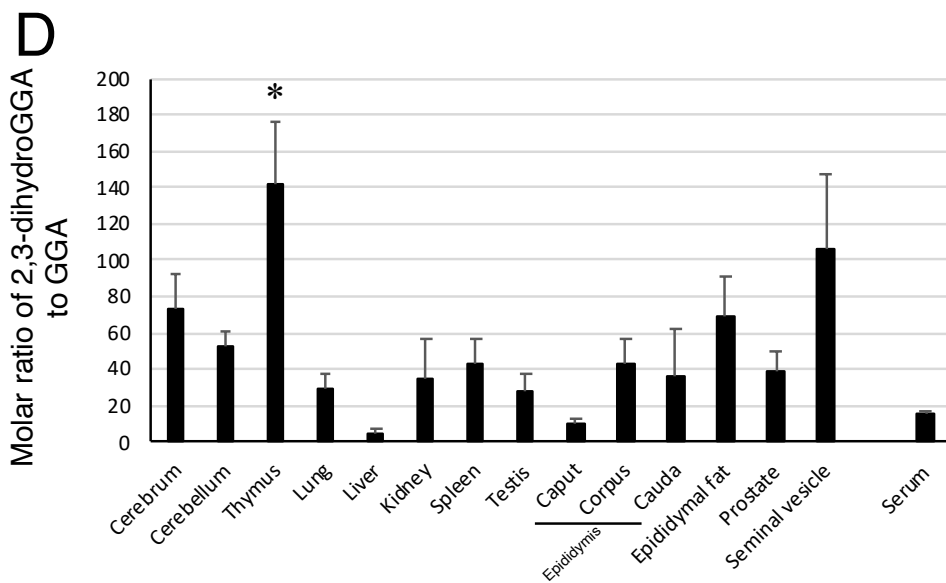
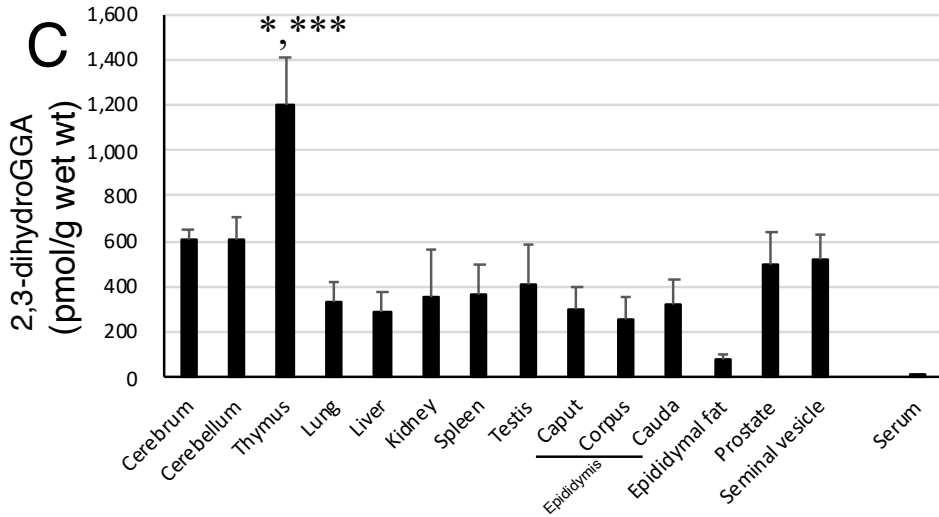
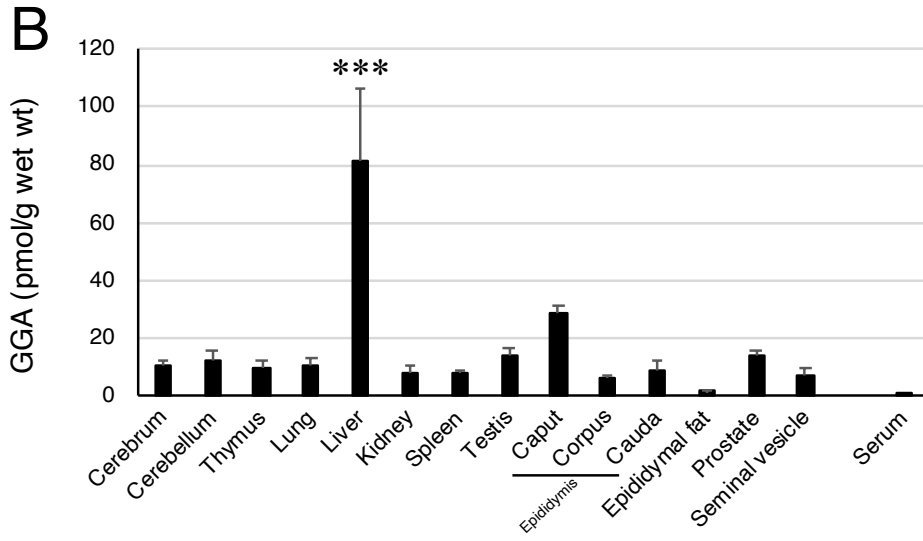


Fig. 2-1 Continued.

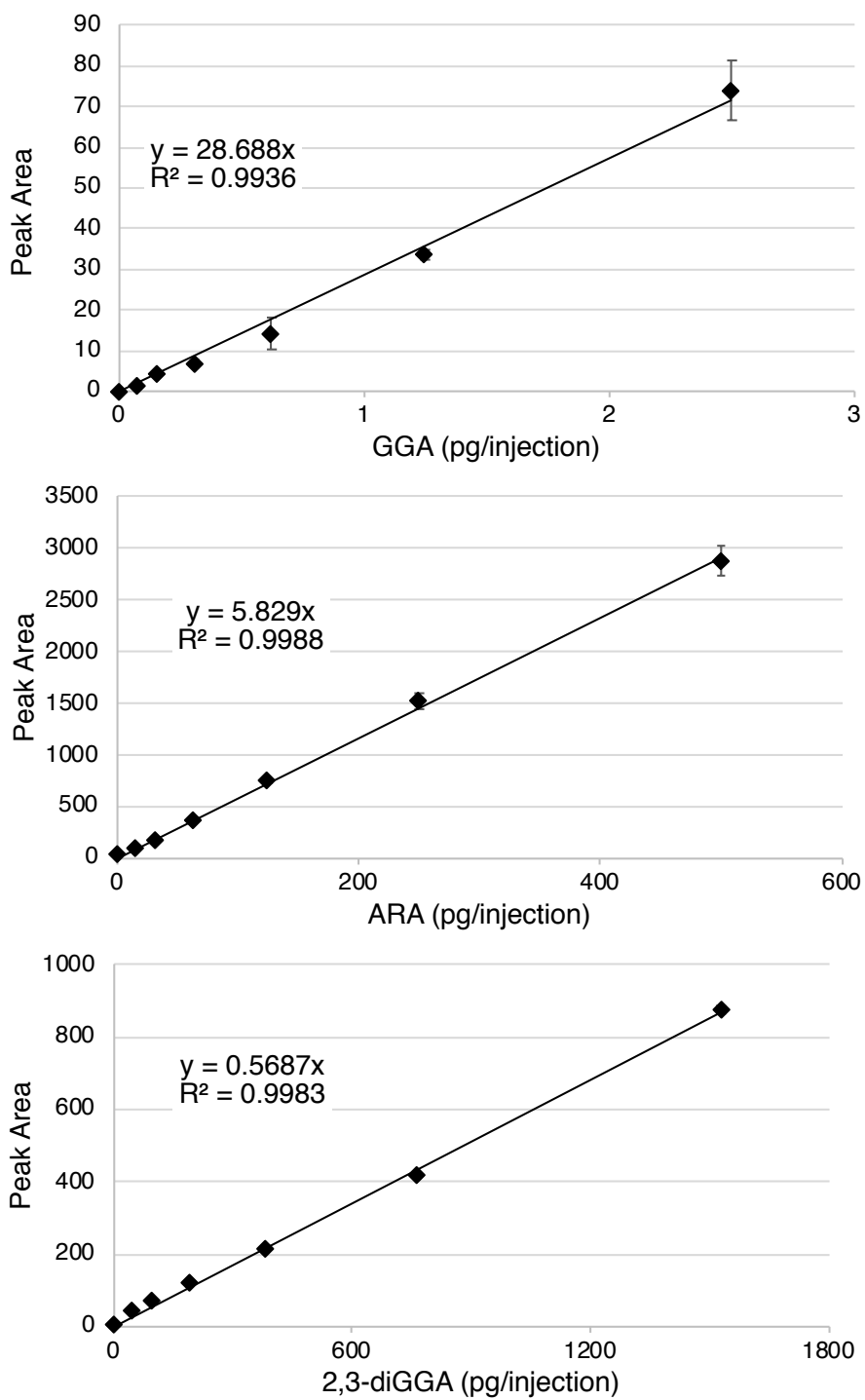


Figure 2-2. Calibration curves of GGA, ARA and 2,3-dihydroGGA.
 GGA, geranylgeranoic acid; ARA, arachidonic acid.

Table 2-1 Distribution of GGA, 2,3-dihydroGGA, ARA and their molar ratios in several organs of male Wistar rats.

Organ	GGA			2,3-diGGA			ARA			GGA/ARA			2,3-diGGA/ARA			2,3-diGGA/GGA		
	(pmol/g)			(pmol/g)			(nmol/g)			(Molar ratio x 10 ⁴)			(Molar ratio x 10 ⁴)			(Molar ratio)		
Cerebrum	*10.29	±	2.03	612.47	±	42.73	645.54	±	26.33	0.16	±	0.04	9.60	±	0.86	72.86	±	19.28
Cerebellum	12.44	±	2.63	604.38	±	105.28	611.82	±	48.37	0.20	±	0.04	9.71	±	1.35	53.15	±	7.60
Thymus	9.74	±	2.21	1205.03	±	205.63	497.13	±	42.71	0.19	±	0.04	23.94	±	3.40	141.15	±	34.28
Lung	10.04	±	2.78	330.92	±	89.53	741.48	±	63.23	0.13	±	0.03	4.14	±	1.12	29.08	±	8.33
Liver	80.97	±	25.68	292.17	±	82.60	580.60	±	40.21	1.43	±	0.43	5.02	±	1.30	5.12	±	1.48
Kidney	8.10	±	2.53	350.92	±	215.26	714.46	±	77.50	0.10	±	0.03	4.30	±	2.63	34.44	±	22.48
Spleen	7.97	±	0.87	363.60	±	137.78	848.41	±	165.75	0.11	±	0.02	4.84	±	1.75	42.83	±	13.16
Testis	13.96	±	2.36	408.56	±	172.14	318.53	±	25.96	0.43	±	0.07	12.17	±	4.65	28.25	±	9.42
Epididymis (Caput)	28.82	±	2.13	298.24	±	99.24	287.32	±	14.79	1.00	±	0.12	10.38	±	3.01	10.35	±	2.11
Epididymis (Corpus)	5.96	±	1.13	258.46	±	98.23	174.22	±	13.08	0.34	±	0.05	14.84	±	3.64	43.37	±	12.89
Epididymis (Cauda)	8.75	±	3.07	320.10	±	113.25	271.73	±	55.39	0.32	±	0.05	11.78	±	2.99	36.58	±	25.78
Epididymal fat	1.22	±	0.31	76.66	±	25.63	244.60	±	35.89	0.05	±	0.01	3.05	±	0.90	69.29	±	21.83
Prostate	13.58	±	2.08	498.07	±	144.04	463.92	±	45.43	0.30	±	0.04	11.31	±	3.16	38.78	±	11.06
Seminal vesicle	7.13	±	1.96	522.83	±	106.91	823.62	±	100.55	0.09	±	0.03	6.20	±	1.03	105.98	±	41.44
	(pmol/mL)			(pmol/mL)			(pmol/mL)											
Serum	0.27	±	0.04	4.21	±	0.79	12.89	±	1.92	0.21	±	0.01	3.18	±	0.19	15.38	±	1.89

*: Data are mean ± SE of male Wistar rats (5-weeks old, n=5).
GGA, geranylgeranoic acid; ARA, arachidonic acid.

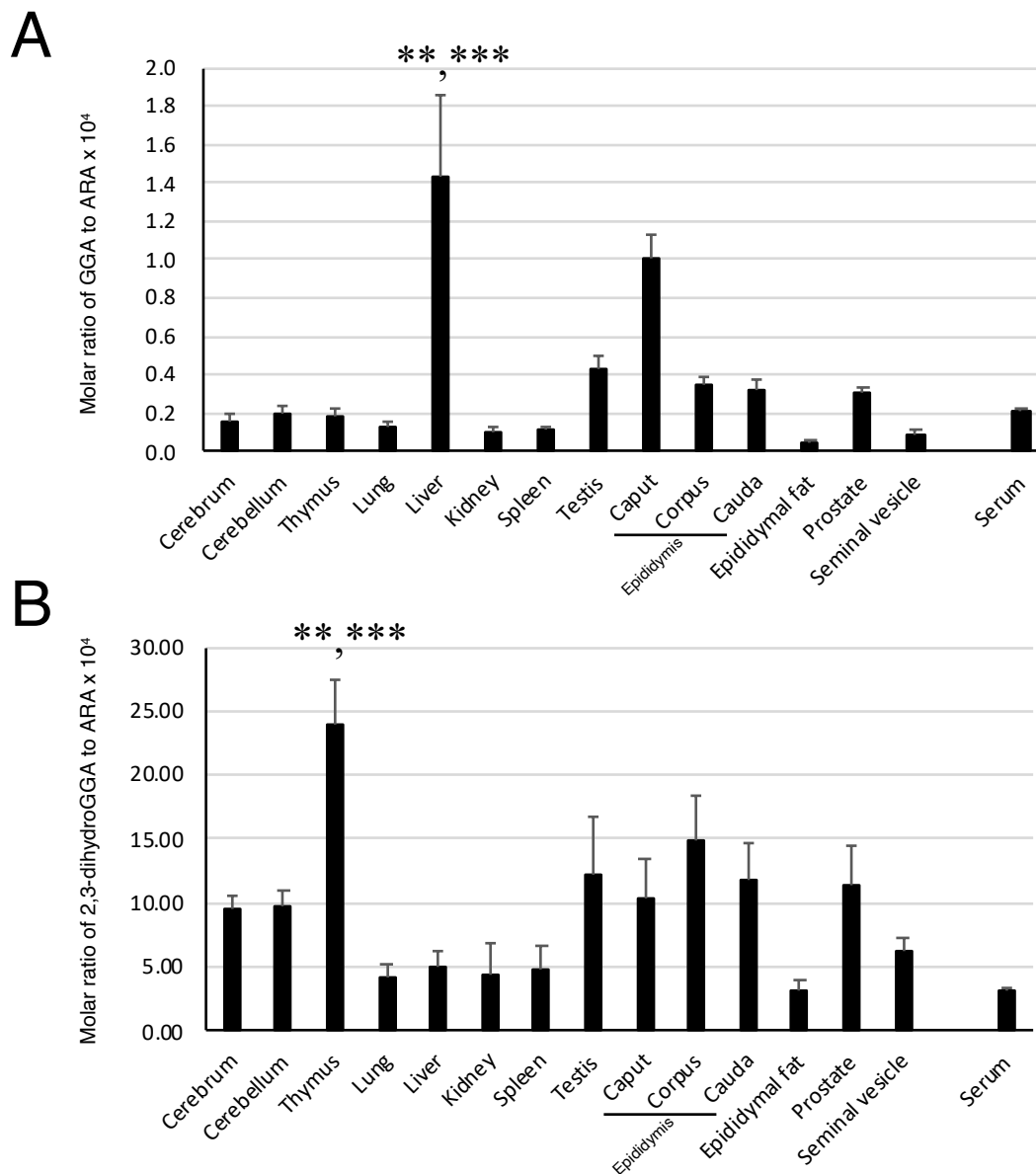


Figure 2-3. Molar ratio of each endogenous acyclic diterpenoid to ARA in each tissue.

(A) Molar ratio of endogenous GGA to ARA in each tissue.

** $p < 0.01$ vs testis and *** $p < 0.001$ vs all other organs except testis.

(ANOVA with post hoc Scheffe)

(B) Molar ratio of endogenous 2,3-dihydroGGA to ARA in each tissue.

** $p < 0.01$ vs lung, liver, kidney, spleen. *** $p < 0.001$ vs seminal vesicle and serum.

(ANOVA with post hoc Scheffe)

All bars represent the mean \pm SE ($n = 5$).

GGA, geranylgeranoic acid; ARA, arachidonic acid.

2-4. Inhibition of biosynthesis of cellular GGA by tranylcypromine (TCP)

First of all, I confirmed whether TCP, an inhibitor of MAOs, worked as a micromolar inhibitor of biosynthesis of GGA in a cell culture system. Fig. 2-4A clearly shows that TCP added in the culture medium decreased the cellular level of endogenous GGA in HuH-7 cells in a dose-dependent manner with apparent IC_{50} of approximately 33 μ M. Furthermore, 100 μ M TCP not only decreased the endogenous GGA (Fig. 2-4B and C), but also suppressed the conversion of exogenously added GGOH to GGA in cultured HuH-7 cells (Fig. 2-4D and E).

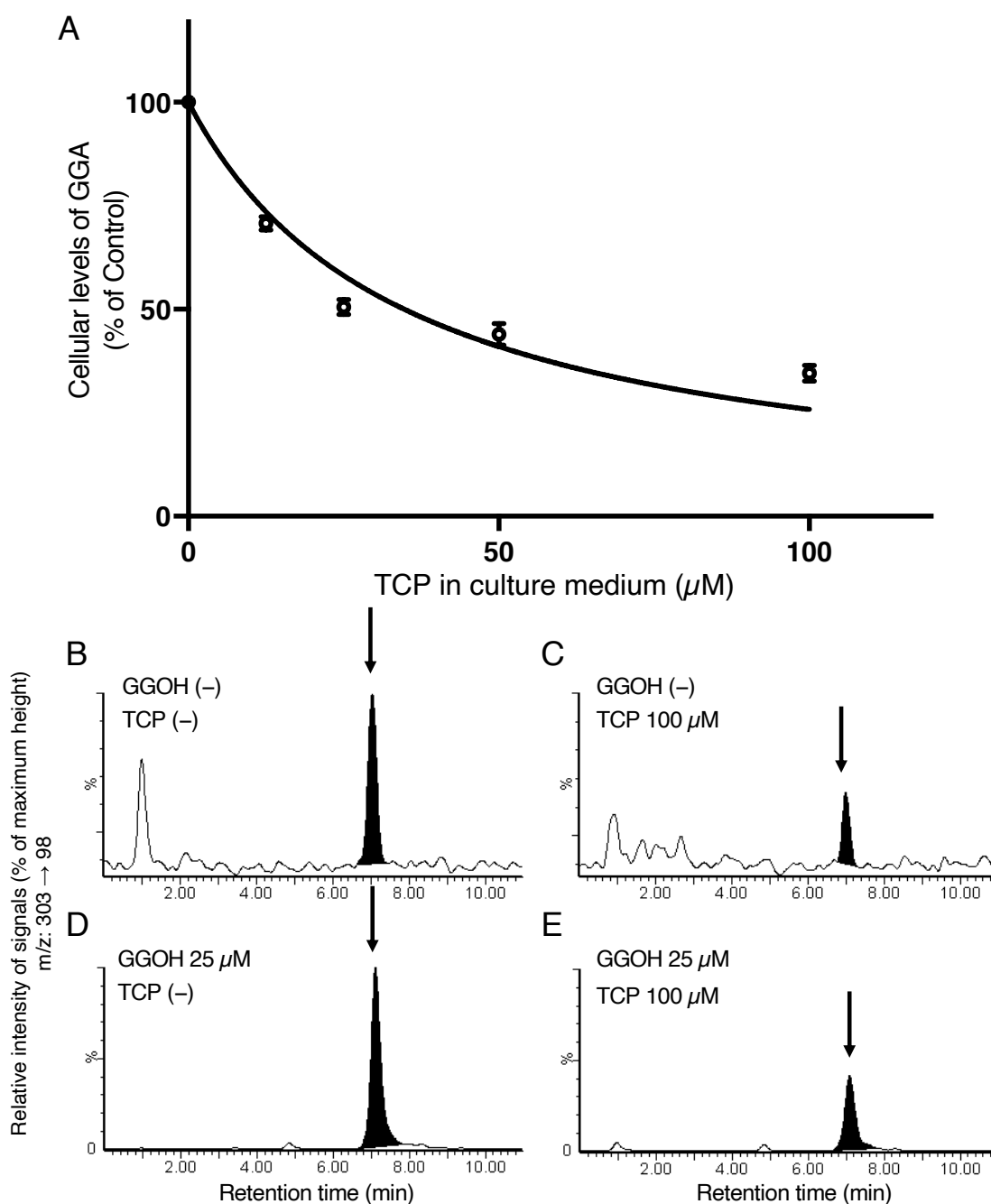


Figure 2-4. Tranilcypromine-induced downregulation of cellular GGA levels in HuH-7 cells.

(A) Dose-dependent changes of endogenous GGA in HuH-7 cells after treatment with 0-100 μM of TCP for 24 h. The amount of the intracellular GGA represents the mean ± SD of three measurements. IC₅₀ of TCP was obtained using GraphPad Prism 7.0.

(B-E) LC/MS/MS chromatograms of GGA in the lipid extracts from the nontreated control HuH-7 cells (B), the cells treated for 48 h with 100 μM TCP (C), with 25 μM GGOH (D) or the cells treated for 24 h with 25 μM GGOH after 24-h pretreatment with 100 μM TCP (E).

The arrows indicate the elution position of authentic GGA. The vertical axes of chromatograms show signal intensity of 85 as 100% (B and C), and 2,210 as 100% (D and E).

TCP, tranilcypromine; GGA, geranylgeranoic acid; ARA, arachidonic acid; LC/MS/MS, liquid chromatography mass spectrometry; GGOH, geranylgeraniol.

2-5. Downregulation of cellular GGA by MAOB siRNA

Even though TCP decreased the cellular level of both endogenous GGA and exogenous GGOH-derived GGA in HuH-7 cells, I cannot exclude a possibility that some other TCP-sensitive enzymes such as monoamine oxidase A (MAOA) and CYPs may be involved in biosynthesis of GGA. Therefore, I performed knockdown of the *MAOB* gene in HuH-7 cells using *MAOB* siRNA. The *MAOB* mRNA levels in HuH-7 cells transfected with *MAOB* siRNA were significantly decreased 72 h after the transfection (Fig. 2-5A), followed by a significant decrease in endogenous GGA at 120 h (*siCtrl* 8.95 ± 0.74 pmol/g; *siMAOB* 2.22 ± 0.18 pmol/g, $p < 0.05$, their representative LC/MS/MS chromatograms are shown in Fig. 2-5B).

Furthermore, the dramatic increase in the intracellular GGA level induced by the exogenous GGOH was significantly suppressed by *MAOB* knockdown (*siCtrl* 205.14 ± 7.36 pmol/g; *siMAOB* 77.19 ± 3.36 pmol/g, $p < 0.05$, see Fig. 2-5C). In addition, *MAOB* knockdown significantly suppressed the squalene synthase inhibitor zaragozic acid A (ZAA)-induced accumulation of endogenous GGA (*siCtrl* 44.23 ± 1.36 pmol/g; *siMAOB* 13.37 ± 2.14 pmol/g, $p < 0.05$, see Fig. 2-5D).

According to the literature, MAOA, prenylcysteine oxidase (*PCYOX1*) and ADH are potential enzymes that generate GGal, a direct precursor of GGA (Fig. 2-6A). Hence, here, I knocked down each gene encoding these enzymes and measured the amount of endogenous GGA. Although the transfection of *MAOA* siRNA, *PCYOX1* siRNA, or *ADH1A* siRNA significantly reduced each gene mRNA level compared to negative control siRNA 72 h after transfection (Fig. 2-6B, C and D). In contrast to the case of the *MAOB* knockdown (Fig. 2-5B), the cellular levels of endogenous GGA in HuH-7 cells were not decreased and unexpectedly increased in the *PCYOX1* siRNA-treated cells at 120 h (Fig. 2-6E). When the relative cellular level of *MAOB* mRNA in each siRNA-treated cell was examined, the *MAOB* expression level was significantly increased by *PCYOX1* siRNA treatment (Fig. 2-6F). When the intracellular levels of endogenous GGA were plotted against *MAOB* mRNA levels in these cells, a strong correlation was detected between endogenous GGA and *MAOB* mRNA levels ($r^2 = 0.8465$, Fig. 2-6G).

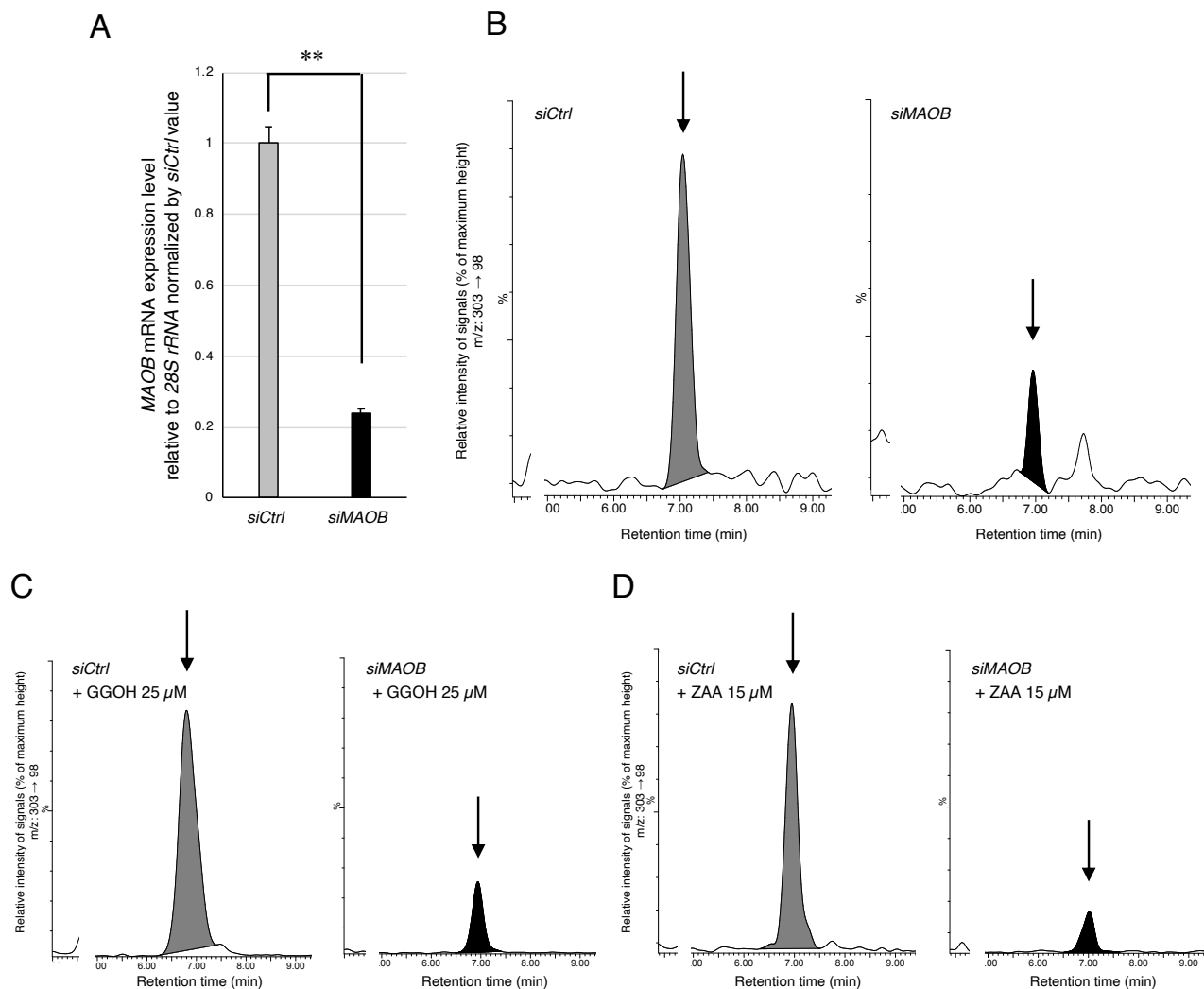


Figure 2-5. MAOB siRNA-induced downregulation of cellular GGA levels in HuH-7 cells.

A, Total RNA was prepared from HuH-7 cells after 72-h incubation with each siRNA to measure the cellular levels of MAOB mRNA by RT-qPCR. Each bar represents the mean \pm SE ($n = 3$). B, C, and D, LC/MS/MS chromatograms of GGA in the lipid extract from each sample treated as described as follows. After HuH-7 cells incubated with each siRNA for 96 h, the cells were incubated for another 24 h in the absence (B) or presence of 25 μ M GGOH (C) or 15 μ M ZAA (D).

The arrows indicated the elution position of authentic GGA. The vertical axes of the chromatograms show of 60 as 100% (B), 1460 as 100% (C) and 246 as 100% (D).

** $, p < 0.01$ compared with control (*siCtrl*).

MAOB, monoamine oxidase B; siRNA, small interfering RNA; GGA, geranylgeranoic acid; LC/MS/MS, liquid chromatography mass spectrometry; GGOH, geranylgeraniol; ZAA, zaragozic acid A.

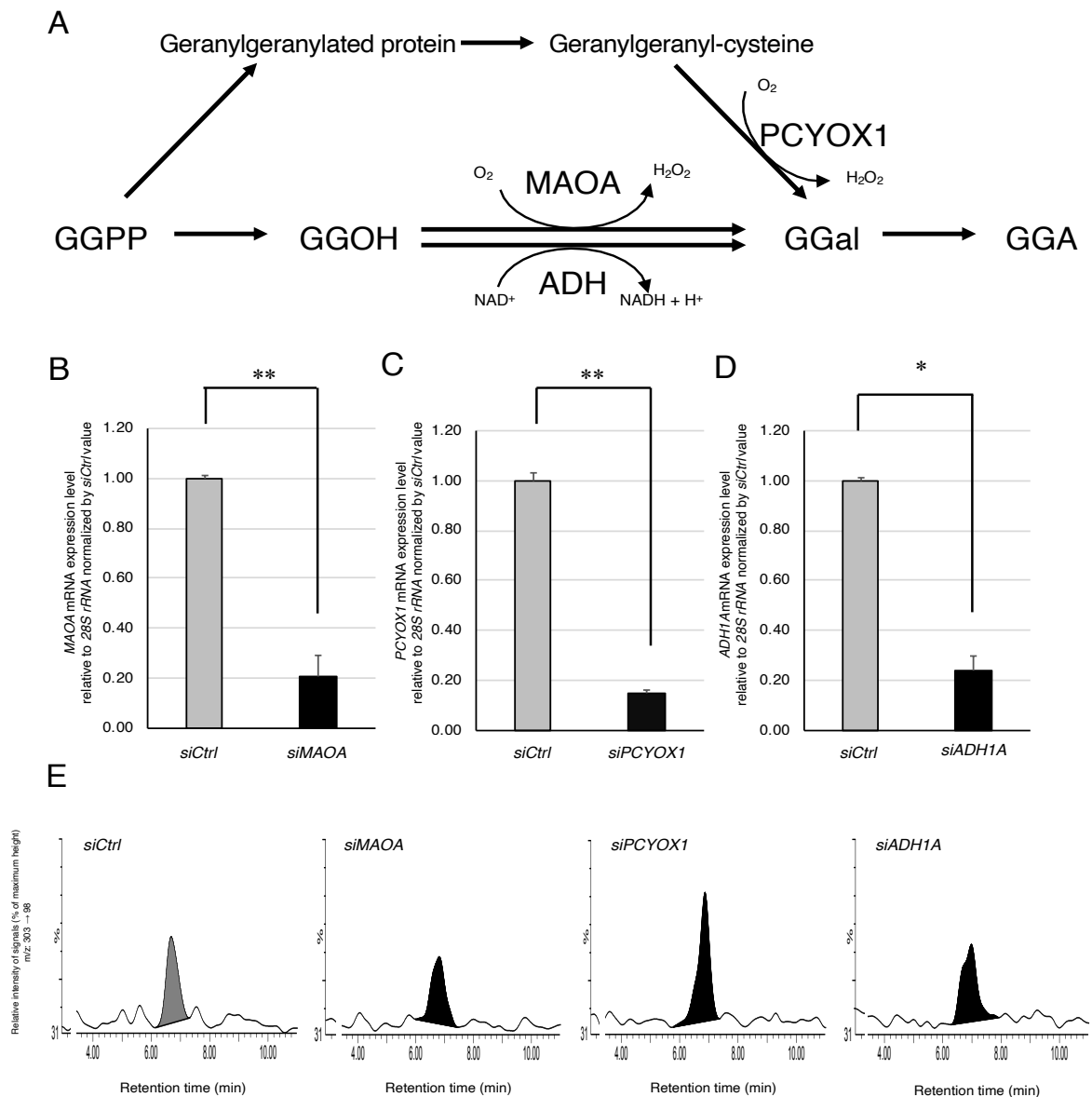


Figure 2-6. Knockdown of *MAOA*, *PCYOX1*, and *ADH1A* genes using each siRNA in HuH-7 cells does not induce a decrease in endogenous GGA level.

(A) According to the literature, possible metabolic pathways to produce GGA are depicted besides oxidation of GGOH to GGal catalyzed by MAOB.

(B, C and D) Total RNA was prepared after HuH-7 cells were incubated with each siRNA for 72 h to measure the cellular levels of *MAOA*, *PCYOX1* and *ADH1A* mRNA by RT-qPCR, respectively. Each bar represents the mean \pm SE (n = 3).

(E), LC/MS/MS chromatograms of GGA in the lipid extract from HuH-7 cells incubated with control siRNA (*siCtrl*), *MAOA* siRNA (*siMAOA*), *PCYOX1* siRNA (*siPCYOX1*), or *ADH1A* siRNA (*siADH1A*) for 120 h. The chromatograms show a peak height of 58 as 100% (*siCtrl*, *siMAOA*, *siADH1A*), and 84 as 100% (*siPCYOX1*).

(F) The expression level of *MAOB* mRNA in HuH-7 cells knocked down with each siRNA.

(G) Correlation between *MAOB* mRNA expression level and intracellular GGA level in HuH-7 cells knocked down with each siRNA.

*, $p < 0.05$ compared with control (*siCtrl*). **, $p < 0.01$ compared with control (*siCtrl*) (t-test).

GGPP, geranylgeranyl diphosphate; GGOH, geranylgeraniol; GGal, geranylgeranial; GGA, geranylgeranoic acid; MAOA, monoamine oxidase A; PCYOX1, prenylcysteine oxidase 1; ADH1A, alcohol dehydrogenase 1A; NAD, nicotinamide adenine dinucleotide; siRNA, small interfering RNA; MAOB, monoamine oxidase B.

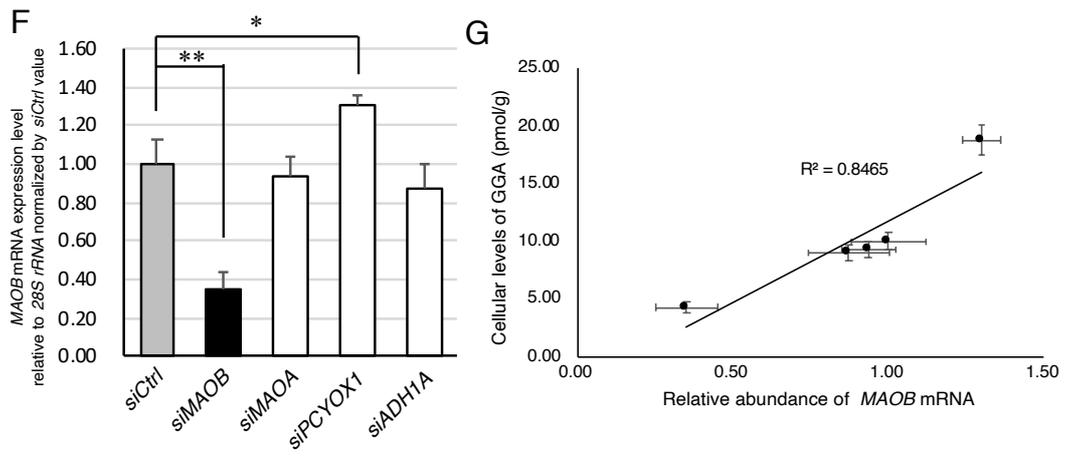


Fig. 2-6 Continued.

2-6. Catalytic activity of recombinant human MAOB in oxidation of GGOH to GGal

Since the results so far obtained in the present study strongly indicate that MAOB enzyme may be involved in GGA biosynthesis, I next decided to examine whether recombinant human MAOB protein is able to catalyze oxidation reaction of acyclic isoprenols with increasing isoprene unit from 2 to 4 to produce the corresponding aldehydes. As a result, MAOB had no ability to oxidize geraniol (GOH, C₁₀-acyclic monoterpene), Fig. 2-7A), but undoubtedly produced farnesal (Fal, Fig. 2-7B) from farnesol (FOH, C₁₅-acyclic sesquiterpene) and GGal (Fig. 2-7C) from GGOH (C₂₀-acyclic diterpene). Then, kinetic analysis using increasing concentrations of GGOH or FOH as a substrate was performed. As shown in Fig. 2-7D, a reaction that oxidizes GGOH to GGal showed a Michaelis-Menten-type kinetics (Fig. 2-7D) and the *K_m* value of the recombinant human MAOB was calculated to be $34.34 \pm 5.35 \mu\text{M}$ for GGOH, which is in the range of those of rat hepatic (36) and human hepatoma GGOH oxidase (37). The kinetic analysis also tells that the *K_m* value was $35.22 \pm 7.77 \mu\text{M}$ for FOH, which is established to competitively inhibit MAOB activity in previous studies (51–53). Although the same amount of the recombinant protein was used in enzyme assay, *V_{max}* was calculated to be $72.51 \pm 6.87 \text{ pmol/h}$ for FOH and $102.2 \pm 6.77 \text{ pmol/h}$ for GGOH (Fig. 2-7D), indicating that the turnover number should be 1.4-times greater for GGOH than for FOH.

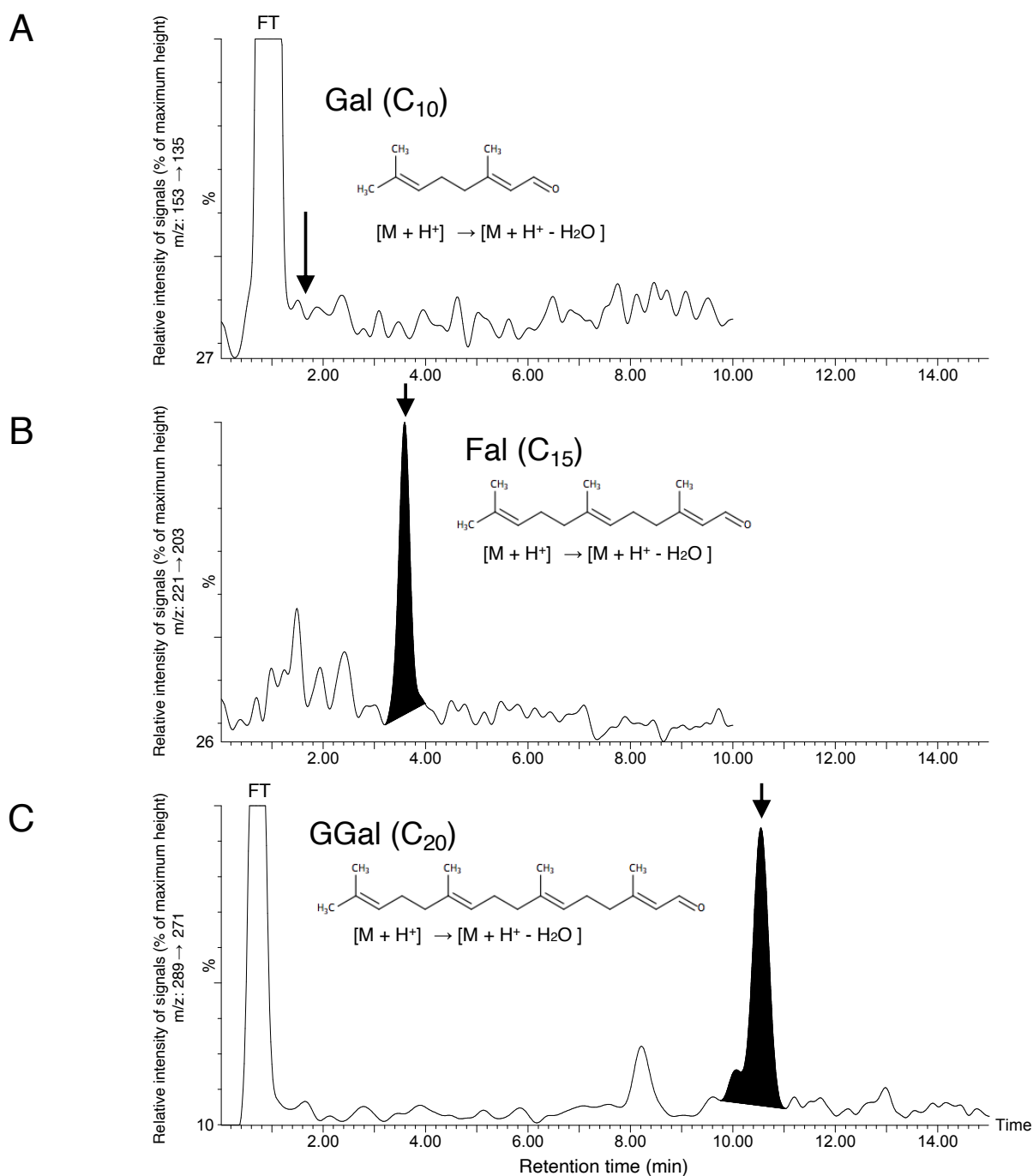


Figure 2-7. Recombinant human MAOB catalyzes oxidation of GGOH and FOH to GGal and Fal, respectively. LC/MS/MS elution profiles of ethanol extracts after 1-h incubation of the recombinant MAOB at 37°C with 25 μM GOH, detecting a signal of geranial (m/z(+) 153–135) (A), 25 μM FOH, detecting a signal of Fal (m/z(+) 221–203) (B) or 25 μM GGOH, detecting a signal of GGal (m/z(+) 289–271) (C). The elution position of authentic corresponding aldehydes was indicated by arrows. (D). The increasing concentrations of GGOH or FOH were incubated with the recombinant MAOB protein (0.15 μg) at 37°C for 1 h. Amounts of GGal or Fal products were measured by LC/MS/MS analysis. Values of K_m were obtained by fitting to plots of amounts of GGal or Fal products versus GGOH or FOH concentration, respectively, using GraphPad prism 7.0. Each point represents the mean ± SD (n = 3). FT is the flow through.

MAOB, monoamine oxidase B; GGOH, geranylgeraniol; FOH, farnesol; GGal, geranylgeranial; Fal, farnesal; LC/MS/MS, liquid chromatography mass spectrometry; GOH, geraniol; Gal, geranial.

D

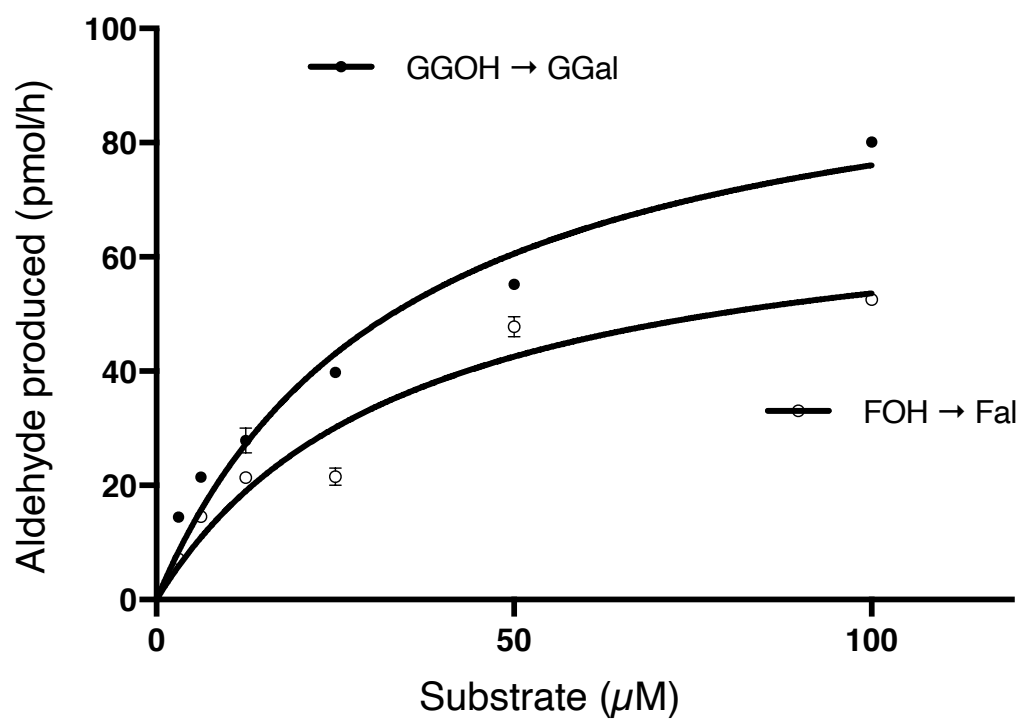


Fig. 2-7 Continued.

2-7. *MAOB* gene knockout by CRISPR-Cas9/HDR system and the resultant cellular endogenous GGA changes.

From the above results, I was convinced that *MAOB* is at least partly involved in GGA biosynthesis in HuH-7 cells. However, the above knockdown experiments show transient changes, so I next attempted to induce stable depletion of endogenous GGA in human hepatoma cells by establishing *MAOB* knockout cell clones using the CRISPR-Cas9/HDR system. Since *MAOB* knockout cells could not be established in HuH-7 cells by puromycin selection after several trials, another human hepatoma-derived cell line, Hep3B, that does not harbor any translocation in the X chromosome was used, because the *MAOB* gene is located on the X chromosome. A puromycin-resistant clone of Hep3B was successfully obtained and it dramatically reduced *MAOB* expression at both the mRNA and protein levels (Fig. 2-8A and B). However, unexpectedly, the endogenous GGA of the knockout cells (Hep3B/*MAOB*-KO) did not decrease at all compared to the wild-type Hep3B cells (Hep3B/*MAOB*-WT) (Fig. 2-8C).

In order to exclude a possibility that *MAOB* siRNA-induced reduction of endogenous GGA level in HuH-7 cells may be due to its off-target effect, I conducted further knockdown experiments by the *MAOB* siRNA in Hep3B/*MAOB*-KO and Hep3B/*MAOB*-WT. The *MAOB* siRNA induced a significant decrease in *MAOB* mRNA levels followed by a significant decrease of the intracellular GGA also in Hep3B/*MAOB*-WT. On the other hand, the *MAOB* siRNA did not further suppress the cellular *MAOB* mRNA level that was hardly expressed in the knockout cells (Fig. 2-8D), nor did it cause a decrease in endogenous GGA of Hep3B/*MAOB*-KO (Fig. 2-8E), suggesting that the *MAOB* siRNA-induced reduction of endogenous GGA may not be due to its off-target effect in both HuH-7 and Hep3B cells. Next, in order to investigate another possibility that metabolic redundancy of GGA biosynthesis by other enzyme(s) may be evoked in the Hep3B/*MAOB*-KO cells, I conducted further knockdown experiments by each siRNA of some potential enzymes (shown in Fig. 2-6A) that may produce GGal in Hep3B/*MAOB*-KO and Hep3B/*MAOB*-WT. As for other enzymes potentially involved in GGA biosynthesis, efficient knockdown of each gene did not cause

any decrease in endogenous GGA either in Hep3B/*MAOB*-WT or Hep3B/*MAOB*-KO (Fig. 2-9).

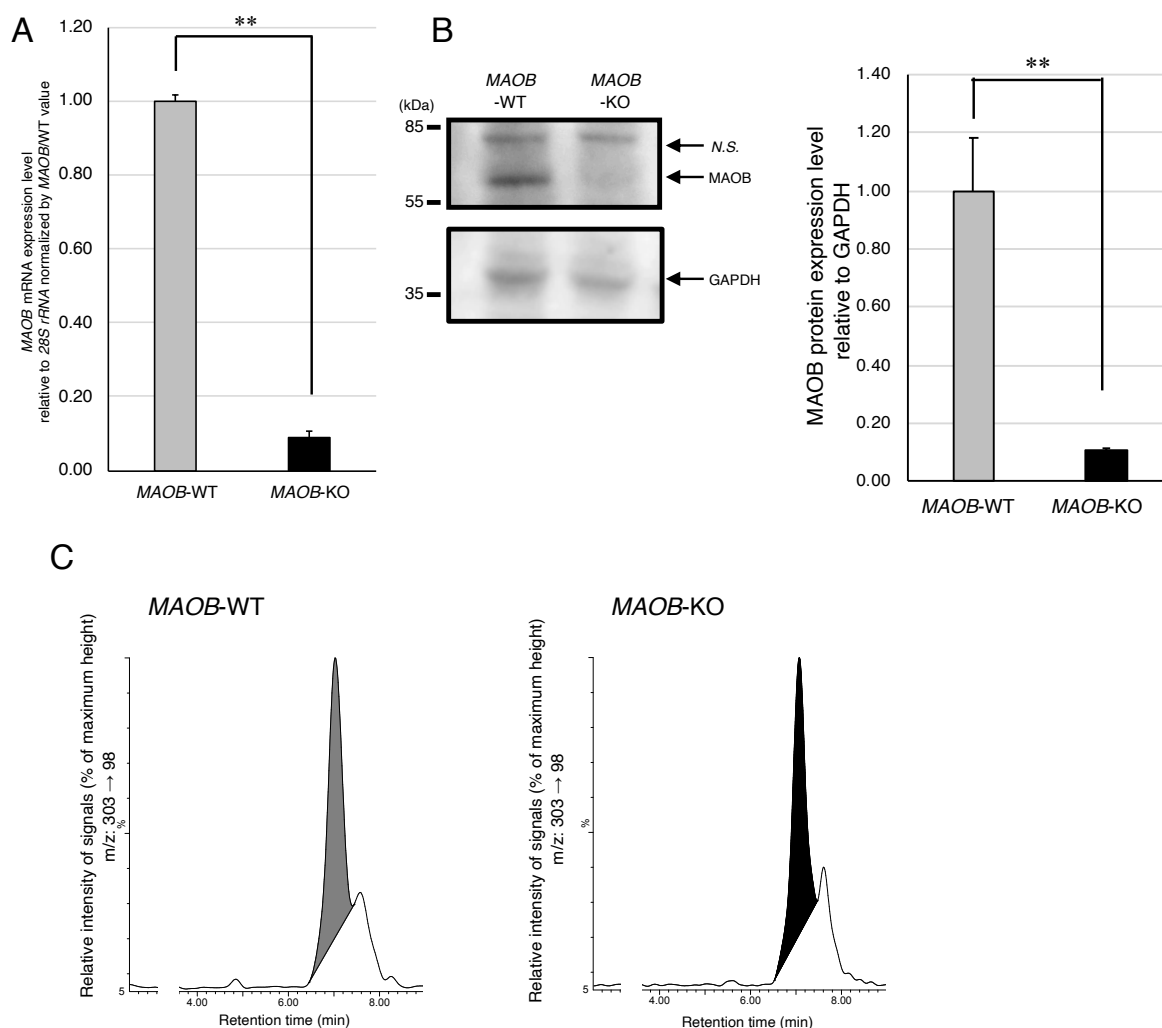


Figure 2-8. The endogenous GGA in Hep3B/MAOB-KO cells lose MAOB sensitivity.

(A) *MAOB* mRNA expression level in *MAOB* knockout cells and wild type cells established by the CRISPR-Cas9/HDR system. Each bar represents the mean \pm SE (n = 3).

(B) Total cell lysates of Hep3B *MAOB*-WT cells and Hep3B *MAOB*-KO cells were analyzed by Western blotting to measure the level of MAOB.

(C) LC/MS/MS chromatograms of the lipid extract from Hep3B/*MAOB*-WT and Hep3B/*MAOB*-KO.

(D) The relative expression level of *MAOB* mRNA to that of *siCtrl*-treated Hep3B/*MAOB*-WT cells upon *MAOB* siRNA treatment in Hep3B/*MAOB*-WT or Hep3B/*MAOB*-KO.

Each bar represents the mean \pm SE (n = 3).

(E) The endogenous GGA level of the lipid extract from Hep3B/*MAOB*-WT or Hep3B/*MAOB*-KO after incubation with *MAOB* siRNA for 120 h. The amount of the intracellular GGA represents the mean \pm SD of three measurements.

*, $p < 0.05$ compared with control (Hep3B/*MAOB*-WT *siCtrl*).

**, $p < 0.01$ compared with control (Hep3B/*MAOB*-WT *siCtrl*).

N.S. is a non-specific band.

GGA, geranylgeranoic acid; MAOB, monoamine oxidase B; GAPDH, glyceraldehyde-3-phosphate dehydrogenase; CRISPR-Cas9/HDR, Clustered Regularly Interspaced Short Palindromic Repeats CRISPR-Associated proteins 9/homology directed repair; LC/MS/MS, liquid chromatography mass spectrometry; siRNA, small interfering RNA.

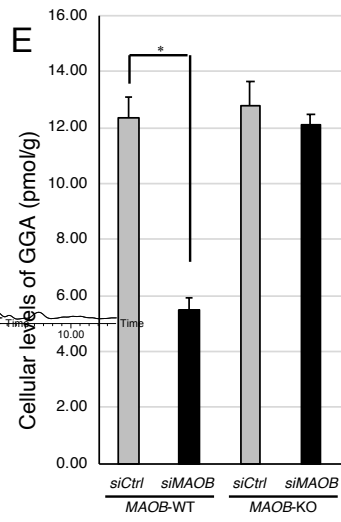
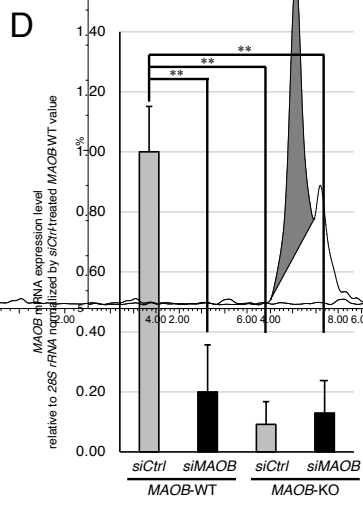


Fig. 2-8 Continued.

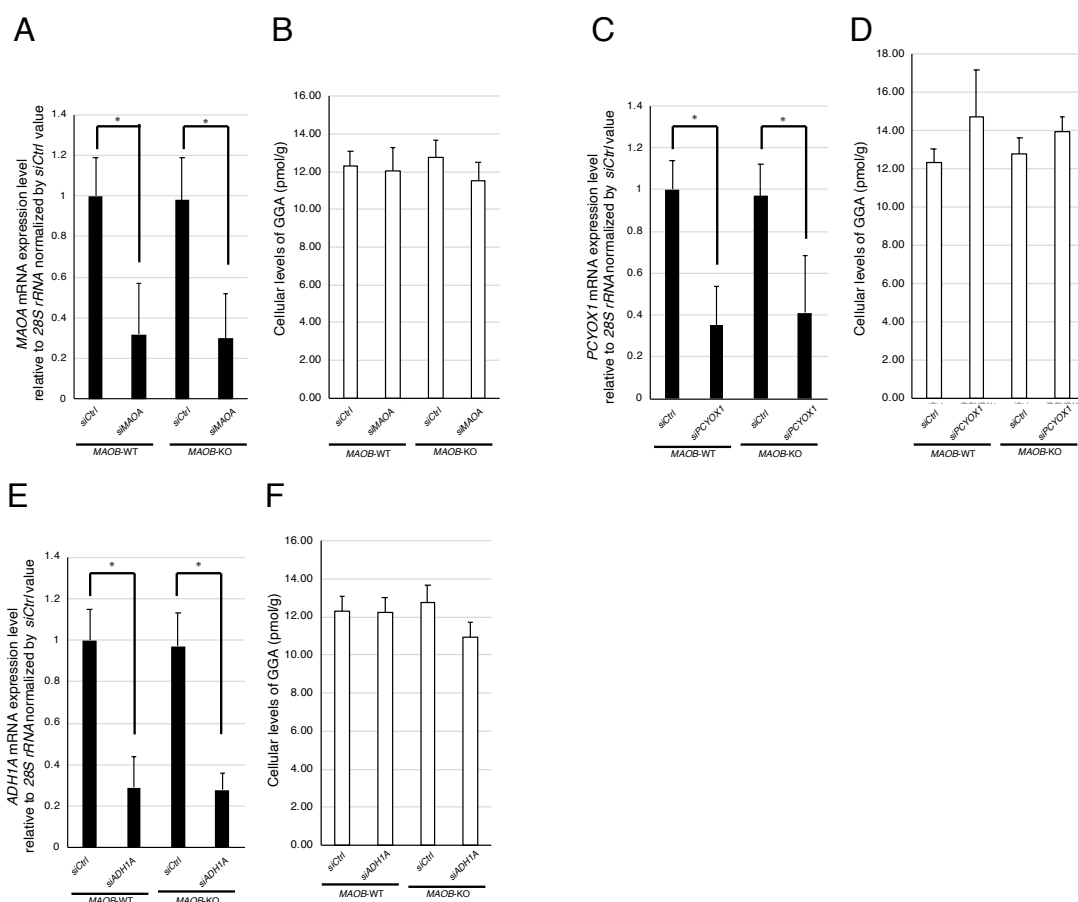


Figure 2-9. Knockdown of *MAOA*, *PCYOX1*, and *ADH1A* using siRNA in Hep3B/*MAOB*-KO cells does not induce a decrease in endogenous GGA.

The relative expression level of each target mRNA upon (A), *MAOA* siRNA, (C), *PCYOX1* siRNA and (E), *ADH1A* siRNA treatment in Hep3B/*MAOB*-WT cells or Hep3B/*MAOB*-KO cells. Each bar represents the mean \pm SE (n = 3). The endogenous GGA level of the lipid extract from Hep3B/*MAOB*-WT cells or Hep3B/*MAOB*-KO cells incubated with (B), *MAOA* siRNA, (D), *PCYOX1* siRNA and (F), *ADH1A* siRNA for 120 h.

The amount of intracellular GGA represents the mean \pm SD of three measurements.

*, $p < 0.05$ compared with control (siCtrl). (ANOVA with post hoc Scheffe).

MAOA, monoamine oxidase A; PCYOX1, prenylcysteine oxidase 1; ADH1A, alcohol dehydrogenase 1A; siRNA, small interfering RNA; MAOB, monoamine oxidase B; GGA, geranylgeranoic acid.

2-8. Back-transfection of the *MAOB* gene into *MAOB* knockout cells restores the *MAOB* dependence of intracellular GGA.

Finally, in order to understand how tightly the *MAOB* gene is linked to metabolic maintenance of the intracellular level of endogenous GGA, Hep3B/*MAOB*-KO/TG cells were established by transfecting Hep3B/*MAOB*-KO with *MAOB* gene expression plasmid. The back-transfection of the *MAOB* gene into the knockout cells restored *MAOB* protein level in the knockout cells to the level of the wild type cells (Fig. 2-10A), in accordance with the cellular *MAOB* mRNA levels (Fig. 2-10B). Knockdown of the transgenic *MAOB* gene in Hep3B/*MAOB*-KO/TG cells with the *MAOB* siRNA significantly reduced the cellular level of *MAOB* mRNA level (Fig. 2-10B) as well as the endogenous GGA level (Fig. 2-10C). Regarding the nature of wild-type cells (*MAOB*-WT) that *MAOB* siRNA reduces intracellular GGA content, the knockout cells (*MAOB*-KO) were rescued to the same extent as wild-type cells by back-transfection of the *MAOB* gene into the knockout cells (*MAOB*-KO/TG), as clearly illustrated in Fig. 2-10D.

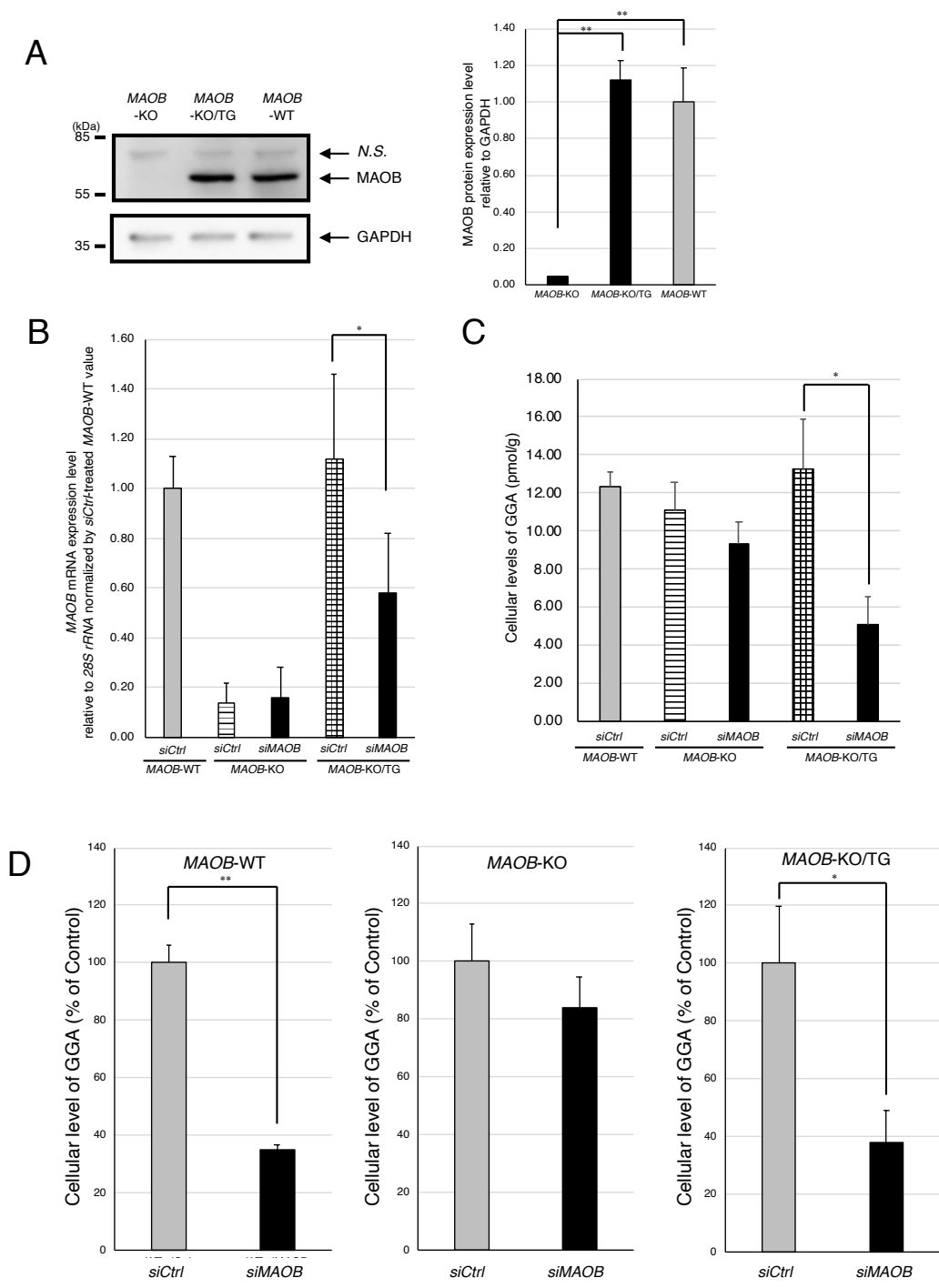


Figure 2-10. Rescue of MAOB siRNA sensitivity of the cellular GGA level in Hep3B/MAOB-KO cells by transgenic MAOB expression.

(A) and (B), Total cell lysates of Hep3B/MAOB-KO, Hep3B/MAOB-KO/TG and Hep3B/MAOB-WT were analyzed by Western blotting with anti-MAOB antibody. GAPDH was analyzed as a loading control. (C), The relative expression level of MAOB mRNA upon MAOB siRNA treatment in Hep3B/MAOB-WT, Hep3B/MAOB-KO or Hep3B/MAOB-KO/TG. (D), The endogenous GGA level in the lipid extract from Hep3B/MAOB-WT, Hep3B/MAOB-KO, or Hep3B/MAOB-KO/TG incubated with MAOB siRNA for 120 h. (E), Changes in intracellular GGA level by MAOB siRNA treatment in Hep3B/MAOB-WT, Hep3B/MAOB-KO or Hep3B/MAOB-KO/TG. The amount of intracellular GGA represents the mean \pm SD of three measurements. *, $p < 0.05$ compared with control. **, $p < 0.01$ compared with control (ANOVA with post hoc Scheffe).

GGA, geranylgeranoic acid; MAOB, monoamine oxidase B, GAPDH, glyceraldehyde-3-phosphate dehydrogenase.

2-9. Discussion

In chapter 2, first, I demonstrated endogenous free GGA in mammalian cells. Endogenous free GGA was definitely present at high levels in various tissues of 5-week-old male Wistar rats, especially in the liver. Given that the liver is an active organ for cholesterol synthesis in mammals and GGA may be biosynthesized from MVA through FPP and GGPP, it can be reasonably considered that the endogenous GGA concentration must be high in the rat liver. Indeed, the highest concentration of endogenous GGA was observed in the liver of male Wistar rats; its concentration is about 80 nM, which is relatively higher than the level of that in human hepatoma-derived HuH-7 cells [10–15 nM (37)], but is much lower than the concentrations [5–20 μ M (29)] inducing cell death in human hepatoma-derived HuH-7 cells. Regarding tissues tested herein other than liver, it is worth mentioning that the GGA concentrations in the testis, prostate and epididymis (especially in the caput) of male Wistar rats were relatively high among all tissues tested in the present study. Before the observations of the present study, I have coincidentally found that, when compared with a commercially available breeding feed relatively rich in DHA and EPA, a GGA supplemented diet increased the reproductive index (RI; the number of weaning mice divided by the number of mated couples) of senescence-accelerated SAM mice (54). Hence, I speculate that endogenously synthesized GGA may play an important role at least in male reproductive organs. Another noteworthy point about tissue distribution is that 2,3-dihydroGGA, which is considered to be a further metabolite of GGA, is distributed at the highest level in the thymus gland. As mentioned above, Kodaira et al reported that 2,3-dihydroGGA was a major metabolite from exogenous GGOH or GGal, presumably via GGA in the primary culture of rat thymocyte (48). In the present study, I also found that a molar ratio of 2,3-dihydroGGA to GGA was extremely high in the thymus, whereas it was the lowest in the liver (Fig. 2-1D and Table 2-1). This suggested that conversion rate from GGA to 2,3-dihydroGGA is very fast and 2,3-dihydroGGA may play a specific role in thymocytes, which should also be explored in the future. As the concentration of endogenous GGA and 2,3-dihydroGGA in blood and adipose tissue was extremely low, I can exclude the possibility that GGA and 2,3-dihydroGGA observed in the above-mentioned organs

might be contaminated with blood GGA.

Next, I provide concrete evidence that hepatic MAOB is involved in the biosynthesis of GGA, which has been expected to prevent hepatocarcinogenesis.

Shidoji's group have provided several lines of evidence for the possibility that MAOB may catalyze the oxidation of GGOH to GGal (36, 37). The reason why I started thinking that "monoamine oxidase" might be involved in the oxidation of amine-free GGOH, a 20-carbon acyclic isoprenol, is that FOH, a 15-carbon acyclic isoprenol in tobacco smoke, has been identified as a selective inhibitor against MAOB (51–53). X-ray crystallography illustrates that FOH is inserted into the substrate-binding pocket of MAOB and is close to the cofactor flavin adenine dinucleotide (FAD) site and these authors described "if the bound *trans,trans*-farnesol is considered as a substrate mimic, these structural data provide support for the polar nucleophilic mechanism" (51). Hence, I hypothesized that GGOH is one isoprene unit longer than FOH, so that the α -CH bond of GGOH and FAD will be closer than the 3.4 Å-distance between the α -CH bond of FOH and FAD attached to MAOB, and such a topological speculation would predict the α -CH of GGOH to be oxidized and converted to GGal by the proposed polar nucleophilic attack mechanism (51). I have previously reported that recombinant hMAOB protein definitely oxidized GGOH to GGal and the activity was inhibited by TCP, an inhibitor of MAO, and the same thing was true with mitochondrial fractions of HuH-7 cells as enzyme sources (37).

In this study, I decided to show that MAOB enzyme activity is involved in the oxidation reaction from GGOH to GGal using cell culture systems. I first tested whether TCP of MAO inhibitor can inhibit the GGA biosynthetic pathway in a cell-culture system. As mentioned in section 2-4, TCP induced dose-dependent downregulation of endogenous GGA content in HuH-7 cells with IC_{50} of 33 μ M (Fig. 2-4A). However, the cellular GGA was not completely depleted by TCP treatment even at 100 μ M (Fig. 2-4B and C) and over 50 μ M the changes in the cellular GGA amount became marginal. Hence, I supposed that some part (roughly 40%) of endogenous GGA might be produced by other enzymes than MAOB. After subtraction of this value, the IC_{50} of TCP is recalculated to be 10.7 μ M, which is in the range of the IC_{50} of TCP for MAOB enzyme

activity (7.0 μM)(55). It is interesting that the similar proportion of the cellular GGA from exogenous GGOH remained after 100 μM TCP treatment (Fig. 2-4D and E). These results indicate that TCP-sensitive enzymes are partly involved in the oxidation of GGOH to GGal to produce the cellular GGA, but I cannot yet conclude TCP-sensitive enzyme is MAOB. Because, TCP-sensitive enzymes include MAOA ($\text{IC}_{50} = 11.5 \mu\text{M}$) (55), CYP2A6 (0.42 μM) (56), and CYP2E1 (3.0 μM) (56) other than MAOB.

The next knockdown experiment provided more strong evidence that the *MAOB* gene is mainly responsible for maintenance of the cellular GGA level in HuH-7 cells. In other words, *MAOB* siRNA-mediated downregulation caused more than 80% reduction of not only endogenous GGA level but also intracellular GGA levels upregulated by either ZAA or exogenous GGOH (Fig. 2-5), suggesting the greater part of the cellular GGA were produced through MAOB-mediated process. Nevertheless, I still see a certain amount of GGA still remained in the cells after the downregulation of the *MAOB* gene.

In the literature (9,11,20,21), several enzymes other than MAOB are reported to be able to produce GGal (Fig. 2-6A), however, knockdown of these genes did not change the intracellular GGA (Fig. 2-6B-E), except that the knockdown of the *PCYOX1* gene significantly and inversely upregulated the GGA level. Although I was able to show how the downregulation of *PCYOX1* gene expression is linked to the upregulation of the cellular GGA level, at present I have no idea how the downregulation of the *PCYOX1* gene resulted in the upregulation of *MAOB* gene expression (Fig. 2-6F). Anyhow, the cellular levels of endogenous GGA are significantly correlated with the expression levels of the *MAOB* gene in any knocked-down cells (Fig. 2-6G).

Now, I am quite confident that MAOB is one of putative enzymes responsible for biosynthesis of GGA in human hepatoma cells. Then, using LC/MS/MS technique I confirmed previous findings that recombinant human MAOB is active to oxidize GGOH (acyclic C₂₀-isoprenol) to GGal (37). This time, I provide additional evidence that MAOB catalyzes oxidation reaction of acyclic isoprenol by showing FOH (acyclic C₁₅-isoprenol) as an additional substrate, but GOH (acyclic C₁₀-isoprenol) was not oxidized to geranial. Taking account that recombinant human MAOA did not oxidize GGOH (37), I suggest that the recombinant

human MAOB recognizes FOH and GGOH as a specific substrate and catalyzes oxidation reaction. As for other acyclic isoprenols longer than GGOH, I have never tried to use them as substrate for MAOB.

At third, I knocked out *MAOB* in the hepatoma cell and attempted to deplete intracellular GGA, but I failed to deplete it by the knockout method. The *MAOB*-knockout Hep3B (Hep3B/*MAOB*-KO) cells established by CRISPR-Cas9/HDR system, drastically reduced both mRNA and protein levels of the *MAOB* gene, as expected. However, the amount of endogenous GGA content in Hep3B/*MAOB*-KO cells was unexpectedly not reduced, which is apparently inconsistent with the *MAOB*-knockdown-mediated reduction of the endogenous GGA level in HuH-7 cells. Thus, I considered three possibilities, as follows: 1) Hep3B cells may produce endogenous GGA by other enzyme(s) than MAOB, different from HuH-7 cells. 2) The decrease in endogenous GGA content in HuH-7 cells by *MAOB* siRNA may be due to off-target effect. 3) When the *MAOB* gene is knocked out, other GGal-producing enzymes may be upregulated instead of MAOB and this putative compensatory mechanism may have helped maintain the original GGA level in Hep3B/*MAOB*-KO cells.

Among 3 possibilities described above, the first possibility was immediately excluded, since introduction of *MAOB* siRNA significantly reduced intracellular GGA level in Hep3B/*MAOB*-WT to the same extent as in HuH-7 cells. On the other hand, *MAOB*-siRNA-treated Hep3B/*MAOB*-KO cells did not change the amount of intracellular GGA, implying that there are no off-targets other than the *MAOB* gene of *MAOB* siRNA used in the present study to deny the second possibility. Finally, in order to verify the third possibility, I knocked down the other GGal-producing *ADH1A* and *PCYOX1* genes or the *MAOA* gene in Hep3B/*MAOB*-KO cells, but I found no change in the cellular GGA content of the knockout cells (Fig. 2-9). At present, a compensatory mechanism for maintaining the GGA concentration in the knockout cells has not been proved, but enzymes of the CYP family are under investigation on the premise that there is a compensatory mechanism.

The last question arose in this context; may MAOB be no longer needed for GGA biosynthesis once compensatory mechanisms begin to work? Or which is dominant in GGA biosynthesis, MAOB or

compensatory mechanism(s)? To answer this question, I performed back-transfection of the *MAOB* gene into Hep3B/*MAOB*-KO cells to make Hep3B/*MAOB*-KO/TG cells. As a result, although Hep3B/*MAOB*-KO/TG cells showed no change in the intracellular GGA content compared to Hep3B wild type cells and *MAOB*-knockout cells, the *MAOB*-siRNA-mediated knockdown of the transgenic *MAOB* significantly reduced intracellular GGA levels in Hep3B/*MAOB*-KO/TG, which means the back-transfection of the *MAOB* gene completely rescued the knockout cells from *MAOB*-siRNA insensitivities of endogenous GGA (Fig. 2-10D). From these results, I can conclude that MAOB-mediated metabolic pathway is primary process to maintain the cellular GGA level in human hepatoma cells. Although it was not possible to identify a putative compensatory enzyme in this study, it is absolutely essential to prove it in the future to establish GGA biosynthesis. Whatever compensatory enzyme works instead of MAOB, it is of note that the existence of a putative maintenance mechanism of the cellular level of endogenous GGA in the *MAOB*-knockout cells suggests that GGA may be an essential metabolite having an important function for cell life other than cell death induction in malignant cells. Indeed, Shidoji's group observed another biological function of GGA not in malignant cells, that is, dietary supplement with GGA during mating period significantly improved reproduction index (RI) in SAM P1 mice (54).

In conclusion, here, I show that MAOB is principally involved in GGA biosynthesis through oxidation of GGOH in human hepatoma cells. MAOB has been established to be involved in the degradation of catecholamines in the brain (57), and the hepatic-MAOB function was speculated to work in the degradation of amine-containing xenobiotics in bulk, despite its high expression level. The present study clearly demonstrates that hepatic MAOB has a completely new metabolically role that has not been so far reported, in the biosynthesis of GGA, a biologically active lipid. Therefore, I propose with confidence that hepatic MAOB can be called "GGOH oxidase".

Chapter 3.

Supplementation with geranylgeranoic acid during mating, pregnancy and lactation improves reproduction index in C3H/HeN mice

Abstract

GGA, an acyclic retinoid of diterpenoid, is a natural compound found in some medicinal herbs such as turmeric. The previous study, Shidoji et al demonstrated that oral supplementation of GGA during mating, pregnancy and lactation periods significantly increased the reproductive index (RI; the number of weaning pups divided by the number of mated couples) of AKR/J strain of mouse by 3 times compared to the non-supplemented control group. Here, I carried out the following experiments to confirm the GGA-mediated improvement of the RI by using C3H/HeN mice. At first, the mice were divided into 2 groups fed on either a commercial chow diet or supplemented with GGA (50 µg/day) during a whole reproduction period. As a result, GGA supplementation increased the RI by 1.60 ± 0.50 times compared to the control group. When the mice were supplemented with GGA only after mating (GGA was supplied only for pregnancy period, or only for gestation period), their pregnancy rate declined. However, these two groups showed that their RIs were both higher than the control group, indicating that GGA supplementation helps to secure healthy pups after conception. Taken together with previous finding, the present results strongly suggested that dietary supplementation of GGA during mating, gestational and lactating periods has potential to upregulate RI in mammals.

3-1. Introduction

In the field of animal breeding such as pet breeder and livestock industries, improvement of reproduction index (RI; the number of weaning animals divided by the number of mated couples) is a principal issue. For improvement of RI, it is essential not only to increase the pregnancy/birth rate, but also to promote the health of mothers and babies after delivery. Improvement by diet is highly recommended rather than by drugs for this purpose. In general, it has been recognized that supplementations with n-3 polyunsaturated fatty acids (PUFAs) such as DHA and EPA and fat-soluble vitamins such as vitamin A, vitamin D and vitamin E are effective in breeding diet in mammals including dogs and cats (58), cows (59), horses (60), rats (61) and mice (62). The effectiveness of n-3 PUFAs and fat-soluble vitamins in the fertility has been observed indeed in several studies. For example, it has been reported that DHA and vitamin E can protect sperm from ROS-mediated damages and improve sperm motility in some animals and humans (63–66). Furthermore, it is suggested that ingestion of DHA improves embryo morphology (67). Other fat-soluble vitamins D and A have been also reported to play important role(s) in maintaining the function of ovary, testis and sperm in animals and humans (68–72).

GGA (all-*trans* 3,7,11,15-tetramethyl-2,6,10,14-hexadecatetraenoic acid), polyunsaturated branched-chain fatty acid, was originally developed as a preventive agent against hepatoma (19, 21, 22). GGA has been called as one of "acyclic retinoids" because it acts on nuclear retinoid receptors to exhibit antitumor activity like retinoids (30). Thereafter, it has reported that it is a natural nutrient present in some herbs such as turmeric and licorice (33). Furthermore, in chapter 2, I found that endogenous GGA was also present in various organs of male Wistar rats, particularly higher in liver, brain and male reproductive organs than other organs (73).

During previous studies on GGA, this laboratory coincidentally found that ingesting GGA during the mating, gestational and lactating periods increased the RI of senescence-accelerated SAM mice (54). I focused that GGA might be involved in the improvement of RI as one of the physiological roles other than the

cancer-preventive effect of GGA. Although improvement of the RI by GGA intake has been demonstrated in SAM mice, I am not sure whether it is effective also in other strains of mice or other mammalian species. Therefore, I decided to perform the same previous study confirming the reproducibility in other strains of mouse. This is because SAM mice, which are age-related disease models, may have different effects of GGA on fertility than other common mouse strains. Here, I have selected the C3H/HeN mouse as a common mouse strain.

3-2. GGA-induced improvement of RI in C3H/HeN mice

As shown in Table 3-1, the data of Experiment I show that there was no significant difference in both pregnant/birth rate and litter size between the control and the GGA intake groups. However, the WR significantly increased in the GGA intake group, as compared with the control group ($p < 0.001$). As a result, the data of Experiment I clearly indicated that supplementation with GGA during a whole reproduction period increased the RI from 3.67 to 5.00 in C3H/HeN mice. In experiment I, the survival curves of the pups in the control group clearly show that more than half of the pups died in 5 days after birth (Fig. 3-1A), and GGA supplementation significantly increased the survival rate of pups ($p = 0.0027$), indicating that most of the early death of the control offspring were apparently prevented by GGA supplementation. Next, I confirmed the reproducibility of the present results of Experiment I, which was performed in February, 2018. Then, I conducted Experiment II in July, 2018 (Table 3-2) and Experiment III in October, 2018 (Table 3-3) and observed whether GGA supplementation increased RI, as in Experiment I. As a result, the RI values of both control (3.50) and GGA (5.17) groups in Experiment II were quite similar to those (3.67 and 5.00) in Experiment I, respectively (Table 3-2). The same thing was true in Experiment III. I found that GGA feeding upregulated the RI value from 2.20 to 5.00 in Experiment III (Table 3-3). The average RI value of GGA group (5.61) was close to that (6.00) of CA-1 group.

Table 3-1. Effect of GGA feeding on reproduction index and weanling rate (Experiment I).

	Control	GGA
Total dams (n)	6	6
Pregnant dams (n)	6	6
Pregnancy/Birth rate	1.00	1.00
Litter size	8.0 ± 0.63	6.8 ± 1.33
Delivery (n)	48	41
Weanling (n)	22	30
WR	0.458	0.732**
RI	3.67	5.00

WR (Weanling rate) = Number of weanling pup/Number of delivery pup

RI (Reproduction index) = Number of weanling pup/Total dams

GGA, geranylgeranoic acid.

** : p < 0.001 (vs Control)

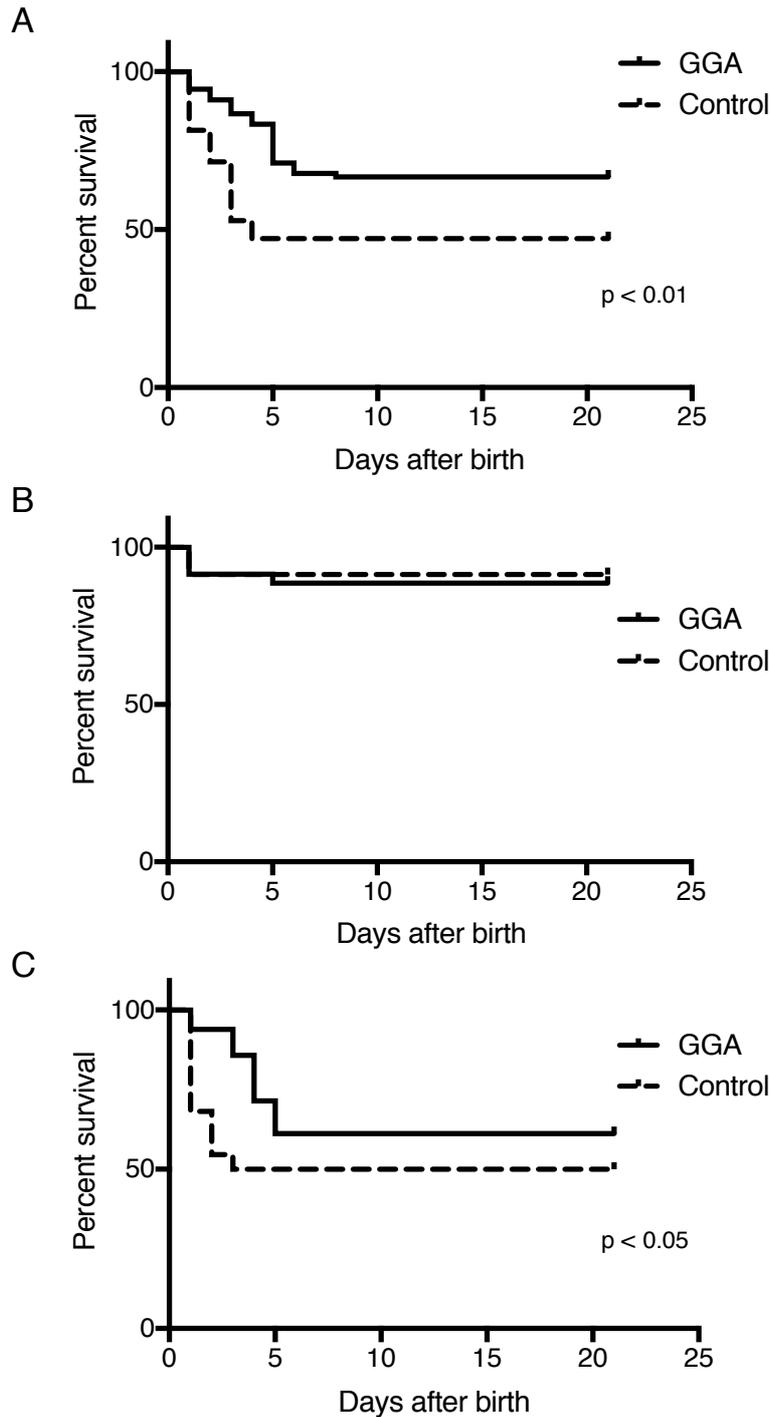


Figure. 3-1 Survival curves of pups in control and GGA groups.

Kaplan-Meier curves of survival rate of pups on Experiment I (A), Experiment II (B) and Experiment III (C), respectively. The statistically significant difference between control group and GGA group was determined using a generalized Wilcoxon test with Gehan-Breslow method.

GGA, geranylgeranoic acid.

Table 3-2.
Effects of GGA feeding or breeding diet on reproduction index and weanling rate (Experiment II).

	Control	GGA	CA-1
Total dams (n)	6	6	6
Pregnant dams (n)	3	5	6
Pregnancy/Birth rate	0.50	0.83	1.00
Litter size	7.7 ± 0.58	7.0 ± 0.71	7.8 ± 1.33
Delivery (n)	23	35	47
Weanling (n)	21	31	36
WR	0.913	0.886	0.766
RI	3.50	5.17	6.00

WR (Weanling rate) = Number of weanling pup/Number of delivery pup

RI (Reproduction index) = Number of weanling pup/Total dams

GGA, geranylgeranoic acid.

Table 3-3.
Effect of difference in GGA feeding period on reproduction index and weanling rate (Experiment III).

	Control	GGA	GGA-I	GGA-II
Total dams (n)	5	6	6	6
Pregnant dams (n)	4	6	4	5
Pregnancy/Birth rate	0.80	1.00	0.67	0.83
Litter size	5.5 ± 3.00	8.2 ± 1.47	6.8 ± 1.50	7.0 ± 2.92
Delivery (n)	22	49	27	35
Weanling (n)	11	30	26	23
WR	0.500	0.612	0.963**	0.657
RI	2.20	5.00	4.33	3.83

WR (Weanling rate) = Number of weanling pup/Number of delivery pup
 RI (Reproduction index) = Number of weanling pup/Total dams
 GGA, geranylgeranoic acid.

** : p < 0.001 (vs Control)

3-3. Timing effects of GGA supplementation on the RI

As described above, I demonstrated the improving effect of GGA on the RI in C3H/HeN mice. However, since GGA was administered for a whole period of mating, pregnancy and lactation, it is unclear whether GGA acts on male, female or both, or even pups through placenta and mother's milk. In breeding experiments, it is very difficult for only males to feed GGA with ad lib. Therefore, in Experiment III, I decided to change the timing of GGA supplementation. In particular, I can observe the effect of GGA on females when the mating period is removed from the time of GGA administration. As a result, the RI was the highest value in GGA (continuously fed on GGA-diet) group, followed by the GGA-I (GGA administration only during pregnant period to putative mothers), GGA-II (GGA supplied only during lactation period) and control groups in the order. In other words, GGA administration over the whole reproduction period was most important for improving the RI, and its administration only during pregnancy did not improve pregnancy/birth rate but contributed to improving the RI by significantly increasing WR, and GGA administration only during lactation also improved the RI to some extent.

3-4. Discussion

The results presented in chapter 2 suggested that GGA may be an essential metabolite having an important function for cell life other than cell death induction. Therefore, next, I demonstrated the improvement of GGA fertility. Since it had already reported that the RI of SAM mice increased by ingesting GGA during the mating, gestational and lactating periods, I decided to do the same experiment to see if similar results are obtained using another strain mouse, C3H/HeN. In the three experiments performed, I demonstrated that the GGA intake during a breeding period also improves the RI of C3H/HeN strain. The survival rate of pups in the control group seems to be too low, however, their survival rate is in the range of the reported values for C3H/HeN mice (74) or is even above that in AKR mice (75). Early death of mouse pups is a commonly facing problem in breeding mice colonies, which is still often regarded as ‘normal’ or is even overlooked due to the counting procedures applied (76). In addition, according to the website of CLEA Japan (http://www.clea-japan.com/en/animals/animal_f/f_11.html), the RIs of other strains such as C3H/HeJ (4.2), C57BL/6N (4.5) and Jcl:ICR (11.5) are than that (2.3) of C3H/HeN mice, which is even lower than the RI (3.67) of the control group in Experiment I.

From these three experiments, I can conclusively state that GGA supplementation during the mating, pregnancy and lactation periods significantly improves the RI in C3H/HeN mice (Fig. 3-2). However, among these three experiments there were clearly some differences that were not reproduced in the data. For example, in contrast to Experiment I, there was no difference in the WR values between the control and GGA groups in either Experiment II (Table 3-2) or Experiment III (Table 3-3). Furthermore, there were apparent differences in the pregnancy/birth rate and in WR of both control and GGA groups between Experiments I and II. In other words, GGA supplementation apparently increased the pregnancy/birth rate from 0.50 of the control mice to 0.83, approaching to that (1.00) of mice fed on CA-1, a commercially-available breeding diet rich in n-3 PUFAs in Experiment II (Table 3-2). In Experiment I, however, the birth rate was 1.00 in both control and GGA supplemented groups. The data in Experiment II tells that the pregnancy/birth rate of the control group was

just halved in Experiment II compared with Experiment I. At the moment, I am speculating a reason why I found such a low value of the pregnancy/birth rate in Experiment II as follows; even though environment of the animal breeding room in an animal facility of my university was maintained at 22-25°C and 60-80% humidity, I considered that the difference in pregnancy/birth rate between Experiments I and II might be conveyed by seasonal variation. Because in Experiment III conducted in October 2018, the pregnancy/birth rate of both groups tended to return back to the values in Experiment I (Table 3-3). In brief, I am supposing that even if breeding is done at the animal facilities of my university, the pregnancy/birth rates may decline in Summer season. In the present study, almost half of the pups died in 5 days after birth in control group in Experiments I (performed in Winter) and III (in Fall), but most of the pups in Experiment II (in Summer) survived (Fig. 3-1BC). Since the litter size has not changed among three experiments, it is thought that the survival rate of the pups is higher in Summer season, because the growth environment might be favorable for the survival of newborn mice in Summer. Alternatively, the increased survival rate of the pups may be simply due to a decrease in pregnancy/birth rates in Summer. The amount of GGA (50 µg/day) used in this study is only about 1% compared to DHA and EPA (approximately 4 mg in total per day) contained in CA-1. So, the fact that almost the same effect as the conventional CA-1 is obtained by very small intake of GGA may be helpful for the development of more efficient breeding feed. GGA-I group significantly increased the WR value from 0.5 to 0.963 ($p < 0.01$), which is higher than that (0.612) of GGA group in Experiment III (Table 3-3), although the pregnancy/birth rate of GGA-I group was apparently less than that of control group. This indicates that maternal supplementation of GGA may support proper embryogenesis and result in delivery of healthier pups. On the other hand, regarding the pregnancy/birth rate, a group administered with GGA for whole periods of mating, pregnancy and lactation showed the highest, suggesting that GGA may enhance male reproductive functions besides female reproductive functions. Further studies are needed in order to adjust the amount that can obtain the maximum efficiency of GGA to be fortified according to the target animal.

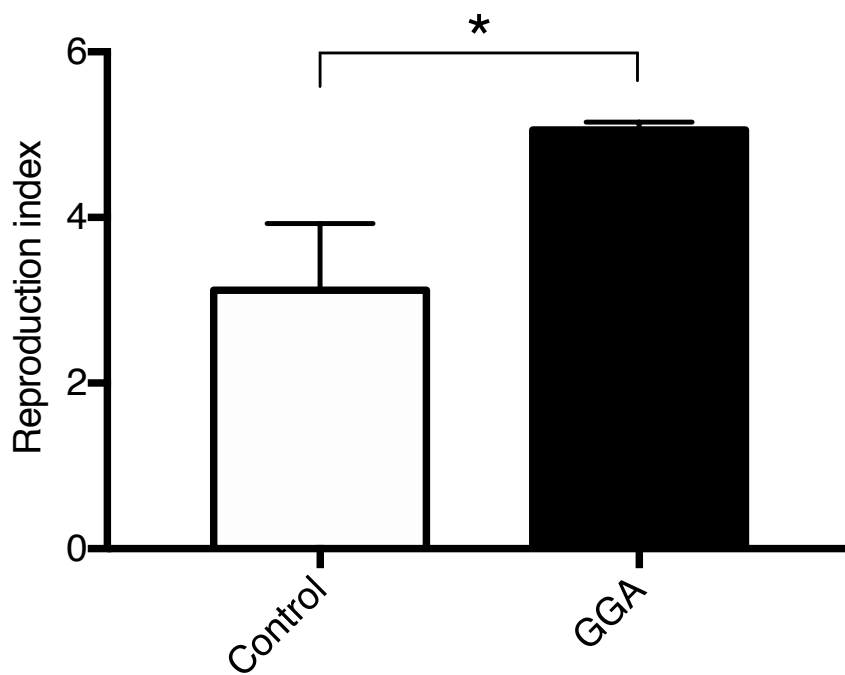


Figure 3-2. Reproduction index of control and GGA groups in Experiments I-III
Data represent mean RI SE of each group in Experiments I-III (n = 3). *: p < 0.05

GGA, geranylgeranoic acid.

Here, I am now ready to discuss how GGA improves the RI by comparing it with a commercially available breeding diet, CA-1. The CA-1 diet contains more DHA and EPA than CE-2. It is well established that these n-3 polyunsaturated fatty acids (PUFAs) have a close relationship with the quality and function of sperm. Besides n-3 PUFAs, GGA may also have similar promoting activity especially in male reproductive organs. In chapter 2, I found that GGA is abundantly present in testis, epididymis and prostate of Wistar rat (73). Furthermore, GGA is found also in testis, epididymis and prostate more than other organs of male C3H/HeN mice (unpublished observations). Accordingly, GGA may play an important role in normal development of sperm in male reproductive organs and it is possible to consider that GGA may enhance the male reproductive function(s) and boost embryonal growth. Additionally, previous study revealed that the protein expression of brain-derived neurotrophic factor (BDNF) increased in the hippocampus of 7-day old mice born from a mother that ingested GGA for a whole period of the mating, gestational and lactating (54). A previous study reported that BDNF-knockout mice were killed by mothers in a few days after birth (77). These authors suggested that mother mice selectively killed the pups in which abnormal development of neurons occurs due to the decline of BDNF. Furthermore, Smarr et al reported that along with hypermethylation of stress-related genes including the *Bdnf* gene, maternal stress was associated with increases in maternal cannibalism of pups (78). In this context, GGA feeding may protect the pups from maternal cannibalism by elevating hippocampal BDNF expression in the pups as well as their mothers.

In summary, taken together with the previous findings on GGA-induced improvement of the RI in SAM mice (54), I propose that the continuous GGA intake during a breeding period also improves the RI of mouse species such as C3H/HeN strain. More quantitative analysis of GGA dose and more extensive studies with other mammalian species will warrant more efficient and healthier mammalian reproduction by GGA in an animal breeding field.

Chapter 4.

Unequivocal evidence for endogenous geranylgeranoic acid biosynthesized from mevalonate in mammalian cells

Abstract

GGA has been developed as a preventive agent for second primary hepatoma. Thereafter, I found natural GGA present as acyclic diterpenoids in some medicinal herbs. In chapter 2, I demonstrated that with normal male Wistar rats, the endogenous GGA content in liver were found to be far greater than those in other organs analyzed. In addition, I had shown that MAOB oxidizes GGOH to GGal, a precursor of GGA, in human hepatoma-derived cells. Here, I provide unequivocal evidence for de novo GGA biosynthesis from MVA pathway. In this chapter 4, first, I attempted to modulate the MVA pathway with inhibitors, such as pravastatin, an HMG-CoA reductase inhibitor, and ZAA, a squalene synthase inhibitor. As a result, inhibition of MVA synthesis by pravastatin was depleted GGA. On the other hand, inhibition of squalene synthesis by ZAA increased intracellular GGA. Interestingly, ZAA induced dose-dependent upregulation of endogenous GGA content in HuH-7 cells and their concomitant cell death. Second, I demonstrated the metabolic GGA labeling from the ^{13}C -labeled mevalonolactone (MVL) in the human hepatoma-derived cell line HuH-7. Isotopomer spectral analysis revealed that approximately 80% of the cellular GGA was newly synthesized from MVA in 12 h and the acid picked up pre-existing FPP and GGPP, suggesting that GGA is derived from FPP and GGPP through the MVA pathway. These results strongly suggest that a GGA with biological activity such as cancer-prevention is biosynthesized via the MVA pathway in mammals.

4-1. Introduction

GGA is a compound that was first recognized as one of MVA-derived metabolites in cell-free homogenates of bovine retina and then in a parasitic worm. In 1981, all-*trans* GGPP synthetase, which catalyzes two consecutive isoprenyl-transfer reactions from IPP to GPP and to FPP, was found in pig liver (79), but at that time these authors were unaware of the metabolic fate or biologic roles of all-*trans* GGPP. At present, GGPP is well-known as an isoprenoid donor for protein isoprenylation (80). But as Dallner's group has pointed out, GGPP synthetase activity is almost 100-times higher than protein-geranylgeranyl transferase activity in rat brain (81). GGPP may have other metabolic pathways apart from protein-geranylgeranylation or may be required for other as yet-unidentified cellular process. In this context, Bansal & Vaidya have made an interesting finding regarding geranylgeranyl pyrophosphatase (GGPPase) activity in rat liver microsomes (34). The enzyme was the most active at physiologic pH and highly specific for GGPP. In other words, it did not hydrolyze FPP and other allyl diphosphates. As shown in Chapter 2, when GGOH is produced by dephosphorylation of GGPP by a specific diphosphatase, MAOB is thought to oxidize GGOH to GGal. Thereafter, it seems reasonable to assume that the non-specific fatty aldehyde dehydrogenase might produce GGA from GGal.

In chapter 4, I provide unequivocal evidence for the biosynthetic pathway of GGA from MVA in mammalian cells. In this chapter, first, I describe that pharmacological upregulation of endogenous GGA could induce cell death in HuH-7 cells. Furthermore, I demonstrate the metabolic labeling of endogenous GGA with a stable isotope of ^{13}C from ^{13}C -MVL in a human hepatoma-derived HuH-7 cell line. Further metabolites of GGA, including 2,3-dihydroGGA in HuH-7 cells, are also described.

4-2. Changes in endogenous GGA levels when pravastatin and/or ZAA treatment of HuH-7 cells.

Because the liver was the main organ that contained endogenous free GGA, I attempted to observe the biosynthesis of GGA using human liver cancer-derived HuH-7 cells (37). Previous observations give that HuH-7 cells contain endogenous GGA, and that GGA can be produced from GGOH in the HuH-7 cell lysates (37), I examined whether cellular GGA is metabolically labeled with a stable isotope of ^{13}C in the cells after adding ^{13}C -labeled MVL to the culture medium. Prior to the labeling experiment, I confirmed that endogenous GGA was sensitive to pravastatin treatment. After 48 h treatment with 120 μM of pravastatin, endogenous GGA became undetectable in HuH-7 cells (Fig. 4-1A and B). Squalene synthesis is a major flow of the mammalian MVA pathway, so I tried to block the major flow by using ZAA (squalestatin 1) to augment a metabolic flow from FPP to GGPP. As a result, the cellular GGA content was increased by 15–20 times after 48 h treatment with 15 μM of ZAA (Fig. 4-1C), and most of the content was depleted by cotreatment with pravastatin and ZAA (Fig. 4-1D).

4-3. ZAA induced upregulation of GGA and cell death in HuH-7 cells

It had reported that HuH-7 cells are sensitive to treatment with exogenous GGA(24, 29), which induces UPR-mediated cell death (25) with an incomplete autophagic response (26), as mentioned in the chapter 1. In this study, I revealed that HuH-7 cells are capable of producing endogenous GGA from MVA. In this context, I hypothesized that if upregulation of endogenous GGA can be inducible, it is possible to induce cell death in HuH-7 cells by the resultant upregulated GGA without using exogenous GGA. I chose ZAA, which prevents a major flow of MVA into the steroid synthesis pathway and augments GGPP synthesis, to upregulate endogenous GGA synthesis from MVA. As a result, 15 μM of ZAA time-dependently increased endogenous GGA from 111 to 1,372 pmol/g in 72 h, and endogenous 2,3-dihydroGGA from 154 to 4,571 pmol/g (Fig. 4-2A). As expected, ZAA dose-dependently induced cell death of HuH-7 cells in 48 h, as shown in Fig. 4-2B. The LD_{50} of ZAA was $22.0 \pm 0.07 \mu\text{M}$ against HuH-7 cells. Because ZAA is an inhibitor of

squalene synthase, ZAA-treated cells are expected to become deficient in cholesterol. Hence, I performed a rescue experiment of ZAA-induced cell death with exogenous cholesterol. As a result, the exogenously added cholesterol was unable to rescue the cells from ZAA-induced death (Fig. 4-2C). Therefore, to demonstrate that ZAA-induced cell death is due to an increase in GGA synthesis, another rescue experiment was conducted to eradicate endogenous GGA synthesis in the presence of ZAA. When pravastatin was supplied to the culture medium during ZAA treatment, the dose-dependent effect of ZAA on cell death was completely attenuated (Fig. 4-2B).

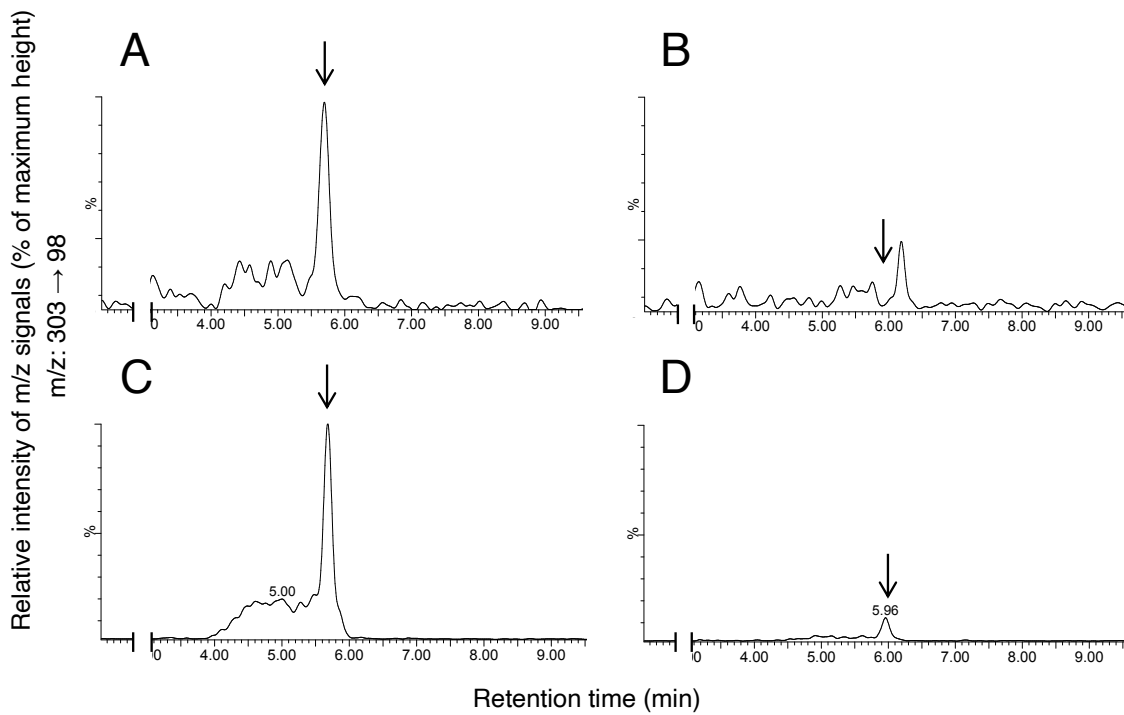


Figure 4-1. Pravastatin-induced downregulation and ZAA-induced upregulation of endogenous GGA levels in HuH-7 cells.

LC/MS/MS chromatograms of the lipid extract from HuH-7 cells, which were non-treated as the control (A), treated for 48 h with 120 μ M pravastatin (B), 15 μ M ZAA (C) or co-treated with pravastatin and ZAA (D). Arrows indicate the elution position of GGA. (A, B) and (C, D) show chromatograms with a peak height of 89 as 100% and of 1380 as 100%, respectively.

ZAA, zaragozic acid; GGA, geranylgeranoic acid; LC/MS/MS, liquid chromatography mass spectrometry.

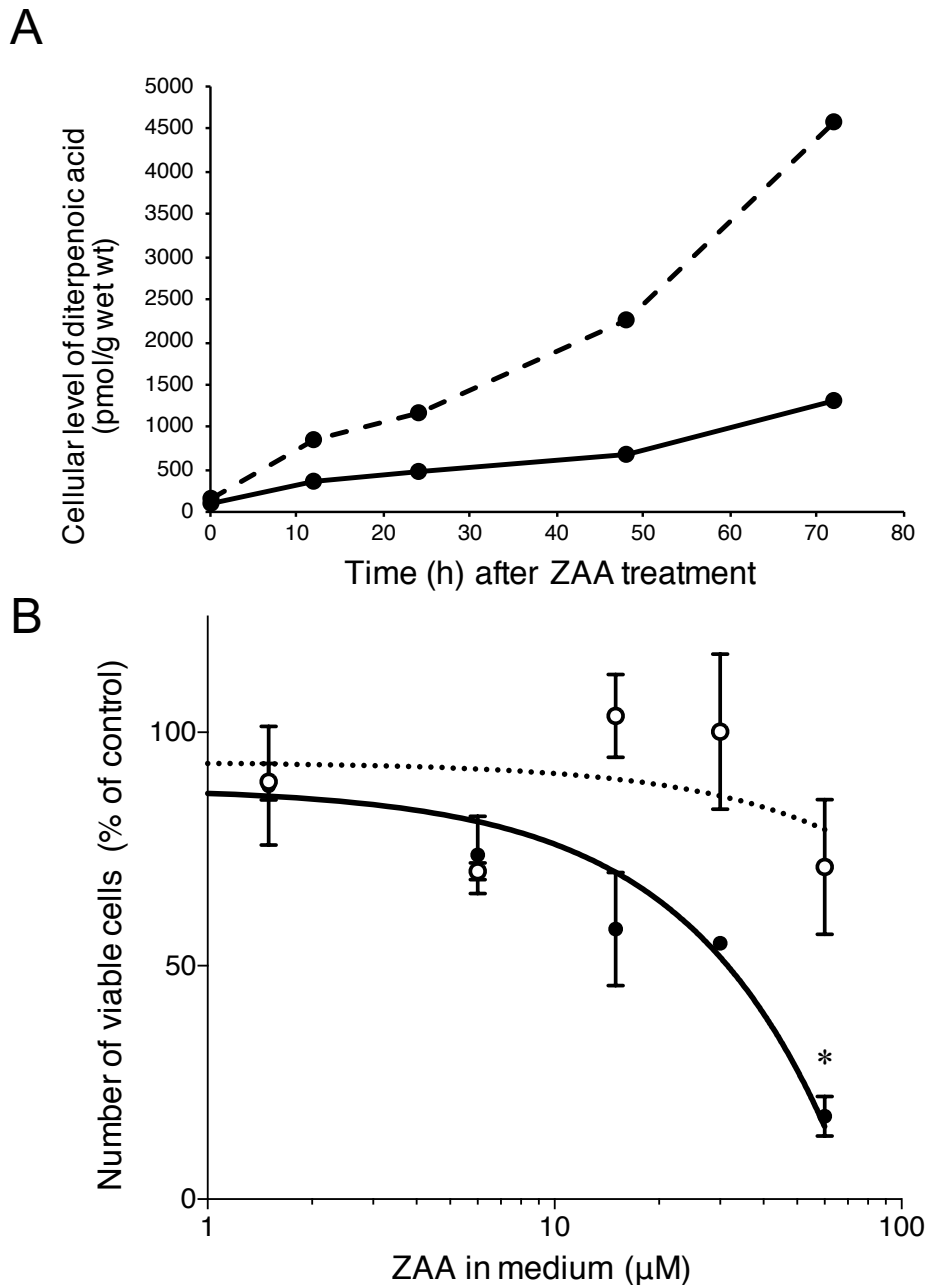


Fig. 4-2. ZAA induced both upregulation of endogenous GGA and 2,3-dihydroGGA and cell death in HuH-7 cells.

(A) Time-dependent changes of endogenous GGA (solid line) and 2,3-dihydroGGA (broken line) in HuH-7 cells after treatment with 15 μM ZAA.

(B) HuH-7 cells were treated with increasing concentrations (0–60 μM) of ZAA in the absence (closed circle) or presence (open circle) of 120 μM pravastatin for 24 h. The number of viable cells were counted using the trypan blue dye exclusion method.

(C) HuH-7 cells were treated with increasing concentrations (0–60 μM) of ZAA in the absence (closed circle) or presence (open circle) of 50 μM cholesterol for 24 h. The number of viable cells was counted using the trypan blue dye exclusion method. The experiment was carried out using duplicate samples. *: $p < 0.05$ vs pravastatin + ZAA at 60 μM (t-test).

ZAA, zaragozic acid; GGA, geranylgeranoic acid.

C

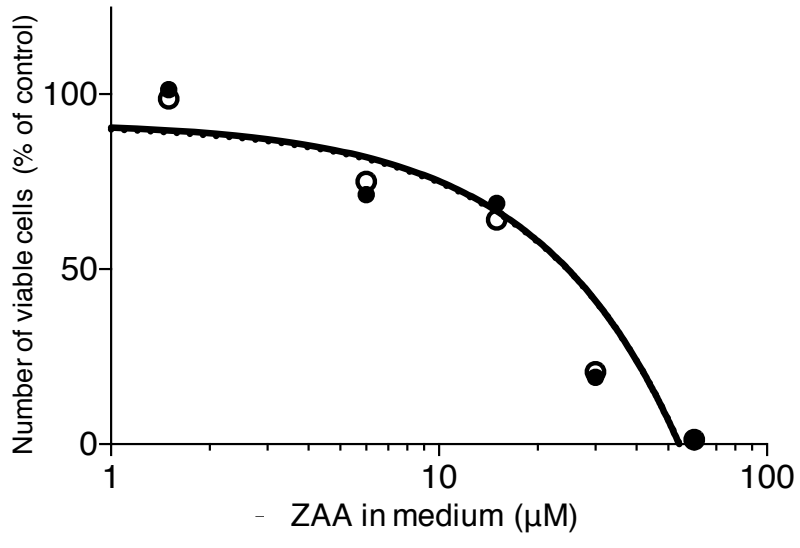


Fig. 4-2 Continued.

4-4. Metabolic labeling of GGA using ^{13}C -MVL in human hepatoma HuH-7 cells

After complete depletion of endogenous GGA by pravastatin, I successfully detected $^{13}\text{C}_4$ -labeled GGA in HuH-7 cells using LC/MS/MS with 2 mM of ^{13}C -MVL in the culture medium (Fig. 4-3A). Then, the labeled GGA could be completely chased by another 48-h treatment with the same concentration of cold MVL (Fig. 4-3B).

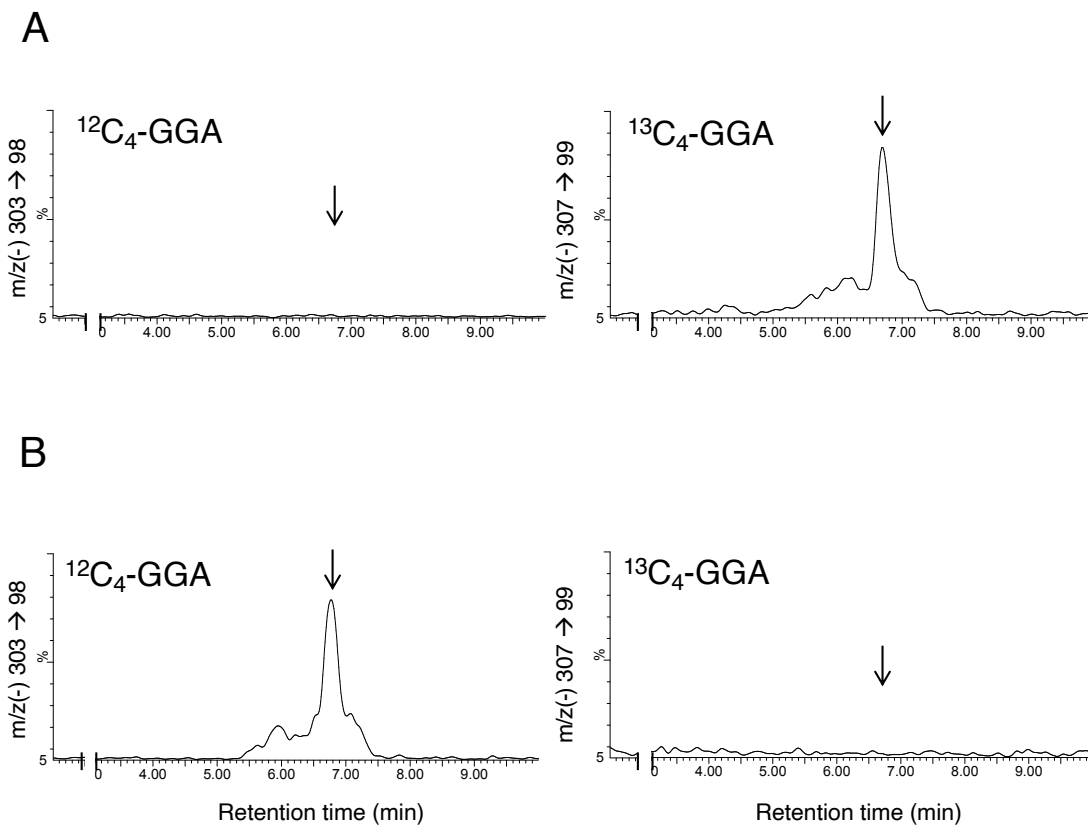


Fig. 4-3. Metabolic labeling of GGA with ^{13}C -MVL and chasing of the labeled GGA with cold MVL.

(A) After depletion of endogenous GGA by 120 μM pravastatin treatment for 24 h, 2 mM of ^{13}C -MVL and 15 μM of ZAA were added and incubated for another 48 h.

(B) The labeled GGA was chased by a further 48 h treatment with the same concentration of cold MVL. (A, B) The left panels show chromatograms of non-labeled GGA and the right panels show chromatograms of $^{13}\text{C}_4\text{-GGA}$. Chromatograms with a peak height of 282 as 100% are shown in both A and B.

GGA, geranylgeranoic acid; MVL, mevalonolactone; ZAA, zaragozic acid.

4-5. ISA with ^{13}C -MVL in HuH-7 cells

I performed isotopomer spectral analysis (ISA) using a stable isotope-labeled ^{13}C -MVL to test for the presence of gradients of precursor enrichment, as illustrated by in vivo sterol synthesis (82). When both ZAA and pravastatin were simultaneously added 24 h prior to addition of ^{13}C -MVL, ^{13}C was incorporated to different extents into newly synthesized GGA in 6 h, which showed all the varieties of mass isotopomers and isotopologues of GGA. As shown in Fig. 4-4A and B, I detected all eight MS/MS peaks at a retention time corresponding to GGA, which had been expected in advance from combinations of five isotopic molecular ions (m/z 303–307) and two isotopic fragment ions (m/z 98 and 99). The peak area of each isotopologue with fragment ion of 98 was 13 for M (a molecular ion of 303), 12 for M+1, 7 for M+2, and 5 for M+3, arranged in descending order (Fig. 4-4C).

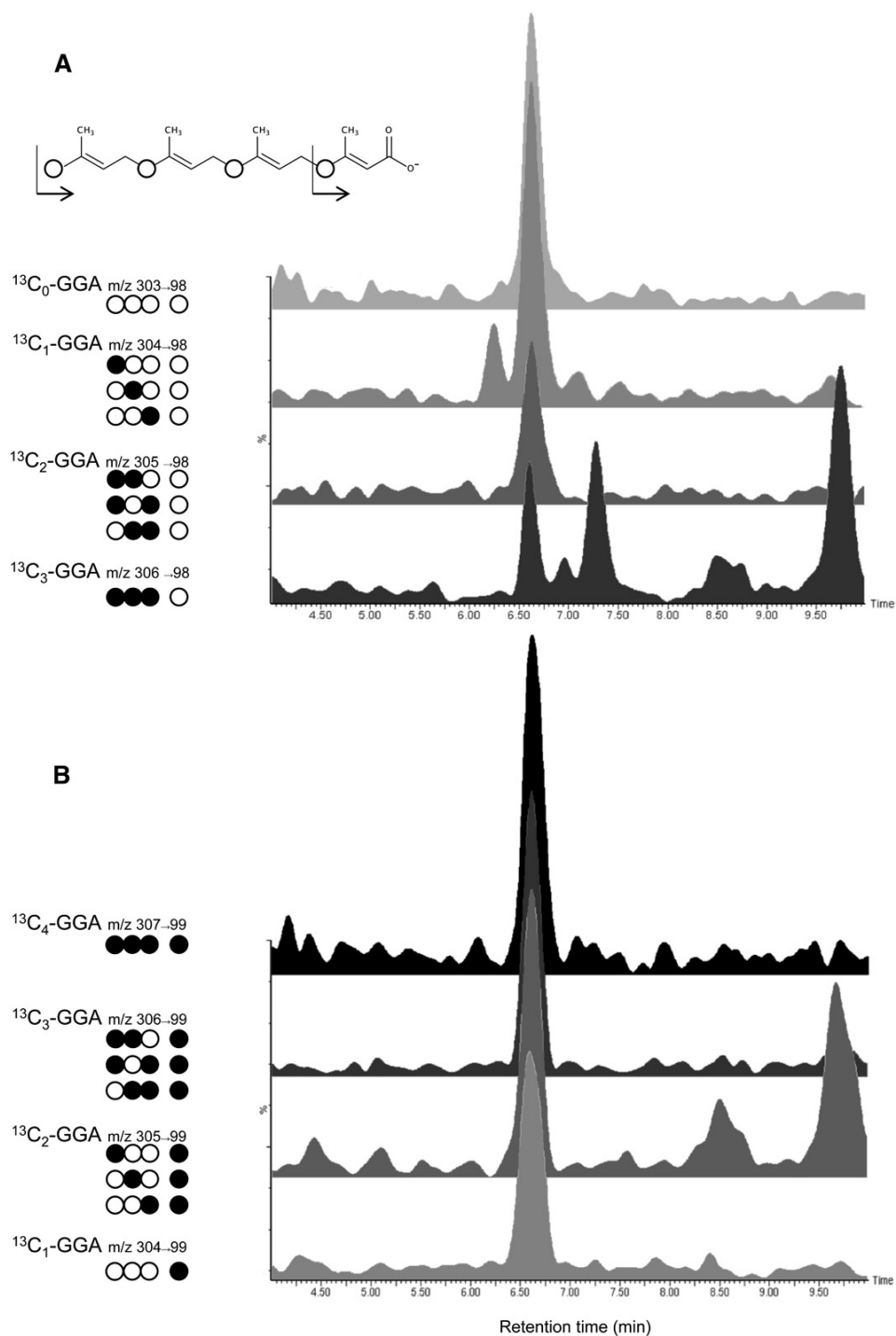


Fig. 4-4. LC/MS/MS chromatograms of mass isotopomers and mass isotopologues of GGA metabolically labeled with ^{13}C -mevalonolactone. (continued)

The eight expected combinations of five molecular ions, m/z 303, 304, 305, 306 and 307, and two fragment ions, [m/z 98 (A) and 99 (B)], were detected at the same retention time in a single run after being metabolically labeled with ^{13}C -MVL for 6 h in HuH-7 cells. Peak areas of GGA mass isotopomers found in (A) and (B) were plotted in a bar graph (C). Here, four isoprene units in GGA are simply illustrated by four circles. Carbon isotopes incorporated in position 1 of each isoprene unit in GGA are indicated by open circle (^{12}C) and closed circle (^{13}C).

LC/MS/MS, liquid chromatography mass spectrometry; GGA, geranylgeranoic acid; MVL, mevalonolactone.

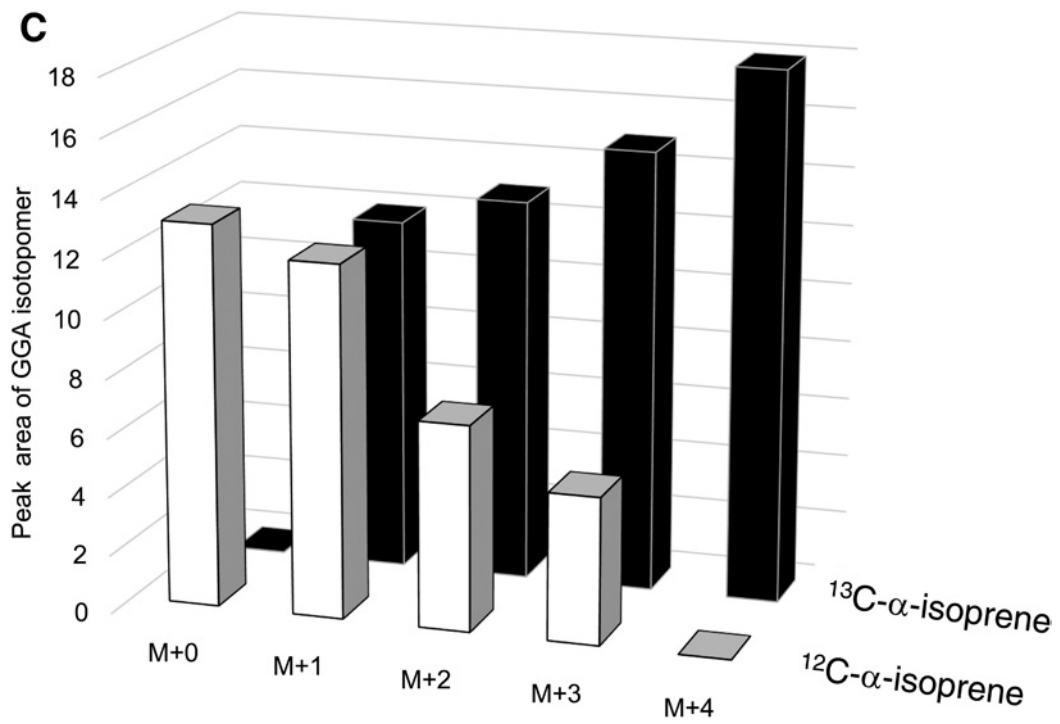


Fig. 4-4 Continued.

However, the peak area of each GGA isotopologue with fragment ion of 99 was 12 for M+1, 13 for M+2, 15 for M+3, and 18 for M+4, each of which was aligned in ascending order, as shown in Fig. 4-4C. I analyzed the data using the ISA framework as measured mass isotopologue distributions of GGA. To elucidate the biosynthetic flow and pathway of GGA from MVA, a simple metabolic model, as shown in Fig. 4-5A, was first constructed and ISA was performed with this model. Here, D is a factor described as the MVA pool dilution with the ^{13}C -MVA. Originally, g(t) is a time-dependent parameter with the time of incubation, representing the product dilution with the newly synthesized product. In the present study, g(t) represented GGA dilution with GGA isotopomers and isotopologues of $^{13}\text{C}_{1-4}$ -GGA. D and g(t) simply represent the flow into product (GGA) pools from precursor (MVA). From the data of each isotopologue (isotopomer) peak, the fractional abundances were calculated for eight MS/MS combinations [303 \rightarrow 98 (M+0); 304 \rightarrow 98 (M+1), 304 \rightarrow 99 (M+1); 305 \rightarrow 98 (M+2), 305 \rightarrow 99 (M+2); 306 \rightarrow 98 (M+3), 306 \rightarrow 99 (M+3), and 307 \rightarrow 99 (M+4)] of GGA (Fig. 4-5B). Then, I applied the “sum of squared error (SSE)” method to estimate for combinations of D and g(t) values with the smallest SSE between observed value and estimated value in each isotopologue by the nonlinear approximation method (82). As a result, the observed values were best fit (SSE = 0.00620) to the estimated values when the combination was as follows: D = 0.68 and g(t) = 0.56 (Fig. 4-5B). These parameter values suggest that nearly 70% of the cellular MVA pool was diluted with 2 mM of ^{13}C -MVL, and HuH-7 cells incorporated MVA into more than a half of the cellular GGA in 6 h, respectively. As mentioned above, D is a factor described as the MVA pool dilution with the ^{13}C -MVA; therefore, D should have been constant during the experiment because I used pravastatin to prevent further dilution of the MVA pool by endogenous MVA synthesis. Indeed, D values were constant from 0.766 at 12 h to 0.768 at 72 h (**Fig. 4-5D**). However, g(t) is a time-dependent parameter. When g(t) was plotted along with incubation time after adding ^{13}C -MVL (**Fig. 4-5E**), it increased from 0.56 at 6 h to 0.88 at 12 h and reached a plateau of 0.9 at 24 h.

4-6. 2,3-DihydroGGA as a metabolite of GGA

ISA was performed on 2,3-dihydroGGA using the same samples. Because the fragment ions of 2,3-dihydroGGA were composed of diterpenoic acid containing alpha- and beta-isoprene units, I detected nine MS/MS combinations [305 \rightarrow 168 (M+0); 306 \rightarrow 168 (M+1), 306 \rightarrow 169 (M+1); 307 \rightarrow 168 (M+2), 307 \rightarrow 169 (M+2); 307 \rightarrow 170 (M+2); 308 \rightarrow 169 (M+3), 308 \rightarrow 170 (M+3); and 309 \rightarrow 170 (M+4)] of 2,3-dihydroGGA (Fig. 4-5C). ISA on 2,3-dihydroGGA also calculated a D value of 0.788, which is similar to the value calculated using ISA on GGA, and it was constant during the experiment. However, g(t) increased from 0.68 at 12 h, and it gradually caught up with the D value of GGA at 72 h, suggesting that GGA may be metabolized to 2,3-dihydroGGA.

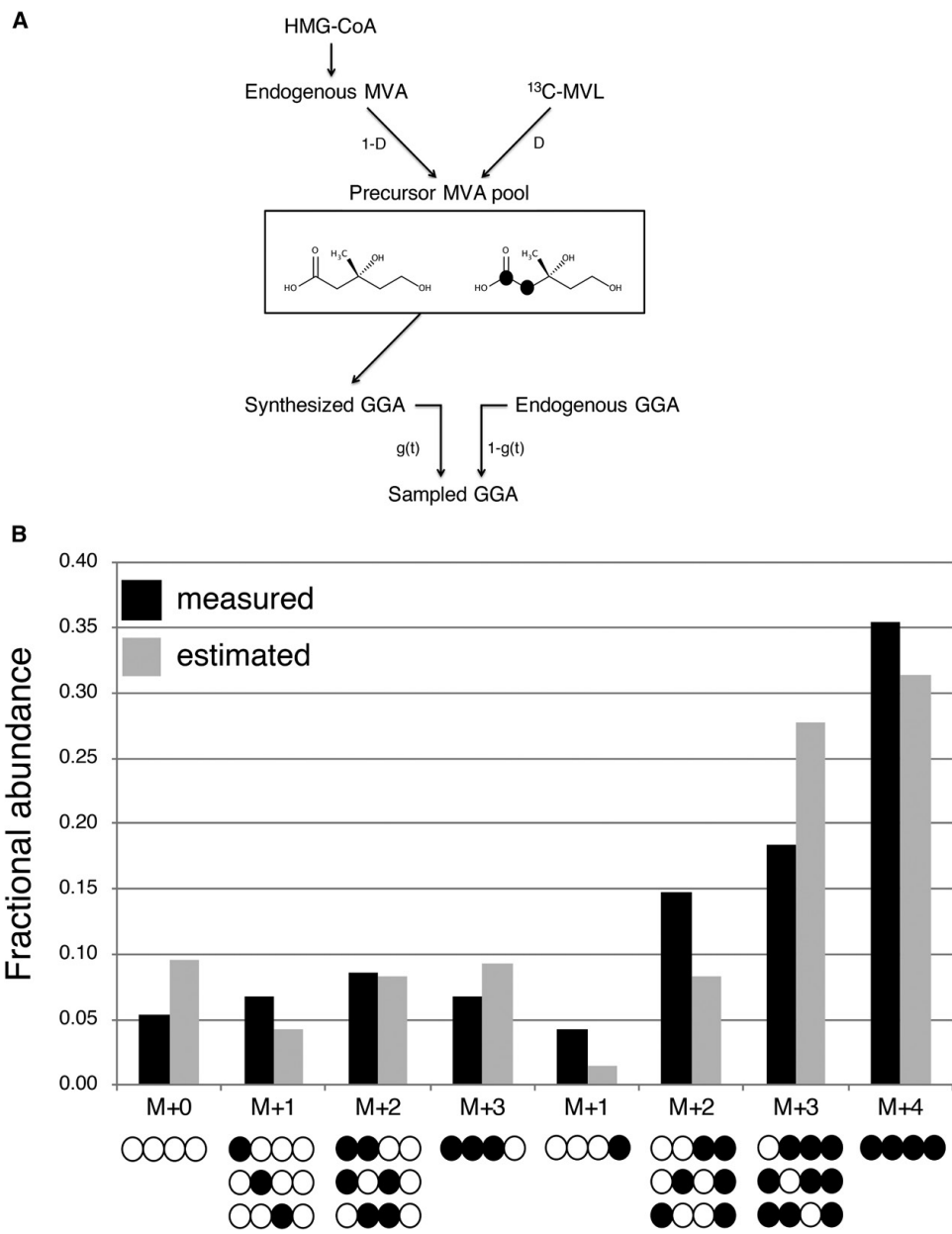


Fig. 4-5. Isotopomer Spectral Analysis on GGA biosynthesis in HuH-7 cells. (continued)

(A) To perform isotopomer spectral analysis (ISA), a simple metabolic model was assumed for the biosynthetic flow and pathway of GGA from MVA. D is a factor of the precursor MVA pool dilution by ^{13}C -MVL and $g(t)$ is a time-dependent parameter of the endogenous GGA pool dilution by newly synthesized GGA.

(B, C) Best fit results found with non-linear approximation of measured values of GGA or 2,3-dihydroGGA mass isotopologues with their estimated values using ISA. Carbon isotopes incorporated in position 1 of each isoprene unit in GGA are indicated by open circle (^{12}C) and closed circle (^{13}C).

(D) Time course changes in D of GGA (closed circle) and 2,3-diGGA (open circle) in HuH-7 cells by isotopomer spectral analysis were plotted along with the incubation time (0–72 h).

(E) Time course changes in $g(t)$ of GGA (closed circle) and 2,3-diGGA (open circle) in HuH-7 cells by isotopomer spectral analysis were plotted along with the incubation time (0–72 h).

HMG-CoA, 3-hydroxy-3-methylglutaryl-CoA; MVA, mevalonate; MVL, mevalonolactone; GGA, geranylgeranoic acid.

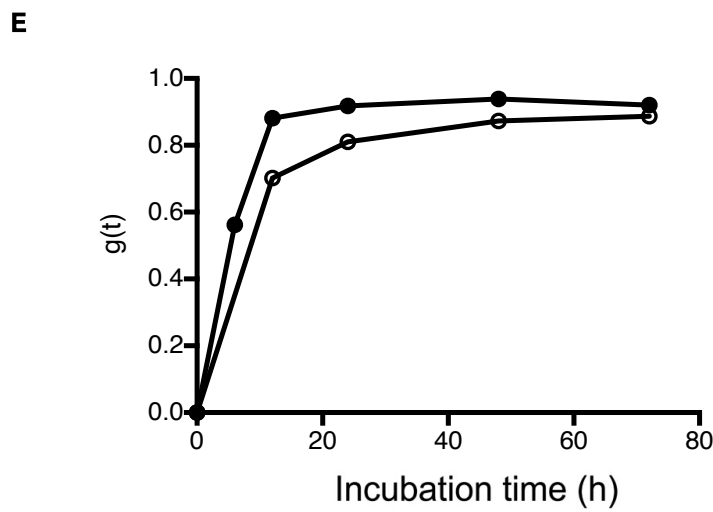
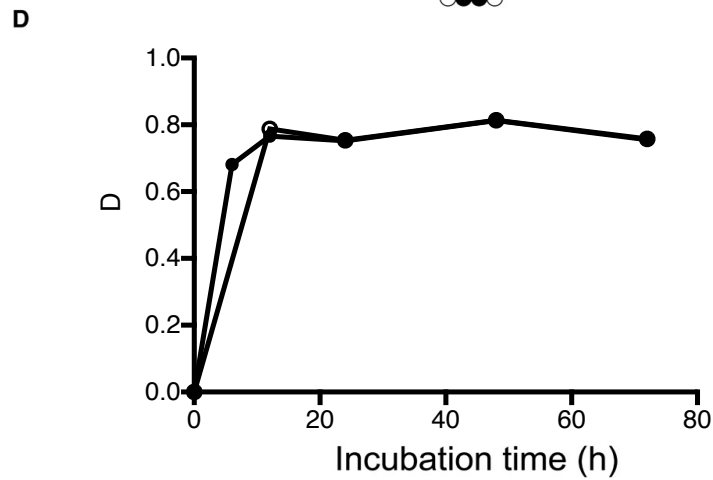
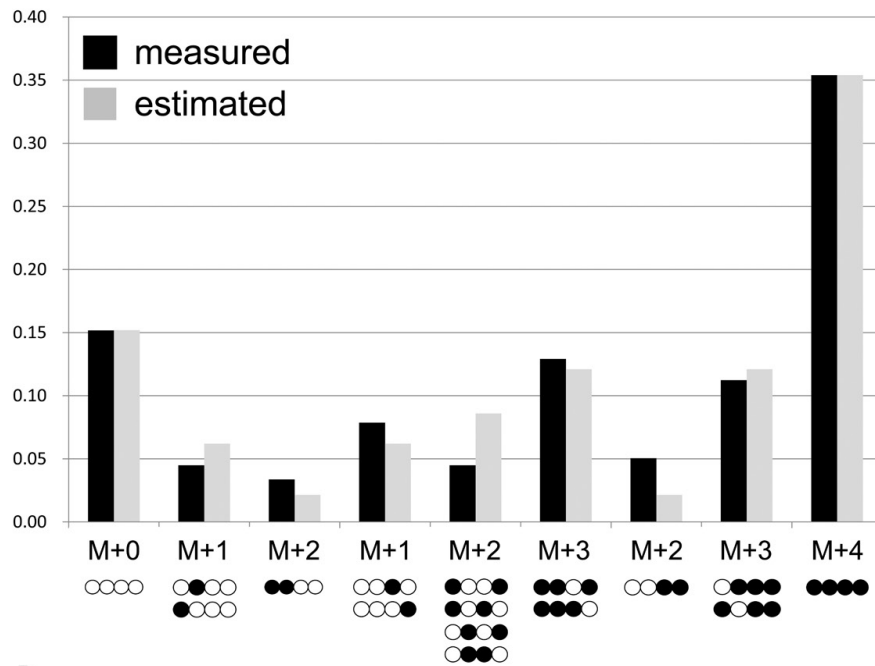
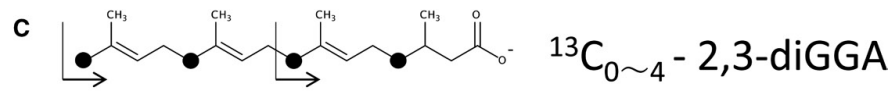


Fig. 4-5 Continued.

4-7. Discussion

In chapter 2, I found that endogenous GGA exists not only in plants but also in mammalian cells. And, at least in male Wistar rats, it was coincidentally distributed at high concentrations specifically in the liver. Because GGA was found to be a hepatic lipid in chapter 2, I analyzed GGA biosynthesis using HuH-7 cells in this chapter. Therefore, first, I tried to induce cell death in HuH-7 cells by upregulating endogenous GGA with ZAA. As a result, I was able to upregulate free endogenous GGA from 0.1 to 1.3 μM and 2,3-dihydroGGA from 0.15 to 4.5 μM in cells by a 3-day treatment with 15 μM ZAA (Fig. 4-2A). Both GGA and 2,3-dihydroGGA actively induce cell death in HuH-7 cells at their micromolar concentration (33). Consistently, ZAA induced cell death in a concentration-dependent manner (Fig. 4-2B), which strongly suggests that the intracellular endogenous GGA and 2,3-dihydroGGA induce cell death. Furthermore, when I canceled MVA synthesis by cotreatment with pravastatin, ZAA-dependent cell death was also canceled. This strongly indicates that the cellular toxicity of ZAA for hepatoma cells is not mediated by deficiency of cholesterol and/or other steroid metabolites, but maybe conveyed through upregulation of GGA and 2,3-dihydroGGA. In other words, I demonstrated for biologically active endogenous free GGA in mammalian tissues.

Next, after confirmation of metabolic incorporation of four atoms of the stable isotope from ^{13}C -labeled MVL into one molecular GGA in the presence of pravastatin, I performed ISA. ISA was initially introduced as a general method for modeling polymerization biosynthesis reactions (83). GGA is a simple tail-to-head tetramer of an isoprene unit derived from consecutive phosphorylation and decarboxylation of MVA. Therefore, the biosynthetic pathway of GGA is an ideal model to which ISA can be applied. In ISA, it is generally assumed that D should be constant, so I performed ISA in the presence of pravastatin to prevent MVA pool dilution with newly synthesized nonlabeled MVA. To prevent the bulk escape of ^{13}C -MVA from FPP to the cholesterol pathway via squalene, I added ZAA, an inhibitor of squalene synthase, into the culture medium during the ISA experiment. When I used 2 mM ^{13}C -MVL, D became 0.77, which means a pool size of endogenous cold MVA was calculated to 0.59 mM at 12 h after pravastatin addition. Because the MVA pool

size in the liver has been reported as 2.55 mM (84), I can conclude that the experimental conditions I performed are restored to the physiological MVA pool size by adding the labeled MVL. However, $g(t)$ is a time-dependent parameter, which means a fractional ratio of newly synthesized GGA after adding ^{13}C -MVL. Surprisingly, very rapid turnover of the cellular GGA was suggested by a time course of the $g(t)$ parameter. In other words, 12 h after adding ^{13}C -MVL, more than 80% of the intracellular GGA was replaced by newly synthesized GGA. Of note, ISA on 2,3-dihydroGGA also revealed that the dihydro-derivative is a metabolite of GGA, consistent with a previous report (48). The metabolite of GGA has the ability to induce lipid droplets in HL-60 cells, whereas GGA has no ability to induce lipid droplets (85). The difference in this biological activity between GGA and 2,3-dihydroGGA is confirmed with HuH-7 cells (Y. Shidoji, K. Okamoto, and H. Sekiguchi, unpublished observations). When the labeled isoprene unit is used for GGA synthesis in the isoprenoid synthesis pathway, theoretically, possible preexisting pools of DMAPP, geranyl diphosphate, and FPP are all available, as shown in Fig. 4-6. However, the data indicate that the observed fractional abundance of the M+1 isotopomer labeled with the alpha isoprene unit was much larger than the estimated value (Fig. 4-4B), which was calculated using the ISA model fitting assumption that the isoprene unit is randomly incorporated into a GGA consisting of four isoprene units (Fig. 4-6). The discrepancy between the observed and estimated values for the M+1 isotopomer labeled with the ^{13}C -alpha isoprene unit suggests that the pool size of FPP is larger than those of other two intermediates in HuH-7 cells (Fig. 4-6D). Consistently, Holstein et al. (86) reported that the FPP levels were higher than the GPP levels in human myeloma cell lines. Taken together with previous reports (36, 37) and chapter 2, I propose a possible metabolic flow from MVA to GGA in Fig. 4-7, where GGOH, a dephosphorylated form of GGPP by GGPPase (34), is enzymatically oxidized to GGal by MAOB, which is further oxidized to GGA in a NAD-dependent manner (36, 37).

In this chapter, I demonstrated unequivocal evidence for the biosynthetic pathway of GGA from MVA via MVA pathway in mammalian cells. The present study paves a road for exploring the metabolism and biological activity of these compounds from the viewpoint of inducing cell death in tumor cells and other

biological activities in reproductive and neural tissues.

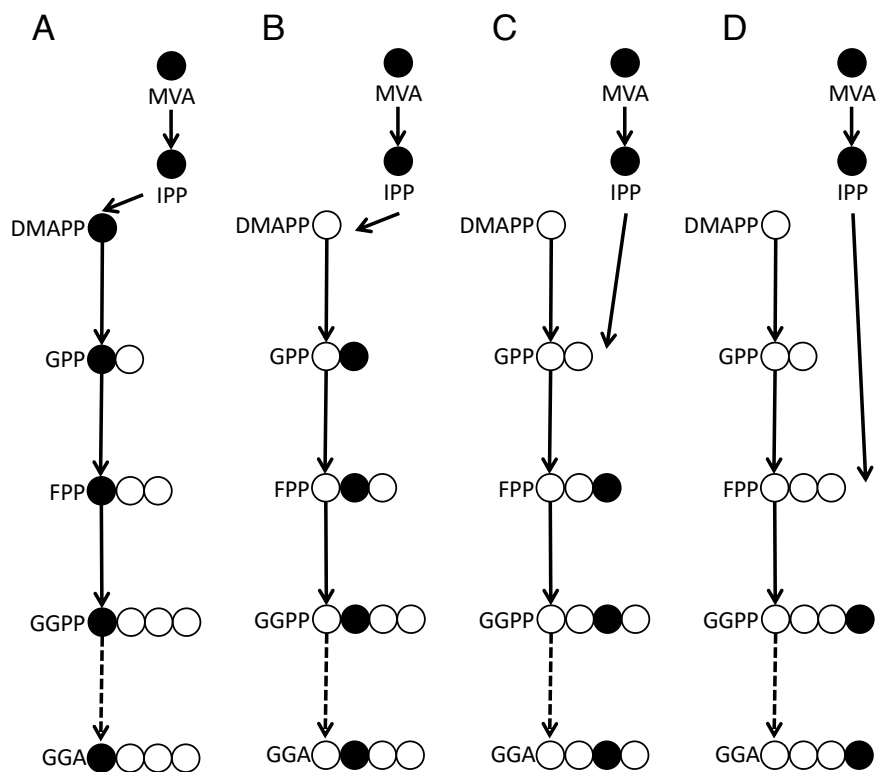


Figure 4-6. Possible metabolic pathways for M+1 isotopomers of GGA labeled from ^{13}C -MVL

MVA, mevalonate; IPP, isopentenyl diphosphate; DMAPP, dimethylallyl diphosphate; GPP, geranyl diphosphate; FPP, farnesyl diphosphate; GGPP, geranylgeranyl diphosphate; GGA, geranylgeranoic acid; MVL, mevalonolactone.

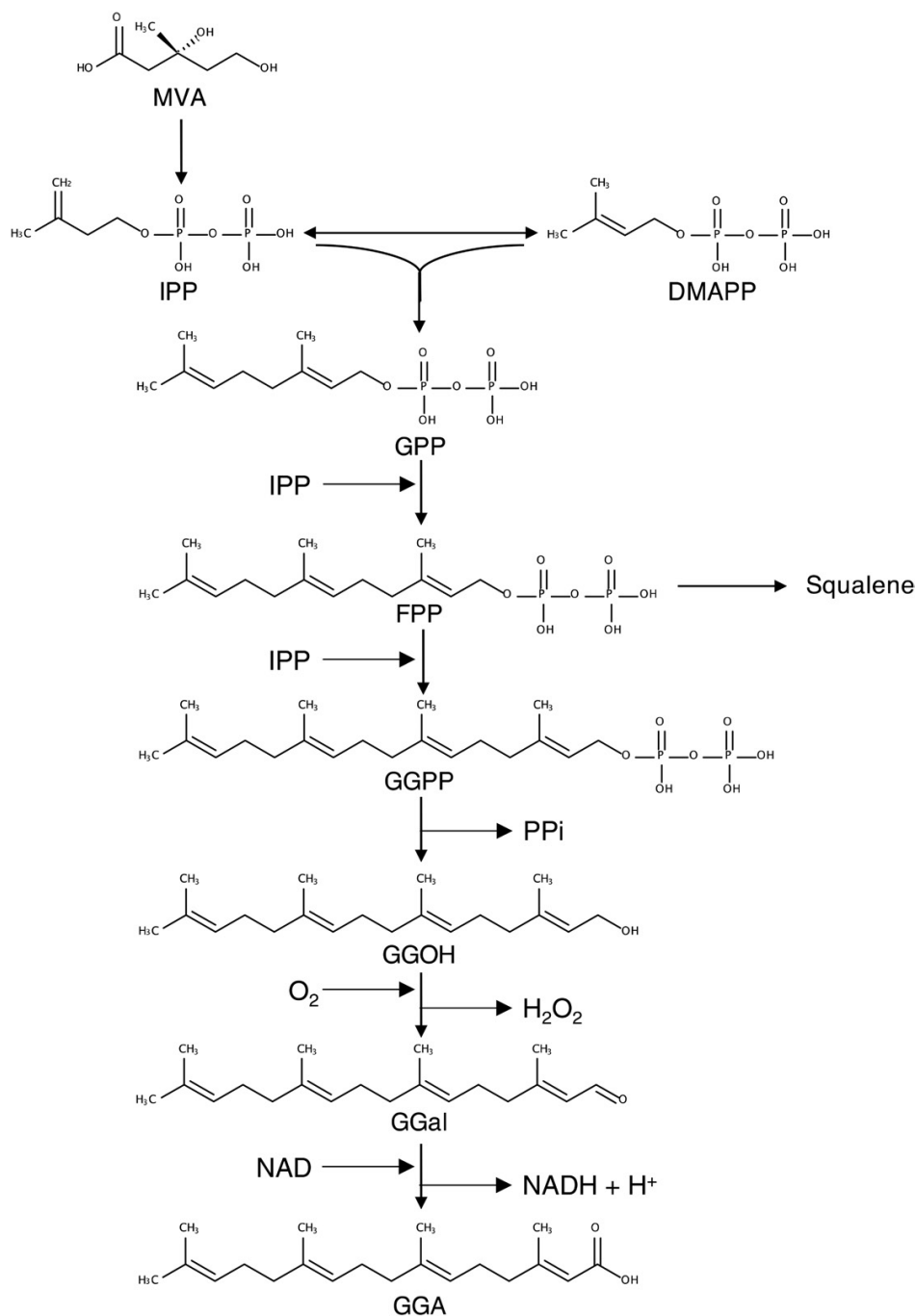


Figure 4-7. Proposed metabolic flow from MVA to GGA in HuH-7 cells.

MVA, mevalonate; IPP, isopentenyl diphosphate; DMAPP, dimethylallyl diphosphate; GPP, geranyl diphosphate; FPP, farnesyl diphosphate; GGPP, geranylgeranyl diphosphate; GGOH, geranylgeraniol; GGal, geranylgeranial; NAD, nicotinamide adenine dinucleotide; GGA, geranylgeranoic acid.

Chapter 5. General Discussion

As the main finding of my thesis, I demonstrated unequivocal evidence for mammalian GGA, a hepatoma-preventive isoprenoid. First, I showed that endogenous GGA is present in each organ of Wistar rat. In addition, previous studies have suggested that MAOB is involved in the oxidation of GGOH in cell-free experiments (37). In this study, I demonstrated that MAOB oxidized GGOH in cultured cells. In Chapter 3, we attempted to improve RI of C3H/HeN mice as biological activities of GGA other than carcinogenesis suppression. Addition of GGA to the feed given to C3H/HeN mice during the breeding period improved RI as in previous studies using SAM mice. Chapter 4 showed for the first time that endogenous GGA is biosynthesized through FPP and GGPP from the MVA pathway in human hepatoma-derived cells using ISA technique.

GGA is a novel, natural, and biologically active acyclic diterpenoid metabolite, not listed in the LIPID MAPS database (<http://www.lipidmaps.org>). Initially, GGA was noted as a chemically synthesized acyclic retinoid to be used as a preventive drug for second primary hepatoma together with peretinoin or 4,5-didehydroGGA (17). It has been reported GGA is a micromolar inducer of cell death in human hepatoma-derived cell lines through both UPR (25) and an incomplete response of autophagy (26). Also, it has reported natural occurrence of GGA in several medicinal herbs (33) and reported enzymatic formation of GGA from GGOH through GGal by rat liver homogenates and human hepatoma derived cell homogenate. Mitake et al reported in cell-free system that MAOB is involved in the oxidation of GGOH (37). However, it has not been clarified whether MAOB is involved in the oxidation of GGOH in cell culture systems.

Therefore, first, I demonstrated evidence for endogenous GGA, a hepatoma-preventive isoprenoid in mammalian cells. Endogenous free GGA was definitely present in various tissues of 5-week-old male Wistar rats, in especially high concentration in the liver. The amount of GGA in each organ of Wistar rat was the highest in the liver, followed by high concentrations in the organs involved in male reproductive organ. Neural tissues such as cerebellum and cerebrum also contained relatively high concentrations of GGA. Kotti et al reported that GGOH acts specifically and quickly to affect LTP (long-term potentiation) in the Schaffer

collaterals of the hippocampus without affecting protein geranylgeranylation (87, 88). GGA metabolized from GGOH may function to affect LTP. Another important finding in chapter 2 is that hepatic MAOB is involved in the synthesis of GGA through oxidation of GGOH. Reduction of MAOB activity by either inhibitor TCP or its siRNA introduction significantly reduced endogenous GGA level in human hepatoma cells. However, the amount of intracellular GGA was not reduced in *MAOB* knockout (Hep3B/*MAOB*-KO) cells compared with *MAOB* wild-type (Hep3B/*MAOB*-WT) cells. Interestingly, back-transfection of the *MAOB* gene into Hep3B/*MAOB*-KO cells completely restored the *MAOB* siRNA-mediated reduction of endogenous GGA, strongly suggesting that the *MAOB* gene is primarily responsible for maintenance of endogenous GGA level in human hepatoma cells. The maintenance of the cellular level of endogenous GGA in the *MAOB*-knockout cells suggests that GGA may be an essential metabolite having another important biological function other than cell death induction.

In chapter 2, GGA might have an essential role in life activity other than cell death induction. So, I examined the improvement of the reproductive index of mice as a biological activity of GGA other than the hepatocarcinogenesis inhibitory effect in chapter 3. In conclusion, taken together with the previous findings on GGA-induced improvement of the RI in SAM mice (54), I propose that the continuous GGA intake during a breeding period also improves the RI of mouse species such as C3H/HeN strain.

Since it showed not only a hepatoma-preventive effect but also an RI-improving effect, I finally decided to clarify the biosynthetic pathway of GGA with biological activities. In chapter 4, I demonstrated unequivocal evidence for mammalian GGA, a hepatoma-preventive isoprenoid. First, I demonstrated that the downregulation of endogenous GGA by pravastatin and upregulation of endogenous GGA by ZAA. Furthermore, ZAA-induced upregulation of endogenous GGA-induced cell death in HuH-7 cells. The most important finding is that GGA is synthesized from MVA in human hepatoma-derived HuH-7 cells through metabolic labeling of endogenous GGA by using ¹³C-labeled MVL.

As shown in chapter 2 and previous studies, GGA is synthesized by oxidation of GGOH. GGOH has

been reported to be obtained by dephosphorylation of GGPP, a metabolite from the MVA pathway, by GGPPase in rat liver microsomes. The MVA pathway is an important pathway that generates sterol and nonsterol isoprenoids, vital for multiple cellular functions. Nonsterol isoprenoids such as ubiquinone, heme A, dolichol, the farnesyl and geranylgeranyl groups of prenylated proteins are incorporated into diverse end products that participate in processes essential to life activities relating to such as cell growth, protein glycosylation and protein prenylation (1). Therefore, GGA, an isoprenoid with various biological activities was also speculated to be an endogenous metabolite derived from the MVA pathway in mammals.

Regarding the metabolic synthesis of GGA from MVA in animal cells, I must mention the pioneering studies by Fliesler and Schroepfer (89) and Foster et al. (90). More than a quarter century ago, they commonly found GGA and 2,3-dihydroGGA in bovine retina and the blood fluke, respectively, without discussion on their biological functions. In particular, it is worth noting that Fliesler and Schroepfer (89) originally observed the metabolic labeling of GGA from ³H-MVA using the tissue culture system of bovine retina, which strongly supports my study of endogenous GGA in mammalian cells.

I speculate that if carcinogenesis or infertility is caused by a decrease in endogenous GGA content, it can be prevented by taking exogenous GGA from daily meals. To validate the author's speculation, it will also be important to establish the analysis for further metabolites of GGA in humans and assessment indicators of endogenous GGA levels in the human body.

In previous studies, the effects of GGA on hepatocellular carcinoma have been demonstrated not only in vitro but also in vivo using C3H/HeN mice. It has been well known that male C3H/HeN mice develop spontaneous hepatoma at high incidence in 2 years after birth in normal raising conditions (91). Therefore, it is often used for experiments as a model animal of hepatic carcinogenesis. However, a mechanism underlying the hepato-carcinogenesis of this mouse has not yet been elucidated. A previous study reported that C3H/HeN mice given with acyclic retinoid, either GGA or 4,5-didehydroGGA, efficiently blocked spontaneous hepato-carcinogenesis (92). In this study, the liver carcinogenesis was most significantly inhibited by a single oral

supplementation of acyclic retinoid at around 11 months of age when observed at 23 months of age. The authors found that acyclic retinoid was effective at around 11 months after birth, but they have not completely elucidated the mechanism of acyclic retinoid-induced inhibition of carcinogenesis yet. At present, I am speculating that GGA may be involved in so-called immune surveillance mechanism against carcinogenesis in this mouse to pick up and remove the buds of tumor cells, and a putative aging-dependent decrease in the tissue GGA contents may lead to development of spontaneous hepatoma in C3H/HeN mice. I think that a narrow window at around 11 months after birth may be a timing when the hepatic GGA content age-dependently decreases down to a critical level that loses an ability to prevent carcinogenesis. Therefore, by oral supplementation of GGA at this time of 11 months after birth, the exogenously administered GGA may be able to suppress carcinogenesis at the age of 23 months by picking up and removing the buds of hepatoma cells at 11 months. Even if oral supplementation was carried out at the earlier stage than the critical point of 11 months, spontaneous hepato-carcinogenesis was not suppressed, because no bud of hepatoma cells appeared at the earlier time and the buds of hepatoma cell will appear after the disappearance of the administered GGA from the mouse body. Furthermore, oral supplementation at the later stage was also ineffective, suggesting that advanced cancer cells may be resistant to GGA treatment. To prove my hypothesis, I am in the middle of observation of age-dependent changes in the hepatic amount of GGA in the C3H/HeN mice in order to demonstrate a mechanistic linkage between a critical time point of GGA dosing and prevention of spontaneous hepato-carcinogenesis. When the amount of GGA in the liver of C3H/HeN mice was actually measured, hepatic GGA decreased depending on the age of the C3H/HeN mice. Interestingly, the mRNA expression level of hepatic MAOB decreased depending on the age of the mouse, and there was a significant correlation between hepatic GGA and hepatic MAOB mRNA expression levels (unpublished observations.). The mechanisms of the decrease in hepatic GGA and hepatic MAOB mRNA expression levels are unknown in C3H/HeN mice. Hence, I expected orally supplemented GGA, as a nutrient, might prevent spontaneous hepato-carcinogenesis, even after endogenous GGA synthesis is suppressed by aging. Previous studies have shown

that serum GGA levels increase in about 2 hours when GGA is taken by mouth (93). However, it is unclear whether absorbed GGA is efficiently transported into the liver. Therefore, it is necessary to find the most efficient way of taking GGA or its precursor for the future.

Arachidonic acid (ARA), a 20-carbon polyunsaturated fatty acid similar to GGA, is a nutrient that is taken from animal food products as lipids, stored into phospholipid and converted into secondary metabolites that exhibit various physiological activities *in vivo*. After release from phospholipid by phospholipase A2, ARA form various bioactive eicosanoids such as prostaglandins by enzymes such as cyclooxygenase. Prostaglandins were first discovered in semen (94). Prostaglandins were thought to be prostate-derived secretions but later found to be synthesized in many other tissues (94). Prostaglandins synthesized from ARA are bioactive as autocrine or paracrine factors. The effects of prostaglandins are diverse and are known to regulate inflammation, control cell growth, be involved in the physiological phenomena of pregnancy and parturition, and so on (62, 67, 95, 96). As well as ARA, the biological activity involved in GGA's inhibition of hepato-carcinogenesis and improvement of reproduction index may be caused by GGA itself or its derivatives. When ester-type lipids in HuH-7 cells were analyzed by TLC, the esterified GGA existed in the fraction of the origin including phospholipids (unpublished observation). As well as ARA, endogenous GGA is speculated to exhibit bioactivity after being released from phospholipids.

GGA has been reported to have RAR/RXR ligand activity (21). Retinoic acid signaling is known to play an important role in the induction of neuroblastoma cell differentiation (97) and normal development in mammalian ovaries and spermatozoa (98–100). Recently, it has been suggested that GGA-induced cell death is a pyroptosis through the activation of NLRP3 and IL-1 beta (101). Recent studies have reported that RAR-related orphan receptor γ (ROR γ) regulates the NLRP3 inflammasome (102). Furthermore, cholesterol precursor metabolites are suggested as a ligand for ROR but have not been fully identified (103, 104). At present, it is difficult to rationally explain GGA's seemingly unrelated biological activity of liver cancer cell death induction and reproduction. However, considering the diversity of bioactivity of eicosanoids such as

prostaglandins, GGA and its derivatives may be defined as the novel C₂₀ bioactive compound “geranylgeranoid”.

If I aim for primary prevention of diseases using GGA, which is both an endogenous metabolite and an exogenous nutrient, we will absolutely need to further elucidate the mechanisms that regulate GGA metabolism and any other biological activities of GGA. In the future, I am convinced that health evaluation of the amount of GGA synthesized in the human body and supplementing GGA and/or its derivatives with food to prevent certain diseases will be a necessary viewpoint for future nutritional science.

As I finish writing my doctoral thesis, I have now sincere hope that basic research on disease preventing endogenous metabolites such as GGA will pave a concrete road to protect future people from non-communicable diseases through major developments of human nutrition.

Chapter 6. Materials and Methods

Materials

Acetonitrile (LC/MS grade) (Sigma-Aldrich)

Arachidonic acid (Sigma-Aldrich)

Chloroform (Kanto Chemical)

Cholesterol (Sigma-Aldrich)

cis-8,11,14-eicosatrienoic acid (di-homo- γ -linolenic acid) (Sigma-Aldrich)

Dulbecco's modified Eagle medium (DMEM; high glucose, Wako Pure Chemical Industries)

Ethanol (Wako Pure Chemical Industries)

Fetal bovine serum (FBS; HyClone, Thermo Fisher Scientific)

All-*trans* FOH (Sigma-Aldrich)

All-*trans* GGA (Kuraray)

All-*trans* 2,3-dihydroGGA (Kuraray)

All-*trans* GGOH (Sigma-Aldrich)

All-*trans* GOH (Sigma-Aldrich)

n-Hexane (Kanto Chemical)

Hygromycin (Sigma-Aldrich)

Lipofectamine^R 2000 (Thermo Fisher Scientific)

Methanol (Wako Pure Chemical Industries)

MVL (Sigma-Aldrich)

DL-[1,2-¹³C₂]-MVL (ISOTEC)

Recombinant human MAOB (Activ-Motif)

Dulbecco's Phosphate Buffered Saline, without calcium chloride and magnesium chloride (PBS (-); Sigma-Aldrich)

Pravastatin (Daiichi Sankyo Co.)

Puromycin (Sigma-Aldrich)

TCP (Sigma Aldrich)

ZAA (Merck)

All chemicals other than those stated above were of reagent grade.

Methods

Animals, housing and sacrifice

Male Wistar rats (5-week old) and C3H/HeN mice were provided by CLEA Japan, Inc. Tokyo, Japan, and have been raised in the animal facility of University of Nagasaki. Animals were housed in individual plastic cages containing wood shavings as bedding. The plastic cage was placed on a shelf in a 12-h (08:00-20:00) light-dark cycle room at 22-25°C and 60~80% humidity with freely available a conventional diet (CE-2, CLEA Japan) and tapping water. The rats were fed a CE-2 for several days, and then the animals under the isoflurane anesthesia were sacrificed by collecting blood through the vena cava and the 12 organs were immediately excised, weighed and instantaneously frozen at -25°C until use. The Mice were used for mating experiments. These research plans were approved by our university's animal experiment ethics committee. (approval no. 28-02, 29-29)

Cell Culture

Human hepatoma-derived cell lines of HuH-7, Cell Bank (RIKEN, Wako, Saitama, Japan) and Hep3B cells, DS Pharma Biomedical (Suita, Osaka, Japan) were maintained with DMEM containing 5% FBS at 37°C in a humidified atmosphere of 5% CO₂.

Lipid extraction and quantitative measurement of GGA contents

Male Wistar rat organs

Each organ was hand-homogenized using a Potter glass grinder in 10 vol of methanol. Then, the homogenates were transferred to a screw-capped glass tube and were added into 20 vol of chloroform. All sample suspensions were covered with aluminum foil and agitated reciprocally at 4°C overnight. After centrifugation, the supernatant was collected into a new screw-capped glass tube and evaporated to dryness under nitrogen stream on a Reacti-Therm™ heating module (Pierce, Rockford, IL, USA). The residues were

dissolved with ethanol, which was 10 volumes of the wet weight of the tissue used. The resultant ethanolic solution was applied onto ethanol-equilibrated C₁₈ solid-phase cartridges (Bond Elute C18, Agilent, Tokyo, Japan) and the flow-through fractions were used as lipid extracts. The lipid extracts were finally filtered through a cartridge of Cosmonice Filter S, PTFE (Nacalai Tesque, Kyoto, Japan, 0.45 µm, 13 mm) just prior to LC/MS/MS analysis.

Human hepatoma-derived cells

HuH-7 or Hep3B cells and the conditioned medium were separately collected in each tube by centrifugation (2700 rpm, 8 min). To extract the total cellular lipid, the cell pellets were added to chloroform/methanol (2:1 v/v; 20-fold volume over cell volume) and sonicated on ice (three times; each 30 s). After standing overnight at room temperature and being centrifuged, the supernatant was transferred to a screw-capped glass tube and evaporated to dryness under nitrogen stream. The residues were dissolved with 100 µL of ethanol and filtered through a cartridge of Cosmonice Filter S (0.45 µm) prior to LC/MS/MS analysis.

LC/MS/MS analysis

LC was performed by using a Waters Acquity Ultra Performance LC apparatus (Waters, Milford, MA, USA) equipped with Acquity UPLC-HSS T3 column, 100 × 2.1 mm, 1.8 µm (Waters). A tandem quadrupole mass detector system was operated in MRM mode. Nitrogen was used as a desolvation gas (800 L/h) and a cone gas (50 L/h). The desolvation temperature was 450°C. Argon was used as the collision gas (0.15 mL/min) and the collision energy was 20 eV. The capillary voltage was set at 3.0 kV, and the source temperature was 135°C for ESI. The chromatographic run was operated by linear gradients between solution A (acetonitrile) and solution B (milli-Q water). The elution was conducted at a constant flow rate of 0.30 mL/min as follows: 0–9 min, isocratic 74% A; 9–10 min, a linear ascending gradient from 74% A to 100% A; 10–15 min, 100% A; 15–16 min, a linear descending gradient from 100% A to 74% A; 16–19 min, 74% A.

The chromatographic run to measure GGOH and GGal was operated by linear gradients between solution A (milli-Q water containing 0.1% formic acid) and solution B (acetonitrile containing 0.1% formic acid). The elution was conducted at a constant flow rate of 0.30 ml/min as follows: 0–12 min, isocratic 74% B; 2–13 min, a linear ascending gradient from 74% B to 100% B; 13–18 min, 100% B; 18–19 min, a linear descending gradient from 100% B to 74% B; 19–22 min, 74% B. The specific combination of molecular ion and fragment ion, cone voltage and collision cell energy for each compound were listed in Table 6-1. For sample analysis, 5 μ L of each sample was injected onto the column.

Table. 6-1. MRM mode conditions, and transition for each compound.

Compound	m/z		Charge	Cone voltage (V)	Collision energy (eV)
	Molecular ion	→ Fragment ion			
GGA	303.11	→ 98.11	–	44	20
ARA	303.11	→ 259.11	–	36	12
2,3-dihydroGGA	305.33	→ 168.23	–	48	18
GGal	289.4	→ 271.3	+	20	10
Fal	221.3	→ 203.3	+	20	11
Gal	153.2	→ 135.2	+	20	10

MRM, multiple-reaction-monitoring; GGA, geranylgeranoic acid; ARA, arachidonic acid; GGal, geranylgeranial; Fal, farnesal; Gal, geranial.

-Chapter 2-

Treatment of HuH-7 and Hep3B cells with TCP

HuH-7 cells (5×10^5 cells/dish, in a 10-cm diameter dish) were inoculated and cultured with DMEM containing 5% FBS for 24 h; thereafter, the medium was replaced with FBS-free DMEM 1 day before tranlycypromine hydrochloride (Sigma Aldrich, St. Louis, MO) treatment. After 24-h treatment of the cells with different concentrations (0 - 100 μ M) of TCP or with 100 μ M of TCP + 25 μ M GGOH (99% pure, kindly provided from Eisai Foods, Tokyo, Japan), the cells were harvested using a plastic cell lifter (Nunc, Roskilde, Denmark) and the cellular GGA was quantitatively measured using liquid chromatography tandem mass spectrometry (LC/MS/MS) as described below. IC₅₀ of TCP on the endogenous GGA levels was calculated using GraphPad Prism version 7.0 for Windows (GraphPad Software, La Jolla, CA).

Transfection with small interfering RNA

Ready-made siRNAs for *MAOB*, *MAOA*, *ADH1A*, and *PCYOX1* genes were purchased from Santa Cruz Biotechnology (Santa Cruz, CA, Table 6-2). For transfection, HuH-7 cells or Hep3B cells were inoculated on 3-cm dishes at a density of 4×10^4 cells/dish. On the next day, 80 pmol of each siRNA were transfected using Lipofectamine^R 2000 (Thermo Fisher Scientific). After 72-h incubation, total RNA was isolated from cells to measure the cellular mRNA levels of each gene. Cells incubated for an additional 48 h (120 h in total after transfection) were used for LC/MS/MS quantification of intracellular GGA.

Table. 6-2. The sequences of each siRNA used for knockdown.

		Sequence (5' – 3')
<i>siMAOA</i>	Sense A	GUGACAACAUCAUCAUAGATT
	Antisense A	UCUAUGAUGAUGUUGUCACTT
	Sense B	CGACUUCUCUAGACAUCUATT
	Antisense B	UAGAUGUCUAGAGAAGUCGTT
	Sense C	GGAUCCUUGUCAGUUGUAATT
	Antisense C	UUACAACUGACAAGGAUCCTT
<i>siMAOB</i>	Sense A	GCAUGAAGAUUCACUUCAATT
	Antisense A	UUGAAGUGAAUCUUCAUGCTT
	Sense B	CUCUGCCAAUGAUGAGAAATT
	Antisense B	UUUCUCAUCAUUGGCAGAGTT
	Sense C	GGCUUAGCGUUCUGUUUCATT
	Antisense C	UGAAACAGAACGCUAAGCCTT
<i>siPCYOX1</i>	Sense A	GGAAAGAUGUGAAGAUAGATT
	Antisense A	UCUAUCUUCACAUCUUUCCTT
	Sense B	CCACUCCGUUGAAUCGAAATT
	Antisense B	UUUCGAUUCAACGGAGUGGTT
	Sense C	GAAGCCCAAUCUGUAUCAATT
	Antisense C	UUGAUACAGAUUGGGCUUCTT
<i>siADH1A</i>	Sense A	GCCUCUAGAGAAAGUCUGUTT
	Antisense A	ACAGACUUUCUCUAGAGGCTT
	Sense B	CCGUACCAUUCUGAUGUUUTT
	Antisense B	AAACAUCAGAAUGGUACGGTT
	Sense C	GCAACAGCUGGGAAAUAUUCTT
	Antisense C	GAUAUUUCCCAGCUGUUGCTT

siRNA, small interfering RNA; MAOA, monoamine oxidase A; MAOB, monoamine oxidase B; PCYOX1, prenylcysteine oxidase 1; ADH1A, alcohol dehydrogenase 1.

RT-qPCR

Total RNA was isolated from each cell cultures using the FastgeneTM RNA Basic kit (Nippon Genetics, Tokyo, Japan). For cDNA synthesis, FastgeneTM Scriptase II (Nippon Genetics) was used according to the manufacturer's instructions. Real-time PCR was performed using LightCycler FastStart DNA Master PLUS SYBR Green I (Roche Diagnostics, Tokyo, Japan) on LightCycler 96 (Roche). Gene expression levels were analyzed using the $2^{-\Delta\Delta Ct}$ method. Primer sequences and real-time PCR settings used in this study are presented in supplementary Table 6-3, 6-4 and 6-5.

Table. 6-3 The nucleotide sequences of each primer used for real-time RT-qPCR.

F: forward primer, R: reverse primer

Genes	Primer	Sequence (5' – 3')
<i>MAOA</i>	F	CAGCTCCTGGTGGAGAGACTA
	R	TGGGTTGGTCCCACATAAGC
<i>MAOB</i>	F	GCAACAAATGCGACGTGGT
	R	AGGATCCTCCAAGGTCCACA
<i>PCYOX1</i>	F	TGAGGAGAGCAACTGGTTCA
	R	ACTGGTAGCGGTAGATCCTCA
<i>ADH1A</i>	F	TCTGGGAAAAGTATCCGTACCATT
	R	TGAAGACTGCCACAAGGGAA
<i>28S rRNA</i>	F	TTAGTGACGCGCATGAATGG
	R	TGTGGTTTCGCTGGATAGTAGGT

MAOA, monoamine oxidase A; MAOB, monoamine oxidase B; PCYOX1, prenylcysteine oxidase 1; ADH1A, alcohol dehydrogenase 1.

Table. 6-4. The condition of thermal cycler for real-time PCR of *MAOA*, *MAOB*, *PCYOX1*, *ADH1A* cDNAs.

Step	Temperature, Duration	Slope
Denature	95°C, 600 s	20°C / s
PCR (40 cycles)	95°C, 15 s	20°C / s
	60°C, 60 s	20°C / s
Melting	95°C, 0 s	20°C / s
	57°C, 15 s	20°C / s
	98°C, 0 s	-
Cooling	40°C, 30 s	20°C / s

MAOA, monoamine oxidase A; MAOB, monoamine oxidase B; PCYOX1, prenylcysteine oxidase 1; ADH1A, alcohol dehydrogenase 1.

Table. 6-5. The condition of thermal cycler for real-time qPCR of *28S rRNA* cDNA.

	Temperature, Duration	Slope
Denature	95°C, 600 s	4.4°C / s
PCR (40 cycles)	95°C, 10 s	4.4°C / s
	60°C, 10 s	2.2°C / s
	72°C, 3 s	4.4°C / s
Melting	95°C, 1 s	4.4°C / s
	65°C, 15 s	2.2°C / s
	95°C, 1 s	-
Cooling	40°C, 30 s	4.4°C / s

Enzyme assays

Aliquots of 3-100 μ M GGOH, FOH, or GOH were incubated at 37°C with the recombinant human MAOB protein (0.15 μ g, >85% pure, Active Motif, Carlsbad, CA) in a final volume of 100 μ L H₂O. The reaction was then stopped by chilling on ice, and the reaction mixture was diluted with 9 vol of ethanol. The resultant ethanolic extract was filtered through a cartridge of Cosmonice Filter S (0.45 μ m) prior to the analyses of GGal, Fal and Gal by LC/MS/MS. *K_m* for each substrate was calculated using GraphPad Prism 7.0.

Knockout of the MAOB gene in hepatoma cells by using CRISPR-Cas9 system

HuH-7 or Hep3B cells (3×10^4 cells/dish, in a 30-mm diameter dish) were transfected with 1 μ g MAOB CRISPR-Cas9 KO plasmids and 1 μ g HDR plasmids (Santa Cruz Biotechnology). After approximately 2-wk screening with 2 μ g/mL puromycin, Hep3B, but no HuH-7 cell clones were established by confirming RFP fluorescence on a laser-scanning confocal fluorescence microscope (LSM-700, Carl Zeiss, Berlin, Germany) and a lack of both *MAOB* mRNA expression using RT-qPCR method and MAOB protein expression using Western blotting method was confirmed in these Hep3B/*MAOB*-KO cells.

Back transfection of the MAOB gene in Hep3B/MAOB KO cells.

Hep3B/*MAOB* KO cells (3×10^4 cells/dish, in a 30-mm diameter dish) were transfected with 1 μ g human *MAOB* gene ORF cDNA clone expression plasmid (Sino Biological, Beijing, China). After approximately 2-wk selection with 200 μ g/mL hygromycin (Sigma Aldrich), re-expression of both *MAOB* mRNA using RT-qPCR method and MAOB protein using Western blotting method were confirmed in Hep3B/*MAOB*-KO/TG cells.

Immunoblotting

Proteins were prepared from the cells with RIPA lysis buffer (Merck Millipore, Tokyo, Japan) containing protease inhibitors (Roche Diagnostic) and the solubilized proteins were quantified by Bradford assay (Bio-Rad, Hercules, CA, USA). Equal amounts (10 μ g) of protein per sample were separated by Mini-PROTEAN TGX precast gels (Bio-Rad) and transferred onto polyvinylidene fluoride membranes. Horseradish peroxidase-labeled secondary antibodies (GE Healthcare, Tokyo, Japan) were detected with ECL plus western blotting detection system (GE Healthcare) or SuperSignal[™] West Femto maximum sensitivity substrate (Thermo Fisher Scientific) using ImageQuant LAS 4000 (GE Healthcare).

-Chapter 3-

Preparation of GGA-containing diets and schedule of feeding each experimental diet.

Aliquots of GGA (50 µg dissolved in 300 µL ethanol) were dropped and soaked into each pellet (roughly 3 g) of CE-2 and the vehicle solvent was removed by overnight air ventilation in a draft chamber. After removal of the solvent, the pellets were kept frozen at -25 °C until use. For a control group, only ethanol was used with the same treatment as CE-2 containing GGA to prepare control CE-2 diet.

Experiment I: Two females (10-week old) and one male (10-week old) were put all together into a plastic cage with each experimental diet. The control diet CE-2 was given to the control group and GGA-containing CE-2 was provided for a GGA group. Six pairs in each group, a total of 12 pairs (6 males and 12 females), were used for Experiment I. After 1-week mating period, each female mouse was separated into a plastic cage one by one. Although male mice were back to conventional maintenance, the putative pregnant mice were continuously fed on each experimental diet throughout the entire experimental term. Therefore, the embryos and pre-weanlings were potentially exposed to the experimental diets through placenta and mother's milk, respectively. After having confirmed the presence of each infant twice a day after delivery, the RI was calculated 3 weeks after pups were born.

Experiment II: The same experimental procedure was conducted to confirm the reproducibility, a few months after Experiment I. In Experiment II, an additional group given commercially-available breeding diet (CA-1, CLEA Japan) was set up. CA-1 is a feed enriched with n-3 polyunsaturated fatty acids and fat-soluble vitamins, etc. for reproduction, compared to conventional chow diet CE-2 for growth. By setting the group fed on CA-1 as a positive control, we compared RI values of the GGA supplemented CE-2 group and the CA-1 group. Six pairs in each group, a total of 18 pairs (9 males and 18 females, 10-week old), were used for Experiment II.

Experiment III: In order to investigate the effects of difference in GGA administration period on the RI, four different groups were set out; as follows, control (Control) and continuous GGA intake (GGA) groups

were the same as those in Experiments I and II, and the other 2 groups consisted of GGA-I group fed on GGA-containing CE-2 only during putative pregnant period (for 3 weeks from the end of the mating period) and GGA-II group fed on GGA-containing CE-2 only during the lactation period (for 3 weeks after delivery). Five to six pairs in each group, a total of 19 pairs (12 males and 19 females, 10-week old), were used for experiment III. Other experimental conditions were the same as in Experiments I and II. For these 3 experiments, all mice used were without any ex-reproductive experience.

Analysis of pups and statistical analysis

As mentioned above, RI was defined as the number of weanling pups divided by the number of the mated females in each experimental group. Weanling rate (WR) was defined as the number of the weaned pups divided by the number of the delivered pups in each group. The difference of WR values between 2 groups was estimated by chi-square test. The difference in the mean values of RI in 3 experiments between control and GGA-treated groups and the difference in the mean values between the corresponding 2 groups were analyzed by Student's t-test. Survival rate of pups: After birth, pups' survival was checked twice a day. The survival rate curves were produced by Kaplan-Meier method, using GraphPad Prism version 7.0 for Windows (GraphPad Software, La Jolla, CA, USA). Statistical significance between 2 groups was estimated by a generalized Wilcoxon test with Gehan-Breslow method.

-Chapter 4-

Treatment of HuH-7 cells with pravastatin and ZAA

HuH-7 cells (5×10^5 cells/dish, in a 100-mm diameter dish) were inoculated and cultured with DMEM containing 5% FBS for 24 h, thereafter the medium was replaced with FBS-free DMEM 1 day before pravastatin and/or ZAA treatment. After 48 h treatment with 120 μ M pravastatin and/or 15 μ M ZAA, the cells were harvested using a plastic cell lifter (Nunc, Roskilde, Denmark).

Concentration-dependent cytotoxicity of ZAA against HuH-7 cells

HuH-7 cells (1.0×10^5 cells/well, 6-well plate) were cultured with DMEM containing 5% FBS for 24 h. Thereafter, the medium was replaced with FBS-free DMEM 1 day before treatment with increasing concentrations (0–60 μ M) of ZAA with or without pravastatin (120 μ M) or cholesterol (50 μ M). After addition of ZAA, the number of viable cells were counted by the trypan blue dye exclusion method at 48 h after addition of ZAA. LD₅₀ was calculated using GraphPad Prism version 7.0 for Windows (GraphPad Software, La Jolla, CA, USA).

Metabolic labeling of GGA with ¹³C-mevalonolactone

HuH-7 cells (5×10^5 cells/dish) were inoculated and cultured with DMEM containing 5% FBS for 24 h, thereafter the medium was replaced with FBS-free DMEM 1 day before pravastatin treatment. After 24-h treatment with 120 μ M pravastatin, 15 μ M ZAA and 2 mM ¹³C-MVL were both added into the culture medium and incubated for 48 h. The cells were harvested using a cell lifter. To chase the labeled GGA, the cells under the same conditions as above were replenished with fresh FBS-free DMEM containing 120 μ M pravastatin and incubated for 24 h. Then, the cells were incubated for a further 48 h with 15 μ M ZAA and 2 mM cold-MVL. They were finally harvested using a plastic cell lifter.

Labeling experiments for Isotopomer Spectral Analysis (ISA):

HuH-7 cells (5×10^5 cells/dish) were preincubated for 12 h with 120 μ M pravastatin and 15 μ M ZAA. Then, 2 mM ^{13}C -MVL was added and the cells were further incubated. The cells were harvested to extract the cellular lipids at the indicated time points (6, 12, 24, 48 and 72 h after addition of ^{13}C -MVL) and the resultant lipid extracts were analyzed by LC/MS/MS to discriminate and measure each isotopologue.

Other statistical analyses

Statistical comparisons were performed using a t-test or ANOVA with Post hoc Scheffe where appropriate. All data, unless specified, are presented as mean \pm SE, with a statistically significant difference defined as $p \leq 0.05$.

7. Acknowledgments

This work was carried out in the Laboratory of Molecular and Cellular Biology, Graduate School of Human Health Science, University of Nagasaki in Nagayo, Nagasaki during the years 2015 – 2019.

My deepest appreciation goes to Prof. Yoshihiro Shidoji who offered continuing support and constant encouragement.

I would also like to thank Prof. Hiroshi Sagami, of Tohoku University for his fruitful discussion on my studies.

I would sincerely express their gratitude to Professor Ken Aoki of the University of Nagasaki for creating a computer program for a nonlinear approximation method in ISA.

I am indebted to Sayaka Uematsu for mice breeding-experiments and wish to thank the present and former members of the Shidoji research group for all your help.

At the end, I owe my deepest gratitude to my parents for their understanding and generous support. I never thank you enough.

8. References

1. Guggisberg, A. M., Amthor, R. E., and Odom, A. R. (2014) Isoprenoid biosynthesis in *Plasmodium falciparum*. *Eukaryot. Cell.* **13**, 1348–1359
2. Crane, F. L. (2001) Biochemical functions of coenzyme Q10. *J. Am. Coll. Nutr.* **20**, 591–598
3. Wang, M., and Casey, P. J. (2016) Protein prenylation: unique fats make their mark on biology. *Nat. Rev. Mol. Cell Biol.* **17**, 110–122
4. Cantagrel, V., Lefeber, D. J., Ng, B. G., Guan, Z., Silhavy, J. L., Bielas, S. L., Lehle, L., Hombauer, H., Adamowicz, M., Swiezewska, E., De Brouwer, A. P., Blümel, P., Sykut-Cegielska, J., Houliston, S., Swistun, D., Ali, B. R., Dobyns, W. B., Babovic-Vuksanovic, D., van Bokhoven, H., Wevers, R. A., Raetz, C. R. H., Freeze, H. H., Morava, É., Al-Gazali, L., and Gleeson, J. G. (2010) SRD5A3 is required for converting polyprenol to dolichol and is mutated in a congenital glycosylation disorder. *Cell.* **142**, 203–217
5. Bergman, M. E., Davis, B., and Phillips, M. A. (2019) Medically useful plant terpenoids: Biosynthesis, occurrence, and mechanism of action. *Molecules.* **24**, 3961
6. Rilling, H., Tchen, T. T., and Bloch, K. (1958) On the mechanism of squalene biogenesis. *Proc. Natl. Acad. Sci. U. S. A.* **44**, 167–173
7. Beyer, P., Al-Babili, S., Ye, X., Lucca, P., Schaub, P., Welsch, R., and Potrykus, I. (2002) Golden rice: introducing the beta-carotene biosynthesis pathway into rice endosperm by genetic engineering to defeat vitamin A deficiency. *J. Nutr.* **132**, 506S-510S
8. Hoeg, J. M., and Brewer, H. B. (1987) 3-Hydroxy-3-methylglutaryl-coenzyme A reductase inhibitors in the treatment of hypercholesterolemia. *JAMA.* **258**, 3532–3536
9. Luckman, S. P., Hughes, D. E., Coxon, F. P., Russell, R. G. G., Rogers, M. J., and Rogers, M. J. (1998) Nitrogen-containing bisphosphonates inhibit the mevalonate pathway and prevent post-translational prenylation of GTP-binding proteins, including Ras. *J. Bone Miner. Res.* **13**, 581–589

10. Fernandes, N. V., Yeganehjoo, H., Katuru, R., Debose-Boyd, R. A., Morris, L. L., Michon, R., Yu, Z. L., and Mo, H. (2013) Geranylgeraniol suppresses the viability of human DU145 prostate carcinoma cells and the level of HMG CoA reductase. *Exp. Biol. Med.* 10.1177/1535370213492693.
11. Onono, F., Subramanian, T., Sunkara, M., Subramanian, K. L., Peter Spielmann, H., and Morris, A. J. (2013) Efficient use of exogenous isoprenols for protein isoprenylation by MDA-MB-231 cells is regulated independently of the mevalonate pathway. *J. Biol. Chem.* **288**, 27444–27455
12. Alberts, A W., Chen, J., Kuron, G., Hunt, V., Huff, J., Hoffman, C., Rothrock, J., Lopez, M., Joshua, H., Harris, E., Patchett, A, Monaghan, R., Currie, S., Stapley, E., Albers-Schonberg, G., Hensens, O., Hirshfield, J., Hoogsteen, K., Liesch, J., and Springer, J. (1980) Mevinolin: a highly potent competitive inhibitor of hydroxymethylglutaryl-coenzyme A reductase and a cholesterol-lowering agent. *Proc. Natl. Acad. Sci. U. S. A.* **77**, 3957–3961
13. Liao, J. K., and Laufs, U. (2005) Pleiotropic effects of statins. *Annu. Rev. Pharmacol. Toxicol.* **45**, 89–118
14. Sacchettini, J. C., and Poulter, C. D. (1997) Creating isoprenoid diversity. *Science.* **277**, 1788–1789
15. Seybold, S. J., and Tittiger, C. (2003) Biochemistry and molecular biology of de novo isoprenoid pheromone production in the Scolytidae. *Annu. Rev. Entomol.* **48**, 425–453
16. Yob, E. H., and Pochi, P. E. (1987) Side effects and long-term toxicity of synthetic retinoids. *Arch. Dermatol.* **123**, 1375–1378
17. Muto, Y., Moriwaki, H., Ninomiya, M., Adachi, S., Saito, A., Takasaki, K. T., Tanaka, T., Tsurumi, K., Okuno, M., Tomita, E., Nakamura, T., and Kojima, T. (1996) Prevention of second primary tumors by an acyclic retinoid, polyprenoic acid, in patients with hepatocellular carcinoma. Hepatoma Prevention Study Group. *N. Engl. J. Med.* **334**, 1561–1567
18. Muto, Y., Moriwaki, H., and Saito, A. (1999) Prevention of second primary tumors by an acyclic retinoid in patients with hepatocellular carcinoma. *N. Engl. J. Med.* **340**, 1046–1047

19. Muto, Y., and Moriwaki, H. (1991) Acyclic retinoids and cancer chemoprevention. *Pure Appl. Chem.* **63**, 157–160
20. Muto, Y., Moriwaki, H., and Omori, M. (1981) In vitro binding affinity of novel synthetic polyprenoids (polyprenoic acids) to cellular retinoid-binding proteins. *Gan.* **72**, 974–977
21. Araki, H., Shidoji, Y., Yamada, Y., Moriwaki, H., and Muto, Y. (1995) Retinoid agonist activities of synthetic geranyl geranoic acid derivatives. *Biochem. Biophys. Res. Commun.* **209**, 66–72
22. Yamada, Y., Shidoji, Y., Fukutomi, Y., Ishikawa, T., Kaneko, T., Nakagama, H., Imawari, M., Moriwaki, H., and Muto, Y. (1994) Positive and negative regulations of albumin gene expression by retinoids in human hepatoma cell lines. *Mol. Carcinog.* **10**, 151–158
23. Muto, Y., and Moriwaki, H. (1984) Antitumor activity of vitamin A and its derivatives. *J. Natl. Cancer Inst.* **73**, 1389–1393
24. Nakamura N, Shidoji Y, Yamada Y, Hatakeyama H, Moriwaki H, and Muto Y (1995) Induction of apoptosis by acyclic retinoid in the human hepatoma derived cell line, HuH-7. *Biochem. Biophys. Res. Commun.* **207**, 382–388
25. Iwao, C., and Shidoji, Y. (2015) Polyunsaturated branched-chain fatty acid geranylgeranoic acid induces unfolded protein response in human hepatoma cells. *PLoS One.* 0.1371/journal.pone.0132761
26. Okamoto, K., Sakimoto, Y., Imai, K., Senoo, H., and Shidoji, Y. (2011) Induction of an incomplete autophagic response by cancer-preventive geranylgeranoic acid (GGA) in a human hepatoma-derived cell line. *Biochem. J.* **440**, 63–71
27. Shimonishi, S., Muraguchi, T., Mitake, M., Sakane, C., Okamoto, K., and Shidoji, Y. (2012) Rapid downregulation of Cyclin D1 induced by geranylgeranoic acid in human hepatoma cells. *Nutr. Cancer.* **64**, 473–480
28. Iwao, C., and Shidoji, Y. (2014) Induction of nuclear translocation of mutant cytoplasmic p53 by geranylgeranoic acid in a human hepatoma cell line. *Sci. Rep.* **4**, 4419

29. Shidoji, Y., Nakamura, N., Moriwaki, H., and Muto, Y. (1997) Rapid loss in the mitochondrial membrane potential during geranylgeranoic acid-induced apoptosis. *Biochem Biophys Res Commun.* **230**, 58–63
30. Muto, Y., and Moriwaki, H. (1991) Acyclic retinoids and cancer chemoprevention. *Pure&App/Chem.* **63**, 157–160
31. Iwao, C., and Shidoji, Y. (2015) Upregulation of energy metabolism-related, p53-target TIGAR and SCO2 in HuH-7 cells with p53 mutation by geranylgeranoic acid treatment. *Biomed. Res.* **36**, 371–381
32. Shidoji, Y., Okamoto, K., Muto, Y., Komura, S., Ohishi, N., and Yagi, K. (2006) Prevention of geranylgeranoic acid-induced apoptosis by phospholipid hydroperoxide glutathione peroxidase gene. *J. Cell. Biochem.* **97**, 178–187
33. Shidoji, Y., and Ogawa, H. (2004) Natural occurrence of cancer-preventive geranylgeranoic acid in medicinal herbs. *J. Lipid Res.* **45**, 1092–1103
34. Bansal, V. S., and Vaidya, S. (1994) Characterization of two distinct allyl pyrophosphatase activities from rat liver microsomes. *Arch. Biochem. Biophys.* **315**, 393–399
35. Endo, S., Matsunaga, T., Ohta, C., Soda, M., Kanamori, A., Kitade, Y., Ohno, S., Tajima, K., El-Kabbani, O., and Hara, A. (2011) Roles of rat and human aldo–keto reductases in metabolism of farnesol and geranylgeraniol. *Chem. Biol. Interact.* **191**, 261–268
36. Muraguchi, T., Okamoto, K., Mitake, M., Ogawa, H., and Shidoji, Y. (2011) Polished rice as natural sources of cancer-preventing geranylgeranoic acid. *J. Clin. Biochem. Nutr.* **49**, 8–15
37. Mitake, M., and Shidoji, Y. (2012) Geranylgeraniol oxidase activity involved in oxidative formation of geranylgeranoic acid in human hepatoma cells. *Biomed. Res.* **33**, 15–24
38. Konradi, C., Riederer, P., Jellinger, K., and Denney, R. (1987) Cellular action of MAO inhibitors. *J. Neural Transm. Suppl.* **25**, 15–25

39. Müller, T., and Möhr, J. (2019) Pharmacokinetics of monoamine oxidase B inhibitors in Parkinson's disease: current status. *Expert Opin. Drug Metab. Toxicol.* **15**, 429–435
40. Saura, J., Luque, J. M., Cesura, A. M., Prada, M. Da, Chan-Palay, V., Huber, G., Löffler, J., and Richards, J. G. (1994) Increased monoamine oxidase b activity in plaque-associated astrocytes of Alzheimer brains revealed by quantitative enzyme radioautography. *Neuroscience.* **62**, 15–30
41. Mallajosyula, J. K., Chinta, S. J., Rajagopalan, S., Nicholls, D. G., and Andersen, J. K. (2009) Metabolic control analysis in a cellular model of elevated MAO-B: relevance to Parkinson's disease. *Neurotox. Res.* **16**, 186–193
42. Yanez, M., and Vina, D. (2013) Dual inhibitors of monoamine oxidase and cholinesterase for the treatment of Alzheimer disease. *Curr. Top. Med. Chem.* **13**, 1692–1706
43. Alborghetti, M., and Nicoletti, F. (2019) Different generations of type-B monoamine oxidase inhibitors in Parkinson's disease: from bench to bedside. *Curr. Neuropharmacol.* **17**, 861–873
44. Fagerberg, L., Hallström, B. M., Oksvold, P., Kampf, C., Djureinovic, D., Odeberg, J., Habuka, M., Tahmasebpoor, S., Danielsson, A., Edlund, K., Asplund, A., Sjöstedt, E., Lundberg, E., Szigartyo, C. A. K., Skogs, M., Takanen, J. O., Berling, H., Tegel, H., Mulder, J., Nilsson, P., Schwenk, J. M., Lindskog, C., Danielsson, F., Mardinoglu, A., Sivertsson, Å., von Feilitzen, K., Forsberg, M., Zwahlen, M., Olsson, I., Navani, S., Huss, M., Nielsen, J., Ponten, F., and Uhlén, M. (2014) Analysis of the human tissue-specific expression by genome-wide integration of transcriptomics and antibody-based proteomics. *Mol. Cell. Proteomics.* **13**, 397–406
45. Gaweska, H., and Fitzpatrick, P. F. (2011) Structures and mechanism of the monoamine oxidase family. *Biomol. Concepts.* **2**, 365–377
46. Zhou, L., Vessby, B., and Nilsson, A. (2002) Quantitative role of plasma free fatty acids in the supply of arachidonic acid to extrahepatic tissues in rats. *J. Nutr.* **132**, 2626–2631
47. Bian, Q., Wang, W., Wang, N., Peng, Y., Ma, W., and Dai, R. (2016) Quantification of arachidonic

- acid and its metabolites in rat tissues by UHPLC-MS/MS: application for the identification of potential biomarkers of benign prostatic hyperplasia. *PLoS One*. **11**, e0166777
48. Kodaira, Y., Usui, K., Kon, I., and Sagami, H. (2002) Formation of (R)-2,3-dihydrogeranylgeranoic acid from geranylgeraniol in rat thymocytes. *J Biochem*. **132**, 327–334
49. Dulaney, J. T., Williams, M., Evans, J. E., Costello, C. E., and Kolodny, E. H. (1978) Occurrence of novel branched-chain fatty acids in refsum's disease. *Biochim. Biophys. Acta*. **529**, 1–12
50. Evans, J. E., and Dulaney, J. T. (1983) Location of double bonds in two unsaturated forms of phytanic acid from Refsum disease as determined by mass spectrometry. *Biochim. Biophys. Acta*. **752**, 346–352
51. Hubálek, F., Binda, C., Khalil, A., Li, M., Mattevi, A., Castagnoli, N., and Edmondson, D. E. (2005) Demonstration of isoleucine 199 as a structural determinant for the selective inhibition of human monoamine oxidase B by specific reversible inhibitors. *J. Biol. Chem*. **280**, 15761–15766
52. Khalil, A. A., Davies, B., and Castagnoli, N. (2006) Isolation and characterization of a monoamine oxidase B selective inhibitor from tobacco smoke. *Bioorg. Med. Chem*. **14**, 3392–3398
53. Sari, Y., and Khalil, A. (2015) Monoamine oxidase inhibitors extracted from tobacco smoke as neuroprotective factors for potential treatment of Parkinson's disease. *CNS Neurol. Disord. - Drug Targets*. **14**, 777–785
54. Shidoji, Y., Okamoto, K., and Sakane, C. (2011) A livestock feed or a promoter for improving birth rate applied to mammals, a tranquilizer applied to mammals (in Japanese) JP patent, JP 2011-207902 A.
55. Ji, Y.-Y., Lin, S.-D., Wang, Y.-J., Su, M.-B., Zhang, W., Gunosewoyo, H., Yang, F., Li, J., Tang, J., Zhou, Y.-B., and Yu, L.-F. (2017) Tying up tranlycypromine: Novel selective histone lysine specific demethylase 1 (LSD1) inhibitors. *Eur. J. Med. Chem*. **141**, 101–112
56. Taavitsainen, P., Juvonen, R., and Pelkonen, O. (2001) In vitro inhibition of cytochrome P450

- enzymes in human liver microsomes by a potent CYP2A6 inhibitor, trans-2-phenylcyclopropylamine (tranylcypromine), and its nonamine analog, cyclopropylbenzene. *Drug Metab. Dispos.* **29**, 217–222
57. Babić Leko, M., Nikolac Perković, M., Klepac, N., Švob Štrac, D., Borovečki, F., Pivac, N., Hof, P. R., and Šimić, G. (2019) Relationships of cerebrospinal fluid Alzheimer’s disease biomarkers and COMT, DBH, and MAOB single nucleotide polymorphisms. *J. Alzheimer’s Dis.* 10.3233/JAD-190991
58. Purushothaman, D., Yvonne Brown, W., Wu, S., and Vanselow, B. (2011) Evaluation of breed effects on n-3 PUFA metabolism with dietary flaxseed oil supplementation in dogs. *Br. J. Nutr.* **106**, S139–S141
59. Kolesnik, Y. N., Yurina, N. A., Yurin, D. A., Danilova, A. A., Korotky, V. P., Ryzhov, V. A., and Zenkin, A. S. (2009) Development of biohacking elements drawn from the example of cows under stress conditions. *Int. J. Pharm. Res.* **10**, 655–660
60. O’Connor, C. I., Lawrence, L. M., and Hayes, S. H. (2007) Dietary fish oil supplementation affects serum fatty acid concentrations in horses. *J. Anim. Sci.* **85**, 2183–2189
61. Davis, P. F., Ozias, M. K., Carlson, S. E., Reed, G. A., Winter, M. K., McCarson, K. E., and Levant, B. (2010) Dopamine receptor alterations in female rats with diet-induced decreased brain docosahexaenoic acid (DHA): interactions with reproductive status. *Nutr. Neurosci.* **13**, 161–169
62. Akerele, O. A., and Cheema, S. K. (2018) A diet enriched in longer chain omega-3 fatty acids reduced placental inflammatory cytokines and improved fetal sustainability of C57BL/6 mice. *Prostaglandins, Leukot. Essent. Fat. Acids.* **137**, 43–51
63. Brinsko, S. P., Varner, D. D., Love, C. C., Blanchard, T. L., Day, B. C., and Wilson, M. E. (2005) Effect of feeding a DHA-enriched nutraceutical on the quality of fresh, cooled and frozen stallion semen. *Theriogenology.* **63**, 1519–1527
64. Buhling, K. J., and Laakmann, E. (2014) The effect of micronutrient supplements on male fertility.

65. Esmaeili, V., Shahverdi, A. H., Moghadasian, M. H., and Alizadeh, A. R. (2015) Dietary fatty acids affect semen quality: a review. *Andrology*. **3**, 450–461
66. Zaniboni, L., Rizzi, R., and Cerolini, S. (2006) Combined effect of DHA and α -tocopherol enrichment on sperm quality and fertility in the turkey. *Theriogenology*. **65**, 1813–1827
67. Wathes, D. (2013) Polyunsaturated fatty acids and fertility in female mammals: an update. *CAB Rev. Perspect. Agric. Vet. Sci. Nutr. Nat. Resour.* **8**, No.41
68. Clagett-Dame, M., and Knutson, D. (2011) Vitamin A in reproduction and development. *Nutrients*. **3**, 385–428
69. Li, H., and Clagett-Dame, M. (2009) Vitamin A deficiency blocks the initiation of meiosis of germ cells in the developing rat ovary in vivo. *Biol. Reprod.* **81**, 996–1001
70. Kwiecinsk, G. G., and Delāca, G. P. A. F. (2018) Vitamin D is necessary for reproductive functions of the male Rat. **119**, 741–744
71. Travers, A., Arkoun, B., Safsaf, A., Milazzo, J.-P., Absyte, A., Bironneau, A., Perdrix, A., Sibert, L., Macé, B., Cauliez, B., and Rives, N. (2013) Effects of vitamin A on in vitro maturation of pre-pubertal mouse spermatogonial stem cells. *PLoS One*. **8**, e82819
72. Voulgaris, N., Papanastasiou, L., Piaditis, G., Angelousi, A., Kaltsas, G., Mastorakos, G., and Kassi, E. (2017) Vitamin D and aspects of female fertility. *Hormones*. **16**, 5–21
73. Shidoji, Y., and Tabata, Y. (2019) Unequivocal evidence for endogenous geranylgeranoic acid biosynthesized from mevalonate in mammalian cells. *J. Lipid Res.* **60**, 579–593
74. Rose, C., Schwegler, H., Hanke, J., and Yilmazer-Hanke, D. M. (2012) Pregnancy rates, prenatal and postnatal survival of offspring, and litter sizes after reciprocal embryo transfer in DBA/2JHd, C3H/HeNCrl and NMRI mice. *Theriogenology*. **77**, 1883–1893
75. Potgieter, F. J., and Wilke, P. I. (1997) Effect of different bedding materials on the reproductive

- performance of mice. *J. S. Afr. Vet. Assoc.* **68**, 8–15
76. Leidinger, C. S., Thöne-Reineke, C., Baumgart, N., and Baumgart, J. (2019) Environmental enrichment prevents pup mortality in laboratory mice. *Lab. Anim.* **53**, 53–62
 77. Kodomari, I., Wada, E., Nakamura, S., and Wada, K. (2009) Maternal supply of BDNF to mouse fetal brain through the placenta. *Neurochem. Int.* **54**, 95–98
 78. Smarr, B. L., Grant, A. D., Perez, L., Zucker, I., and Kriegsfeld, L. J. (2017) Maternal and early-life circadian disruption have long-lasting negative consequences on offspring development and adult behavior in mice. *Sci. Rep.* **7**, 3326
 79. Sagami, H., Ishii, K., and Ogura, K. (1985) Geranylgeranylpyrophosphate synthetase of pig liver. *Methods Enzymol.* **110**, 184–188
 80. Leung, K. F., Baron, R., and Seabra, M. C. (2006) Thematic review series: Lipid posttranslational modifications. geranylgeranylation of Rab GTPases. *J. Lipid Res.* **47**, 467–475
 81. Grünler, J., Ericsson, J., and Dallner, G. (1994) Branch-point reactions in the biosynthesis of cholesterol, dolichol, ubiquinone and prenylated proteins. *Biochim. Biophys. Acta.* **1212**, 259–277
 82. Kelleher, J. K., and Nickol, G. B. (2015) *Isotopomer spectral analysis: utilizing nonlinear models in isotopic flux studies*, 1st Ed., Elsevier Inc., 10.1016/bs.mie.2015.06.039
 83. Kelleher, J. K., and Nickol, G. B. (2015) Isotopomer Spectral Analysis. *Methods in enzymology.* **561**, 303–330
 84. Elmberger, P. G., Kalèn, A., Appelkvist, E. L. L., and Dallner, G. (1987) In vitro and in vivo synthesis of dolichol and other main mevalonate products in various organs of the rat. *Eur. J. Biochem.* **168**, 1–11
 85. Kodaira, Y., Kusumoto, T., Takahashi, T., Matsumura, Y., Miyagi, Y., Okamoto, K., Shidoji, Y., and Sagami, H. (2007) Formation of lipid droplets induced by 2,3-dihydrogeranylgeranoic acid distinct from geranylgeranoic acid. *Acta Biochim. Pol.* **54**, 777–782

86. Holstein, S. A., Tong, H., Kuder, C. H., and Hohl, R. J. (2009) Quantitative determination of geranyl diphosphate levels in cultured human cells. *Lipids*. **44**, 1055–1062
87. Kotti, T. J., Ramirez, D. M., Pfeiffer, B. E., Huber, K. M., and Russell, D. W. (2006) Brain cholesterol turnover required for geranylgeraniol production and learning in mice. *Proc. Natl. Acad. Sci. U. S. A.* **103**, 3869–3874
88. Kotti, T., Head, D. D., McKenna, C. E., and Russell, D. W. (2008) Biphasic requirement for geranylgeraniol in hippocampal long-term potentiation. *Proc. Natl. Acad. Sci. U. S. A.* **105**, 11394–11399
89. Fliesler, S. J., and Schroepfer, G. J. (1983) Metabolism of mevalonic acid in cell-free homogenates of bovine retinas. Formation of novel isoprenoid acids. *J. Biol. Chem.* **258**, 15062–15070
90. Foster, J. M., Pennock, J. F., Marshall, I., and Rees, H. H. (1993) Biosynthesis of isoprenoid compounds in *Schistosoma mansoni*. *Mol. Biochem. Parasitol.* **61**, 275–284
91. Festing, M. F. W., and Blackmore, D. K. (1971) Life span of specified-pathogen-free (MRC category 4) mice and rats. *Lab. Anim.* **5**, 179–192
92. Omori, M., Watanabe, M., Shidoji, Y., Moriwaki, H., and Muto, Y. (1996) Inhibitory effects of a timely dosing of acyclic retinoid on the development of spontaneous hepatomas in C3H/HeNCrj mice. *Recent Adv. Gastroenterol. Carcinogenesis I.* **1**, 523–526
93. Mitake, M., Ogawa, H., Uebaba, K., and Shidoji, Y. (2010) Increase in plasma concentrations of geranylgeranoic Acid after turmeric tablet intake by healthy volunteers. *J Clin Biochem Nutr.* **46**, 252–258
94. Bergström, S., Carlson, L. A., and Weeks, J. R. (1968) The prostaglandins: a family of biologically active lipids. *Pharmacol. Rev.* **20**, 1–48
95. Shapiro, H., Singer, P., and Ariel, A. (2016) Beyond the classic eicosanoids: Peripherally-acting oxygenated metabolites of polyunsaturated fatty acids mediate pain associated with tissue injury and

inflammation. *Prostaglandins Leukot. Essent. Fat. Acids.* **111**, 45–61

96. Mumford, S. L., Chavarro, J. E., Zhang, C., Perkins, N. J., Sjaarda, L. A., Pollack, A. Z., Schliep, K. C., Michels, K. A., Zarek, S. M., Plowden, T. C., Radin, R. G., Messer, L. C., Frankel, R. A., and Wactawski-Wende, J. (2016) Dietary fat intake and reproductive hormone concentrations and ovulation in regularly menstruating women. *Am. J. Clin. Nutr.* **103**, 868–877
97. Teppola, H., Sarkanen, J.-R., Jalonen, T. O., and Linne, M.-L. (2016) Morphological differentiation towards neuronal phenotype of SH-SY5Y neuroblastoma cells by estradiol, retinoic acid and cholesterol. *Neurochem. Res.* **41**, 731–747
98. Teletin, M., Vernet, N., Ghyselinck, N. B., and Mark, M. (2017) Roles of retinoic acid in germ cell differentiation. *Current topics in developmental biology.* **125**, 191–225
99. Jauregui, E. J., Mitchell, D., Topping, T., Hogarth, C. A., and Griswold, M. D. (2018) Retinoic acid receptor signaling is necessary in steroidogenic cells for normal spermatogenesis and epididymal function. *Development.* **145**, dev160465
100. Minkina, A., Lindeman, R. E., Gearhart, M. D., Chassot, A.-A., Chaboissier, M.-C., Ghyselinck, N. B., Bardwell, V. J., and Zarkower, D. (2017) Retinoic acid signaling is dispensable for somatic development and function in the mammalian ovary. *Dev. Biol.* **424**, 208–220
101. Yabuta, S. (2018) Studies on geranylgeranoic acid-induced cell death: with special attention to pyroptosis in human hepatoma cells. Ph.D. thesis, University of Nagasaki
102. Billon, C., Murray, M. H., Avdagic, A., and Burris, T. P. (2019) ROR γ regulates the NLRP3 inflammasome. *J. Biol. Chem.* **294**, 10–19
103. Fauber, B. P., and Magnuson, S. (2014) Modulators of the nuclear receptor retinoic acid receptor-related orphan receptor- γ (ROR γ or RORc). *J. Med. Chem.* **57**, 5871–5892
104. Hu, X., Wang, Y., Hao, L.-Y., Liu, X., Lesch, C. A., Sanchez, B. M., Wendling, J. M., Morgan, R. W., Aicher, T. D., Carter, L. L., Toogood, P. L., and Glick, G. D. (2015) Sterol metabolism controls

TH17 differentiation by generating endogenous ROR γ agonists. *Nat. Chem. Biol.* **11**, 141–147